LICENTIATE THESIS

Microcracking in Fiber Composites and Degradation of Thermo-elastic Properties of Laminates

Mohamed Sahbi Loukil

LULEÅ UNIVERSITY OF TECHNOLOGY

Microcracking in Fiber Composites and Degradation of Thermo-elastic Properties of Laminates

LICENTIATE THESIS

Mohamed Sahbi Loukil

Division of Materials Science
Department of Engineering Sciences and Mathematics
Luleå University of Technology
Luleå, Sweden
SE 97187

December 2011

Printed by Universitetstryckeriet, Luleå 2011

ISSN: 1402-1757
ISBN 978-91-7439-347-7

Luleå 2011

www.ltu.se

Preface

The three scientific papers in the present licentiate thesis contain the results from my work in the Division of Materials Science in Luleå University of Technology, Sweden and in the Division of Mechanics of Materials (SI2M) in Institut Jean Lamour, France during the period October 2009 to October 2011.
There are many people who deserve my gratitude since they have contributed to this work.
First of all, I would like to express my sincerest gratitude to my both supervisors Professor Janis Varna from Sweden and Professor Zoubir Ayadi from France for their scientific guidance and HUGE contribution to this thesis. I am grateful to them for their support, not only in working, but also in personal level and for creating such a warm atmosphere, making work in their divisions a great pleasure.
I am very thankful to Dr. Roberts Joffe for his remarks, ideas and fruitful suggestions, during this period.
My gratitude also goes to Dr. Lennart Wallström for his help and to Professor Ali Kallel and Professor Zouhir Fakhfakh from Tunisia for being the persons who gave me the opportunity to come to Europe.
Special thanks also go to all my colleagues at division of materials science; Andrejs, Erik, Kostis, Liva, Magda and Ylva; who have always been friendly and supportive making the working environment always very fun and warm even though we live and work at -25°C or less.
My list would not be completed if I would not mention my colleagues at division of mechanics of materials; Hana and Benjamin.
I would in particular like to thank my family in Tunisia for their love and support. They always make it wonderful to come back home.

Luleå, December 2011

Mohamed Sahbi Loukil

Abstract

The macroscopic failure of composite laminates subjected to tensile increasing load is preceded by initiation and evolution of several microdamage modes. The most common damage mode and the one examined in this thesis is intralaminar cracking in layers. Due to this kind of microdamage the laminate undergoes stiffness reduction when loaded in tension. For example, the elastic modulus in the loading direction and the corresponding Poisson's ratio will decrease.

The degradation of the elastic properties of these materials is caused by reduced stress in the damaged layer which is mainly due to two parameters: crack opening displacement (COD) and crack sliding displacement (CSD). At fixed applied load these parameters depend on the properties of the damaged and surrounding layers, on layer orientation and on thickness. When the number of cracks per unit length is high (high crack density in the layer) the COD and CSD are reduced because of to crack interaction.

The main objective of the **first paper** is to investigate the effect of crack interaction on COD using FEM and to describe the identified dependence on crack density in a simple and accurate form by introducing an interaction function dependent on crack density. This interaction function together with COD of non-interactive crack gives accurate predictions of the damaged laminate thermo-elastic properties. The application of this function to more complex laminate lay-ups is demonstrated. All these calculations are performed assuming that cracks are equidistant.

However, the crack distribution in the damaged layer is very non-uniform, especially in the initial stage of multiple cracking. In the **second paper**, the earlier developed model for general symmetric laminates is generalized to account for non-uniform crack distribution. This model is used to calculate the axial modulus of cross-ply laminates with cracks in internal and surface layers. In parametric analysis the COD and CSD are calculated using FEM, considering the smallest versus the average crack spacing ratio as non-uniformity parameter. It is shown that assuming uniform distribution we obtain lower bond to elastic modulus. A "double-periodic" approach presented to calculate the COD of a crack in a non-uniform case as the average of two solutions for periodic crack systems is very accurate for cracks in internal layers, whereas for high crack density in surface layers it underestimates the modulus reduction.

In the **third paper**, the thermo-elastic constants of damaged laminates were calculated using shear lag models and variational models in a general calculation approach (GLOB-LOC) for symmetric laminates with transverse cracks in 90° layer. The comparison of these two models with FEM was presented for cross-ply and quasi-isotropic laminates.

List of appended papers

Paper I

MS. Loukil, J. Varna and Z. Ayadi, Engineering expressions for thermo-elastic constants of laminates with high density of transverse cracks, Composite Part A: Applied Science and Manufacturing, submitted, 2011.

Paper II

MS. Loukil, J. Varna and Z. Ayadi, Applicability of solutions for periodic intralaminar crack distributions to non-uniformly damaged laminates, Journal of Composite Materials, submitted, 2011.

Paper III

MS. Loukil, W. Hussain, A. Kirti, A. Pupurs and J. Varna, Thermo-elastic constants of symmetric laminates with cracks in 90-layer: application of simple models, Plastics, Rubber and Composites, accepted, 2011.

List of relevant publications and presentations

Conference papers

1. MS. loukil, J. Varna and Z. Ayadi, Characterization of damaged composite laminates by an optical measurement of the displacement field, IOP Conference Series: Materials Science and Engineering, submitted, 2011

2. H. Zrida, MS. loukil, J. Varna and Z. Ayadi, Crack opening displacement determination in damaged cross-ply laminate using ESPI, IOP Conference Series: Materials Science and Engineering, submitted, 2011

List of Conference Presentations

1. MS. Loukil, J. Varna and R. Joffe, Microdamage initiation and growth in laminated composites, 17th Polychar World Forum on Advanced Materials, Rouen (France), April 2009

2. MS. loukil, L. Farge, J. Varna and Z. Ayadi, Characterization of damage evolution in thermo mechanical loading of composites materials, 5th International EEIGM/AMASE Conference on Advanced Materials Research, Nancy (France), November 2009

3. MS. loukil, J. Varna and Z. Ayadi, Parameter determination in damaged laminate model by optical full-field measurement of the displacement using ESPI , 5th International Conference on Composites Testing and Model Identification, Lausanne (Switzerland), February 2011

4. MS. loukil, J. Varna and Z. Ayadi, Thermo-elastic properties of damaged laminates at high density of cracks in layers, Supply on the Wings, Frankfurt/Main (Germany), November 2011

5. MS. loukil, J. Varna and Z. Ayadi, Characterization of damage composite laminates by an optical measurement of the displacement field, 6th International EEIGM Conference on Advanced Materials Research, Nancy (France), November 2011

Contents

1. Introduction

Composite is a material which has at least two distinct phases or constituents. This material has found usage in many industrial applications and more recently it is increasingly being used in aerospace panels and airframes. The use of aligned fiber reinforced polymeric composites in the aerospace industry is justified by their excellent specific modulus and strength (referred to the property divided by the density).

When a composite laminate is loaded in tension with increasing load it will eventually fail (macroscopically). The failure is preceded by initiation and evolution of several microdamage modes. On the microscale, a part of the matrix can fail, fibers can fail and there can be fiber/matrix interface debonding (Figure 1). On the mesoscale, the first mode of damage is usually intralaminar cracking in off-axes layers with respect to the main load component. These cracks run parallel to fibers in the layer with the crack plane being transverse to the laminate midplane. Intralaminar cracks do not usually cause the final failure of a laminate, but may significantly impair the effective properties of the composite and serve as a source for other damage modes initiation, such as interlayer delamination. Fiber fracture in the adjacent plies is induced only at high loads in the case of monotonic loading or for large cycle number in the case of fatigue loading.

Figure 2 shows a cross-ply laminate with three different modes of damage.

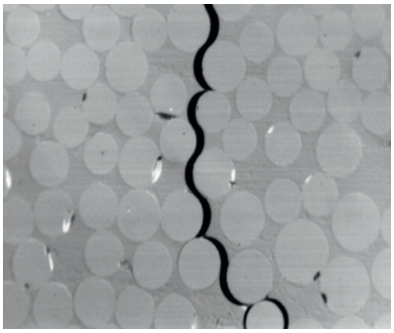

Figure 1. Intralaminar crack initiation from fiber/matrix interface failure.

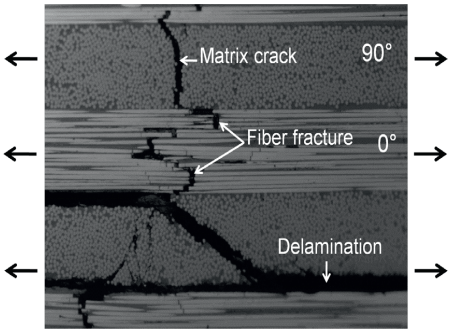

Figure 2. Example of damage modes in laminates.

Since the number of cracks per unit length called crack density increases during service life (Figure 3), a complete model that describes the reduction of thermo-elastic properties must contain damage evolution modeling.

In this work the crack evolution is not considered but there are several approaches that can be used. One is the deterministic approach that ignores the fact that transverse cracking is a progressive damage and predicts appearance of many cracks simultaneously when the first cracking strain is reached. There are also more accurate models that include the statistical nature of the failure process.

Due to damage accumulation (transverse cracks) the effective stiffness of the damaged layer as well as stiffness of the whole laminate is decreasing (Figure 4).

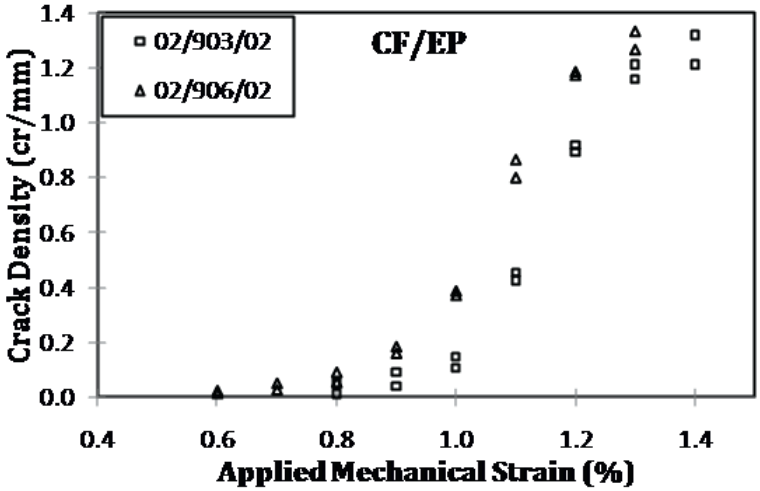

Figure 3. Experimental data for crack evolution with increasing applied strain in carbon fiber/epoxy cross-ply laminates

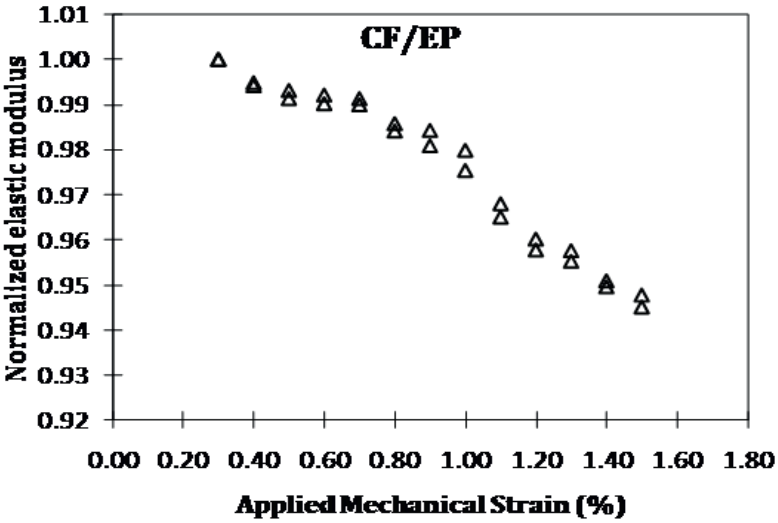

Figure 4. Dependence of the elastic modulus of a cross-ply laminate on the applied strain level

Numerous analytical and numerical models have been developed to study the stiffness degradation due to transverse cracks. The opening and sliding of crack surfaces reduce the average strain and stress in the damaged layer, thus reducing the portion of the load carried by this layer. It results in reduction of the laminate thermo-elastic properties.

All analytical models are based on approximate solution for the stress state between two cracks (repeating element). The simplest type of models leading to linear second order differential equation with constant coefficients is called shear lag models [1-4].

General for all shear-lag models is that the equilibrium conditions are satisfied in average only and the shear stress free condition on crack surfaces is not satisfied. A "shear lag" parameter which is often a fitting parameter is needed in these models. The stress distribution and the stiffness degradation calculated according to these models in [5,6] are affected by the value of this parameter.
The first model based on the principle of minimum complementary energy which was free of these assumptions was developed by Hashin [7] to investigate the axial modulus reduction of cross ply laminate with cracks in inside 90 layers. The approximate stress field derived with this approach satisfies all the necessary equilibrium as well as the boundary conditions including zero tractions on the crack surfaces. Since the approximate nature of the selected stress functions lead to increase of the value of the complementary energy, it does not reach the minimum corresponding to the exact solution and the displacement continuity is satisfied only approximately. Hashin's model is relatively simple to use and it renders lower bond for the axial modulus of the damaged laminate.
Refined variational models based on minimum principle of the complementary energy with more accurate predictions of axial modulus and Poisson's ratio were developed in [8,9].
Homogenization method was used to establish (GLOB-LOC approach) the link between the damaged laminate thermo-elastic properties and the microdamage parameters (crack face opening displacement (COD) and crack face sliding displacement (CSD)) in [10,11]. It was shown that only the average values of COD and CSD enter the stiffness expressions directly. In a linear model the average COD and CSD values are proportional to the applied load. Consequently, they were normalized to be used in stiffness calculations.
FEM studies were performed to understand which material and geometry parameters affect the COD and CSD in [10-12] and simple empirical relationships (power law) were suggested.
The effect of crack density (number of cracks per unit length) on the COD and CSD was analyzed in [12] and studied using FEM in [13]. It was shown that the normalized COD and CSD are smaller for high crack density.
All of these models are based on idealized assumptions, for example, assuming linear elastic material behavior even in high stress concentration region at crack tip as well as linearity in shear loading and assuming idealized geometry of these cracks which would not change during the service life. The only correct way to validate these assumptions is through experiments.

The effect of material properties on COD was measured experimentally using optical microscopy of loaded damaged specimens in [14,15]. It was shown that the measured average values of COD are affected by the constraining layer orientation and stiffness.
The experimental determination of the average COD and CSD requires the measurement of the displacement for all points of the crack surfaces, which justifies the use of full-field measurement techniques Electronic Speckle Pattern Interferometry (ESPI). ESPI is an optical technique that provides the displacement for every point on a surface and offers the possibility to measure both, the in-plane and out-of-plane displacement without surface preparation.
This technique was used in [16,17] to measure the COD for inside cracks on the specimen's edge. It was shown that the profile of the crack on the edge is elliptical.

The objectives of the presented licentiate thesis are

a) to obtain a deeper insight in the mesoscale laminate parameters governing the interaction of cracks in terms of COD's

b) to describe the crack interaction by simple functions obtained analyzing results of FEM parametric analysis and to use these functions for thermo-elastic properties determination of damaged laminates using the GLOB-LOC approach

c) to develop and verify methodology for approximate calculation of the complete set of thermo-elastic constants using any analytical stress model for laminates with cracks

2. Summary of appended papers

In **paper 1** the effect of crack interaction on COD is investigated using FEM in surface layers (surface cracks) and inside layers (inside cracks). The identified dependence on crack density is described in a simple and accurate form by introducing an interaction function dependent on crack density. This interaction function together with COD of non-interactive crack gives accurate predictions of the damaged laminate properties. The application of this function to more complex laminate lay-ups is demonstrated. All these calculations are performed assuming that cracks are equidistant.

However, the crack distribution in the damaged layer is very non-uniform, especially in the initial stage of multiple cracking. In **paper 2** the earlier developed model for general symmetric laminates is generalized to account for non-uniform crack distribution. This model is used to calculate the axial modulus of cross-ply laminates with cracks in internal and surface layers. In parametric analysis the COD and CSD are calculated using FEM, considering the smallest versus the average crack spacing ratio as non-uniformity parameter. It is shown that assuming uniform distribution we obtain lower bond to elastic modulus. A "double-periodic" approach presented to calculate the COD of a crack in a non-uniform case as the average of two solutions for periodic crack systems is very accurate for cracks in internal layers, whereas for high crack density in surface layers it underestimates the modulus reduction.

In paper 3 it is shown that a complete set of damaged laminate thermo-elastic constants can be calculated using any analytical stress distribution model for a region between two cracks, usually developed to calculate only one or maximum two elastic constants. The degradation of thermo-elastic properties of cross-ply and quasi-isotropic laminates with intralaminar cracks in 90° layers is analyzed. Predictions are performed using previously derived general expressions for stiffness (GLOB-LOC) of symmetric damaged laminates as dependent on crack density and crack face opening (COD) and sliding (CSD). It is shown that the average COD can be linked with the average value of axial stress perturbation between two cracks. Using this relationship analytical shear lag and Hashin's models, developed for axial modulus, are applied to calculate thermal expansion coefficients, Young's modulus and Poisson's ratios of damaged laminates. The approach is evaluated using FEM and showing that the accuracy is rather similar as in axial modulus calculation.

3. Reference

1. Highsmith AL, Reifsnider KL. Stiffness-reduction mechanisms in composite laminates. In: Damage in composite materials, ASTM STP 775. Philadelphia (PA): American Society for Testing and Materials 1982; 103-17.
2. Han YM, Hahn HT. Ply cracking and property degradation of symmetric balanced laminates under general in-plane loading. Composite Science and Technology 1989;35:377-97.
3. Smith PA, Wood JR. Poisson's ratio as a damage parameter in the static tensile loading of simple cross-ply laminates. Composite Science and Technology 1990;38:85-93.
4. Lim SG, Hong CS. Prediction of transverse cracking and stiffness reduction in cross-ply laminated composites. Journal of Composite Materials 1989;23:695-713.
5. Krasnikovs A, Varna J. Transverse cracks in cross-ply laminates. Part 1, Stress Analysis, Mechanics of Composite Materials 1997; 33(6):565-582.
6. Varna J, Krasnikovs A. Transverse cracks in cross-ply laminates. Part 2, Stiffness Degradation, Mechanics of Composite Materials 1998; 34(2):153-170.
7. Hashin Z. Analysis of cracked laminates: A Variational Approach. Mech. Mater., North-Holland 1985; 4:121-136.
8. Varna J, Berglund LA. Thermo-Elastic properties of composite laminates with transverse cracks. Journal of Composites Technology and Research 1994; 16(1):77-87.
9. Varna J, Berglund LA. Two-Dimensional Transverse Cracking in $[0m/90n]_S$ Cross-Ply Laminates. European Journal of Mechanics A/Solids 1993; 12(5):699-723.
10. Lundmark P, Varna J. Constitutive relationships for laminates with ply cracks in in plane loading. International Journal of Damage Mechanics 2005;14(3):235-261
11. Lundmark P, Varna J. Crack face sliding effect on stiffness of laminates with ply cracks. Composite Science and Technology 2006; 66:1444-1454
12. Joffe R, Krasnikovs A, Varna J. COD-based simulation of transverse cracking and stiffness reduction in [S/90n]s laminates. Composite Science and Technology 2001; 61:637-656
13. Lundmark P, Varna J. Stiffness reduction in laminates at high intralaminar crack density: effect of crack interaction. International Journal of Damage Mechanics 2011; 20:279-97
14. Varna J, Berglund LA, Talreja R, Jakovics A. A study of the crack opening displacement of transverse cracks in cross ply laminates. International Journal of Damage Mechanics 1993; 2:272-289
15. Varna J, Joffe R, Akshantala NV, Talreja R. Damage in composite laminates with off-axis plies. Composite Science and Technology 1999; 59:2139-2147
16. Farge L, Ayadi Z, Varna J. Optically measured full-field displacements on the edge of a cracked composite laminate. Composite Part A 2008; 39:1245-1252
17. Farge L, Varna J, Ayadi Z. Damage characterization of a cross-ply carbon fiber/epoxy laminate by an optical measurement of the displacement field. Composite Science and Technology 2010; 70: 94-101

Paper I

MS. Loukil, J. Varna and Z. Ayadi

Engineering expressions for thermo-elastic constants of laminates with high density of transverse cracks

Engineering expressions for thermo-elastic constants of laminates with high density of transverse cracks

MS. Loukil[1,2], J. Varna[1] and Z. Ayadi[2]

[1]Luleå University of Technology, SE-971 87 Luleå, Sweden
[2]Institut Jean Lamour, EEIGM 6 Rue Bastien Lepage, F-54010 Nancy Cedex, France

Abstract

Exact analytical expressions for thermo-elastic constants of symmetric and balanced laminates with intralaminar cracks in 90-layers are presented. The normalized crack opening displacement (COD), which is one of the most important parameters in these stiffness reduction expressions, depends on crack density. This dependence is described by interaction function in form of tanh() obtained fitting results of FEM based parametric analysis for cross-ply laminates with cracks in surface and inside layers. It is shown that this interaction function together with COD of non-interactive crack, gives high accuracy predictions of reduced properties of any cross-ply laminate. The derived interaction function can be used to simulate stiffness reduction of more general lay-ups. The application of this function to quasi-isotropic laminates is demonstrated.

Keywords: Laminates, Mechanical properties, Transverse cracking, Finite element analysis (FEA)

1. Introduction

Intralaminar cracks are caused by in-plane transverse and shear stresses in layers with current understanding that the role of transverse stress is much more important. The number of cracks increases during service life reducing laminate thermo-elastic properties. The stiffness degradation phenomenon can be explained in terms of opening and sliding of crack surfaces. Due to crack face relative displacement the average stress between cracks is reduced and, hence, the participation of the damaged ply in bearing the applied load is reduced. In thermal loading it results in release of thermal stresses and dimensional changes of the laminate. In other words the average crack face displacements are uniquely linked to the average stress between cracks.
In modeling, the simplest way to account for reduced average stress in a damaged ply is by reducing the thermo-elastic properties of this ply as it is done in the well know ply-discount model, commonly used together with Classical Laminate Theory (CLT). Physically this approach it is not correct; thermo-mechanical constants in the damaged layer material have not changed. Nevertheless, the reduction of elastic constants is a simple way to include the effect of reduced average stress in the layer, still keeping the concept of iso-strain which in non-bending case builds the basis of CLT. However, assumption in this approach that transverse and shear properties of a ply with cracks are zero is very conservative and does not reflect the real situation where the number of cracks is increasing in a stable manner during the service life.

Therefore, development of reliable and refined stiffness reduction models requires a good understanding of the effect of each crack on stiffness. At higher density of transverse cracks (number of cracks per mm measured transverse to the fiber direction in a layer) the local stress states of individual cracks start to overlap and the effect of each individual crack on stiffness is reduced. This overlapping of stress perturbations we call ”interaction” and cracks at high densities as ”interactive”. Interactive cracks have smaller opening. One can visualize it by imagining two existing cracks and a new crack (a “cut” in 90-layer) created between them. The “cut” will reduce the stress between existing cracks and the displacement of the corresponding faces of these two cracks.

Most of the analytical stress distribution modeling has been performed for cross-ply laminates [1,2] with cracks in the 90-layer. The simple variational model by Hashin [2], which is free of any fitting parameters, overestimates the stiffness reduction [3]. The accuracy has been improved using more sophisticated variational models [3-4]. The large group of shear-lag models has one in common: the stress distribution is described by second order differential equation with constant coefficients. The equilibrium conditions are satisfied in average only and the shear stress free condition on crack surfaces is not satisfied. These models contain a rather voluntarily defined “shear lag parameter”. Largely different stress distributions and stiffness degradation are calculated dependent on the value of this parameter (which is often used as a fitting parameter) [4-6].

Analytical solutions for more complex lay-ups with cracks in arbitrary layers are not available (except a straightforward generalization for [S/90]s laminates, where S represents the homogenized sublaminate supporting the cracked 90-layer [9]). It is not clear how to transfer to general laminates the knowledge and experience gained studying cross-ply laminates.

A different approach (GLOB-LOC approach), which links the macro-constants of damaged laminate with geometry of the individual crack surface in deformed state, was developed in [7,8]. Exact analytical expressions for thermo-elastic constants of general symmetric laminates with cracks in layers were presented. These matrix expressions are given in Section 2. In addition to laminate lay-up, layer properties and density of cracks in layers they contain two parameters of the deformed crack surface: averaged relative opening (COD) and sliding displacements (CSD) in normalized form.

The COD’d and CSD’s can be obtained from any analytical stress distribution model. In [7,8] FEM analysis was used to identify parameters affecting these quantities. It was found that for low crack densities the average COD and CSD are very robust parameters dependent only on the cracked and the neighboring layer stiffness and thickness ratios. Simple but rather accurate fitting functions (“power laws”) were presented. There is no need to use FEM every time when damaged laminates are analyzed: The GLOB-LOC approach can be used instead. The COD and CSD have been measured also experimentally [10-13] and trends as well as values are confirmed.

These fitting functions for COD and CSD are not valid in high crack density region: due to interaction COD and CSD decrease with crack density. We suggest accounting for interaction in a very simple way: introducing crack density dependent interaction function which multiplied by the COD and CSD of non-interactive cracks would give the opening and sliding at any crack density. Previously the crack interaction for COD was studied in [14], considering cracks only in 90-layer of [0n/90m]s laminate. The interaction function, defined based on FEM data analysis was fit with logarithmic

function with limited range of applicability in terms of laminate lay-up and crack density.

The **objectives** of the presented paper are

a) use FEM to analyze COD's in cross-ply laminates at high crack density in surface layers ("surface cracks") and inside layers ("inside cracks")
b) to present unified interaction functions for COD of surface and inside cracks to be used together with noninteractive crack COD
c) to demonstrate the accuracy of expressions in stiffness prediction for cross-ply and quasi-isotropic laminates

Features of crack face sliding in the interactive region are not considered in this paper.

2. Material model of damaged symmetric laminates with intralaminar cracks

2.1 Model formulation

The upper part of symmetric *N*- layer laminate is shown in Fig. 1. The *k*-th layer of the laminate is characterized by thickness t_k , fiber orientation angle with respect to the global x-axis θ_k and by stiffness in the local axes $[Q]$ (defined by thermo-elastic constants $E_1, E_2, G_{12}, \nu_{12}, \alpha_1, \alpha_2$). The total thickness of the laminate, $h = \sum_{k=1}^{N} t_k$. The crack density in a layer is $\rho_k = 1/(2l_k \sin\theta_k)$ where average distance between cracks measured on the specimen edge is $2l_k$. Dimensionless crack density ρ_{kn} is introduced as

$$\rho_{kn} = t_k \rho_k \tag{1}$$

It is assumed that the damaged laminate is still symmetric et est. the crack density in corresponding symmetrically placed layers is the same. The stiffness matrix of the damaged laminate is $[Q]^{LAM}$ and the stiffness of the undamaged laminate is $[Q]_0^{LAM}$. The compliance matrix of the undamaged laminate is $[S]_0^{LAM} = \left([Q]_0^{LAM}\right)^{-1}$, $\{\alpha\}_0^{LAM}$ is the thermal expansion coefficient vector. Constants of the undamaged laminate are calculated using CLT.

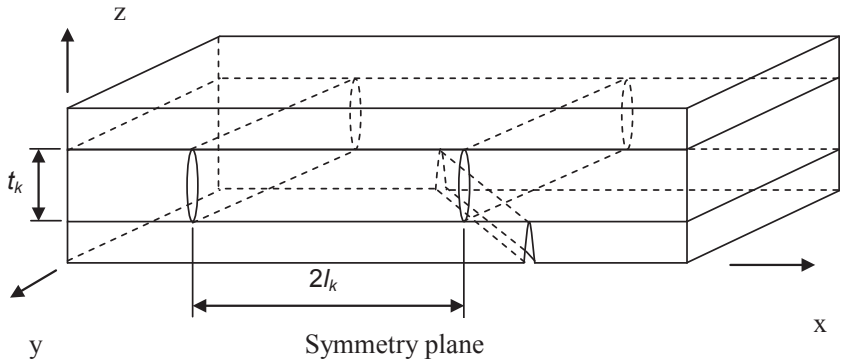

Figure 1. RVE of the damaged laminate with intralaminar cracks in layers.

The expressions for thermo-elastic constants of the damaged laminate presented below are exact.

$$[S]^{LAM} = [S]_0^{LAM}\left([I] + \sum_{k=1}^{N} \rho_{kn} \frac{t_k}{h}[K]_k [S]_0^{LAM}\right) \tag{2}$$

$$\{\alpha\}^{LAM} = \left([I] + \sum_{k=1}^{N} \frac{t_k}{h} \rho_{kn} [S]_0^{LAM} [K]_k\right)\{\alpha\}_0^{LAM} - \sum_{k=1}^{N} \frac{t_k}{h} \rho_{kn} [S]_0^{LAM} [K]_k \{\overline{\alpha}\}_k \tag{3}$$

They were derived in [7,8] expressing the integral effect of cracks in terms of crack density and $[K]_k$ which is a known matrix-function dependent on ply properties and normalized and averaged crack face opening (COD) and sliding displacements (CSD), u_{2an}, u_{1an} which may be different in different layers. In (3) $\{\overline{\alpha}\}_k$ is the vector of thermal expansion coefficients of a damaged layer in global coordinates. The $[K]_k$ matrix for a ply in a laminate is defined as

$$[K]_k = \frac{1}{E_2}[\overline{Q}]_k [T]_k^T [U]_k [T]_K [\overline{Q}]_k \tag{4}$$

The involved matrices $[T]_k$ and $[\overline{Q}]_k$ are defined according to CLT, upper index T denotes transposed matrix and bar over stiffness matrix indicates that it is written in global coordinates. For a layer with fiber orientation angle θ_k , $m = \cos\theta_k$ and $n = \sin\theta_k$

$$[T]_k = \begin{bmatrix} m^2 & n^2 & +2mn \\ n^2 & m^2 & -2mn \\ -mn & +mn & m^2 - n^2 \end{bmatrix}, \qquad [\overline{Q}]_k = [T]_k^{-1}[Q]\left([T]_k^{-1}\right)^T \tag{5}$$

The influence of each crack is represented in (4) by matrix $[U]_k$ which contains the normalized average COD and normalized average CSD of the crack surfaces in k-th layer

$$[U]_k = 2\begin{bmatrix} 0 & 0 & 0 \\ 0 & u_{2an}^k & 0 \\ 0 & 0 & \frac{E_2}{G_{12}} u_{1an}^k \end{bmatrix} \tag{6}$$

Simple and reliable determination of u_{2an}, u_{1an} in high crack density region is the main subject in this paper.

2.2 Thermo-elastic constants of balanced laminates with cracks in 90-layers

For balanced laminates with cracks in 90-layers, $[K]_k$ can be calculated analytically. Using the result in (2) and (3) the following expressions for laminate thermo-elastic constants were obtained.

$$\frac{E_x}{E_x^0}=\frac{1}{1+2\rho_{90n}\dfrac{t_{90}}{h}u_{2an}^{90}c_2} \qquad \frac{E_y}{E_y^0}\frac{1}{1+2\rho_{90n}\dfrac{t_{90}}{h}u_{2an}^{90}c_4} \tag{7}$$

$$\frac{\nu_{xy}}{\nu_{xy}^0}=\frac{1+2\rho_{90n}\dfrac{t_{90}}{h}u_{2an}^{90}c_1\left(1-\dfrac{\nu_{12}}{\nu_{yx}^0}\right)}{1+2\rho_{90n}\dfrac{t_{90}}{h}u_{2an}^{90}c_2} \qquad \frac{G_{xy}}{G_{xy}^0}=\frac{1}{1+2\rho_{90n}\dfrac{t_{90}}{h}u_{1an}^{90}\dfrac{G_{12}}{G_{xy}^0}} \tag{8}$$

$$\frac{\alpha_x}{\alpha_x^0}=1-2\rho_{90n}\frac{t_{90}}{h}u_{2an}^{90}\frac{c_1}{\alpha_x^0}\left(\alpha_2-\alpha_x^0-\nu_{12}\left(\alpha_y^0-\alpha_1\right)\right) \tag{9}$$

$$\frac{\alpha_y}{\alpha_y^0}=1-2\rho_{90n}\frac{t_{90}}{h}u_{2an}^{90}\frac{c_3}{\alpha_y^0}\left(\alpha_2-\alpha_x^0-\nu_{12}\left(\alpha_y^0-\alpha_1\right)\right) \tag{10}$$

$$c_1=\frac{E_2}{E_x^0}\frac{1-\nu_{12}\nu_{xy}^0}{\left(1-\nu_{12}\nu_{21}\right)^2} \qquad c_2=c_1\left(1-\nu_{12}\nu_{xy}^0\right) \tag{11}$$

$$c_3=\frac{E_2}{E_y^0}\frac{\nu_{12}-\nu_{yx}^0}{\left(1-\nu_{12}\nu_{21}\right)^2} \qquad c_4=c_3\left(\nu_{12}-\nu_{yx}^0\right) \tag{12}$$

Index 90 is used for thickness, crack density and COD in 90-layer. The quantities with lower index x,y are laminate constants, quantities with additional upper index 0 are undamaged laminate constants. It is noteworthy that

a) If Poisson's effects are neglected $c_3=c_4=0$. In this approximation E_y and α_y do not change because of damage in 90-ply.

b) Shear modulus is not related to COD and depends on sliding displacement only.

The class of laminates covered by these expressions is broader than just cross ply laminates or laminates with 90-layers. For example, any quasi-isotropic laminate with an arbitrary cracked layer can be rotated to have the damaged layer as a 90-layer. The only limitation of (7)-(12) is that the laminate after rotation is balanced with zero coupling terms in $\left[S\right]_0^{LAM}$.

Application of (7)-(12) requires values of u_{2an}, u_{1an}. Simple and rather accurate expressions are presented in section 3 where FEM parametric analysis is used.

3. Numerical parametric analysis of COD

3.1 Definitions, interaction mechanisms and FEM model

It is assumed that all cracks in the same layer are equal and equidistant. The average CSD and COD are defined as

$$u_{1a}^k=\frac{1}{2t_k}\int_{-\frac{t_k}{2}}^{\frac{t_k}{2}}\Delta u_1^k(x_3)\,dx_3 \qquad u_{2a}^k=\frac{1}{2t_k}\int_{-\frac{t_k}{2}}^{\frac{t_k}{2}}\Delta u_2^k(x_3)\,dx_3 \tag{13}$$

Here Δu_i is the displacement gap between points at both crack faces. Index 1 denotes the displacement in fiber direction (sliding) and index 2 in the transverse direction (opening).

In linear model the average displacements u_{2a}^k and u_{1a}^k are linear functions of the applied stress and the ply thickness. Therefore, they are normalized with respect to the far field (CLT) shear stress σ_{12}^{0k} and transverse stress σ_2^{0k} in the layer (resulting from the macro-load $\{\sigma\}_0^{LAM}$ and temperature difference ΔT) and with respect to the thickness of the cracked layer t_k

$$u_{1an}^k = u_{1a}^k \frac{G_{12}^k}{t_k \sigma_{12}^{0k}} \qquad\qquad u_{2an}^k = u_{2a}^k \frac{E_2^k}{t_k \sigma_2^{0k}} \tag{14}$$

Elastic constants are introduced in (14) to have dimensionless descriptors. The influence of each crack on thermo-elastic laminate constants is represented by u_{2a}^k and u_{1a}^k, see (2),(3) or (7)-(12). They can be deduced from simple stress models like shear lag [1] or variational models [2] as demonstrated in [5], however the accuracy of these models is rather low. Instead, in this paper we present much more accurate expressions based on extensive FEM parametric analysis. They are applicable for wide range of material properties and crack density. Analysis in this paper is limited to crack opening displacements leaving sliding for a separate publication.

When the distance between cracks is much larger than the crack size, the stress perturbations of two neighboring cracks do not overlap and cracks in this region can be considered as non-interactive. The normalized average COD and CSD in this crack density region are independent on crack density. Upper index 0 is used to indicate values in this region ($u_{1an}^{0k}, u_{2an}^{0k}$). Rather accurate fitting expressions to calculate $u_{1an}^{0k}, u_{2an}^{0k}$ are given in [7,8].

When the distance between cracks decreases the stress perturbation regions overlap and the normalized average COD and CSD start to decrease. This phenomenon was studied in [14], however, considering only COD for "inside cracks" (defined in Fig. 2b). Here we extend the analysis to damaged surface layers, see Fig. 2a) and present more reliable description of interaction.

As in [14] in this paper we also express u_{2an}^k through COD of non-interactive cracks, u_{2an}^{0k} by introducing "interaction function" dependent on normalized crack density in the layer

$$u_{2an}^k = \lambda_k(\rho_{kn}) u_{2an}^{0k} \tag{15}$$

The crack interaction function λ depends also on elastic and geometrical parameters of the cracked layer and surrounding layers. For non-interactive cracks $\lambda = 1$.

In [14] the fitting was with logarithmic "master" curve that was rather inaccurate and therefore applicable only for medium crack densities. The role of stiffness and geometrical parameters on crack interaction was not really understood and therefore the "master curve" did not include these parameters. The outcome was a simple interaction function on expense of reduced accuracy.

In the presented paper we analyze the effect of the dimensionless crack density ρ_n on u_{2an} using FEM for $[0_n/90_8]_S$ and $[90_8/0_n]_S$ laminates (n=1,2,4,8,16,24) shown in Fig 2. To have large variation in elastic constants both CF/EP and GF/EP composites

with constants given in Table 1 were analyzed. Since all expressions contain thickness ratios, the thickness of a single ply is irrelevant as long as dimensionless crack density is used.

For calculations the commercial code ABAQUS was used. In order to model the repeating volume element (see Fig. 2), a 3-D model was created. All plies are considered to be transversely isotropic, and hence the thickness direction related properties are taken as $E_2 = E_3; G_{12} = G_{13}$ and $\nu_{12} = \nu_{13}$.

Table 1. Material properties used in simulations, t is the ply thickness.

Material	E_1(GPa)	E_2(GPa)	ν_{12}	ν_{23}	G_{12} (GPa)	G_{23} (GPa)	t (mm)
GF/EP	45	15	0.3	0.4	5	6	0.5
CF/EP	150	10	0.3	0.4	5	6	0.5

In order to mesh volumes, 3D continuum elements (C3D8) 8-node linear brick were used. The same fine mesh with 86400 elements was used in each FE model. The (X, Z) plane consisted of 21600 elements, with refined mesh near the crack surfaces. The number of elements in y-direction was 4 which as described below is more than sufficient for the used edge conditions.

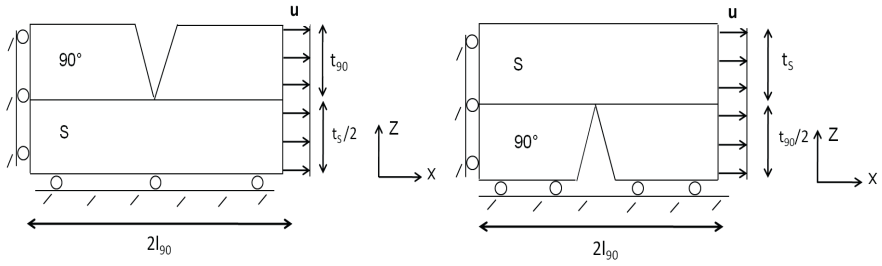

a) surface cracks b) inside cracks

Figure 2. Load cases used for determination of average crack face opening displacement

Constant displacement corresponding to 1% average strain was applied to the repeating unit in x-direction. On the front edge (y=0) and the far-away edge (y=w) coupling conditions were applied for normal displacements (u_y = unknown constant). In this way edge effects are eliminated and the solution does not depend on y-coordinate. It corresponds to solution for an infinite structure in the width direction. Obviously these conditions correspond to generalized plane strain case. The displacement in x-direction for the nodes at the crack surface was used to calculate the average value of the COD. Varying length $2l_{90}$ of the repeating unit, the average strain of 1% corresponds to different values of applied load (laminate stress). Hence, performing normalization according to Equation (14) we have to use corresponding far field stress σ_2^0 and σ_{12}^0 in the 90° layer.

Fig. 3a) shows the normalized crack face opening displacement u_{2an} for $[90_8 / 0_n]_S$ and $[0_n / 90_8]_S$ laminates (n=4,8,16 and 24) for GF/EP and CF/EP materials as a function of normalized crack density ρ_n in the 90-layer.

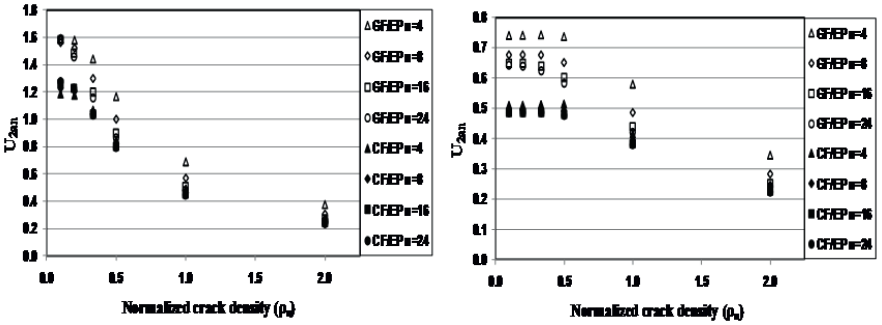

a) $[90_8/0_n]_S$ b) $[0_n/90_8]_S$

Figure 3. The u_{2an} dependence on crack density for GF/EP and CF/EP composites with varying layer thickness ratio calculated using FEM

A large variation in u_{2an} values dependent on the composite elastic properties and laminate lay-up is shown in Fig. 3. For the same value of crack density the normalized average COD is bigger for GF/EP than CF/EP composite because GF/EP 0-layer applies less constraint to COD than the CF/EP 0-layer. The COD decreases with increasing crack density. It is interesting to note that the effect of lay-up and material is stronger for non-interactive cracks. The effect of increasing crack density can be better seen by normalizing the results in Fig. 3 with respect to the COD's of corresponding noninteractive cracks, u^0_{2an}, obtained by FEM et est. introducing the interaction function according to (15).

As a result of many trials we suggest the following form of the 'interaction function' $\lambda(\rho_n)$

$$\lambda(\rho_n) = \tanh\left(\frac{\alpha}{\rho_n}\right) \tag{16}$$

The form (13) is similar to corresponding term in shear lag model's solution for stiffness but the definition of α (14) is different than that of the shear lag parameter.

3.2 Surface cracks

For surface cracks in cross-ply laminates

$$\alpha = C \times \left(\frac{E_s}{E_2}\right)^{1/4} \left(1 + \frac{t_{90} E_2}{t_s/2\, E_s}\right) \tag{17}$$

In (17) and also in (18) E_s is the elastic modulus of the support layer in the transverse direction of the 90-layer. Obviously, $E_s = E_1$ for cross-ply laminates. C is a material and ply geometry independent fitting constant which has different value for "surface" and "inside" cracks. Plotting the FEM values of the interaction function $\lambda(\rho_n)$ versus ρ_n for each lay-up and material, the parameter α in (16) is determined using free software REGRESSI. In this way data for α dependence on geometrical and elastic parameters is obtained. To calculate the constant C, we plot these α data

versus $\left(\frac{E_s}{E_2}\right)^{1/4}\left(1+\frac{t_{90}E_2}{t_s/2\,E_s}\right)$ for $[90_8,0_n]$s laminate (n=1,2,4,8,16,24), using all data for CF/EP and GF/EP materials. According to (17) the relationship has to be linear. Indeed it was linear and fitting with linear trend line gives for surface cracks $C=0.187$. With this value Eq (16) and (17) can be used as surface crack interaction function.

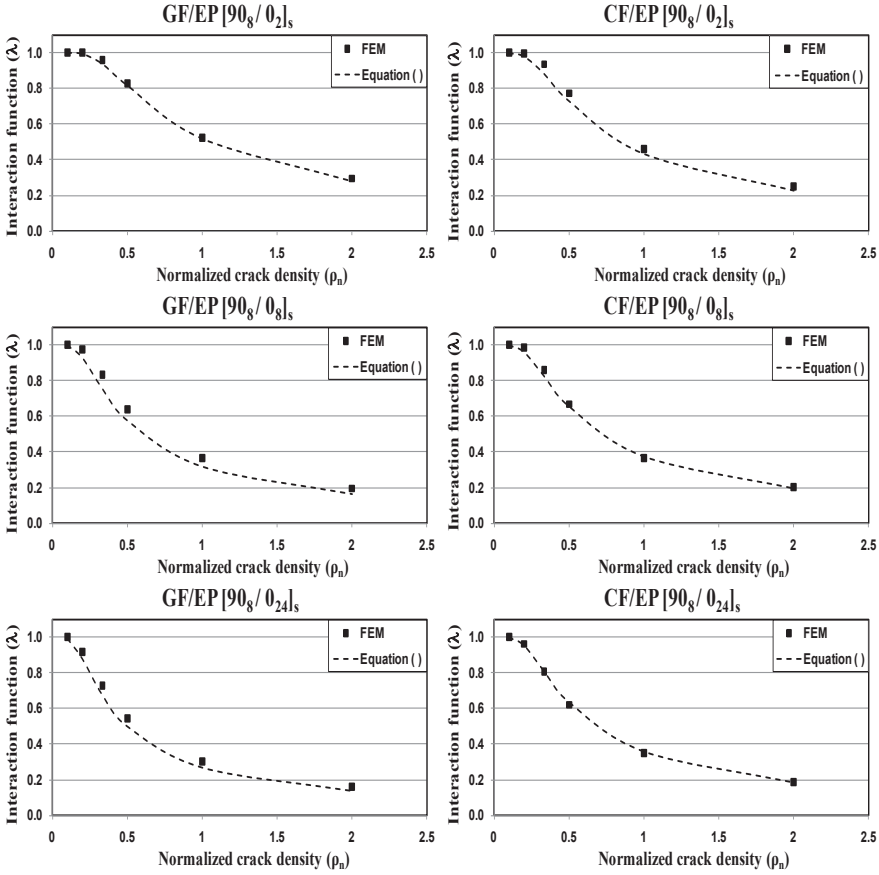

Figure 4. Interaction function according to FEM and equation (16) for surface cracks in **GF/EP** and **CF/EP** cross-ply laminates.

In Fig. 4 the values of the interaction function from direct FE calculations for cracks in GF/EP and CF/EP cross-ply laminate surface layer are compared with values according to the fitting expression (16), (17). A very good agreement was found. Only for GF/EP $[90_8/0]_S$ laminate the fitting function is slightly larger than FEM values (the interaction is underestimated).

3.3 Inside cracks

The interaction function found according to Equation (15) can be seen in Fig. 5. Comparing Fig. 5 and Fig.4 one can notice that interaction of inside cracks starts at almost two times higher normalized crack density and that the value of interaction function at final normalized crack density 2.0 is about two times larger for inside cracks. This is not a real trend but more like an artifact caused by the used definition of the normalized crack density as ply thickness (crack size) and crack spacing ratio. Therefore the same number of cracks per mm in surface and inside layers correspond to two times larger normalized crack density in $[0_n/90_8]$s laminate.
Using (16) for inside cracks (16) the constant α is defined by slightly different expression

$$\alpha = C \times \left(\frac{E_s}{E_2} \right)^{1/4} \left(1 + \frac{t_{90} \diagup 2 \, E_2}{t_s E_s} \right) \tag{18}$$

Determination of C is exactly as for surface cracks leading to $C = 0.497$.
Using this value of C for inside cracks, equations (16) and (18) was used to calculate inside crack interaction function. In Fig. 5 values of the interaction from direct FE calculations for inside cracks in GF/EP and CF/EP cross-ply laminate are compared with values according to expression (16).

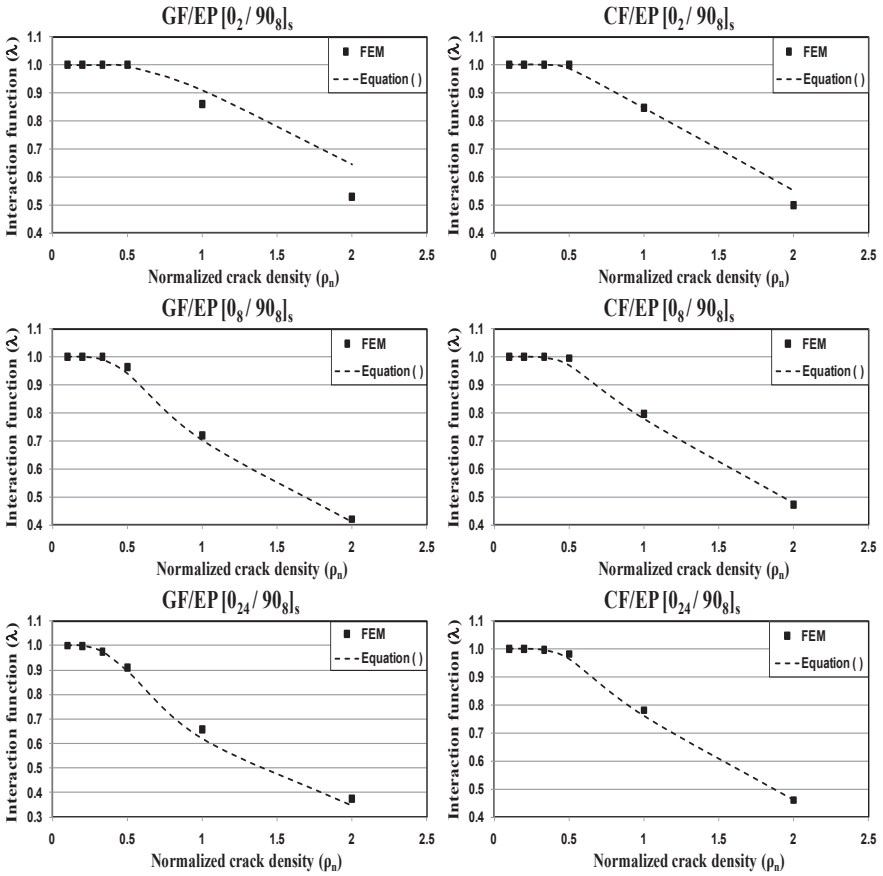

Figure 5 . Interaction function according to FEM and equation (16) for **GF/EP** and **CF/EP** $[0_n/90_8]_S$ cross-ply laminates.

The fitting function values for large t_s/t_{90} are very close to FEM but for small ratios are larger than FEM. The accuracy still is very good except for the rather extreme and non-practical case of GF/EP [0/90$_8$]s and [0$_2$/90$_8$]s laminates where the interaction function (16), (18) underestimates the interaction.

4. Stiffness prediction

In this section equations (7) to (12) are used to calculate elastic constants of damaged laminates. In these expressions $h = t_{90} + t_s/2$ for surface cracks and $h = t_{90} + 2t_S$ for inside cracks. To calculate u_{2an} according to (15) we use the interaction function (16) with (17) and $C = 0.187$ for surface cracks and with (18) and $C = 0.497$ for inside cracks. To evaluate the error on stiffness due to inaccuracy of $\lambda(\rho_n)$ the COD's of non-interactive cracks in (15) was calculated with FEM considering the value as exact. The noninteractive COD's are given in Table 2.

Table 2. FEM calculated values of u_{2an} for non-interactive cracks.

Laminate	**CF/EP**	**GF/EP**
$[0/90_8]$s	0.6044	1.0762
$[0_2/90_8]$s	0.5421	0.8658
$[0_4/90_8]$s	0.5083	0.7402
$[0_8/90_8]$s	0.4927	0.6758
$[0_{16}/90_8]$s	0.4873	0.6487
$[0_{24}/90_8]$s	0.4862	0.6420
$[90_8/0]$s	1.2181	1.9785
$[90_8/0_2]$s	1.1724	1.7188
$[90_8/0_4]$s	1.1852	1.5893
$[90_8/0_8]$s	1.2263	1.5607
$[90_8/0_{16}]$s	1.2640	1.5807
$[90_8/0_{24}]$s	1.2772	1.5925

The elastic properties of damaged cross-ply laminates were calculated also directly from FEM using the same meshes as for interactive COD determination: a) total force and the applied axial strain were used to determine elastic modulus; b) the relative displacement of the coupled edge surfaces was used together with the applied axial strain to find the Poisson's ratio.

4.1 Stiffness of cross-ply laminates with damage in surface layers

Elastic modulus and Poisson's ratio reduction with increasing crack density in $[90_8/0_n]_S$ GF/EP cross-ply laminates is presented in Fig. 6. Ply discount model predictions are also shown as dotted lines. It has to be reminded that normalized crack density larger than 1 is extremely high. The elastic modulus reduction calculated using Equation (7) to (12) with non-interactive COD's in Table 2 and the interaction function (16) is slightly overestimated for small ratio t_s/t_{90}, and slightly underestimated for large ratio. The same observation holds for Poisson's ratio reduction

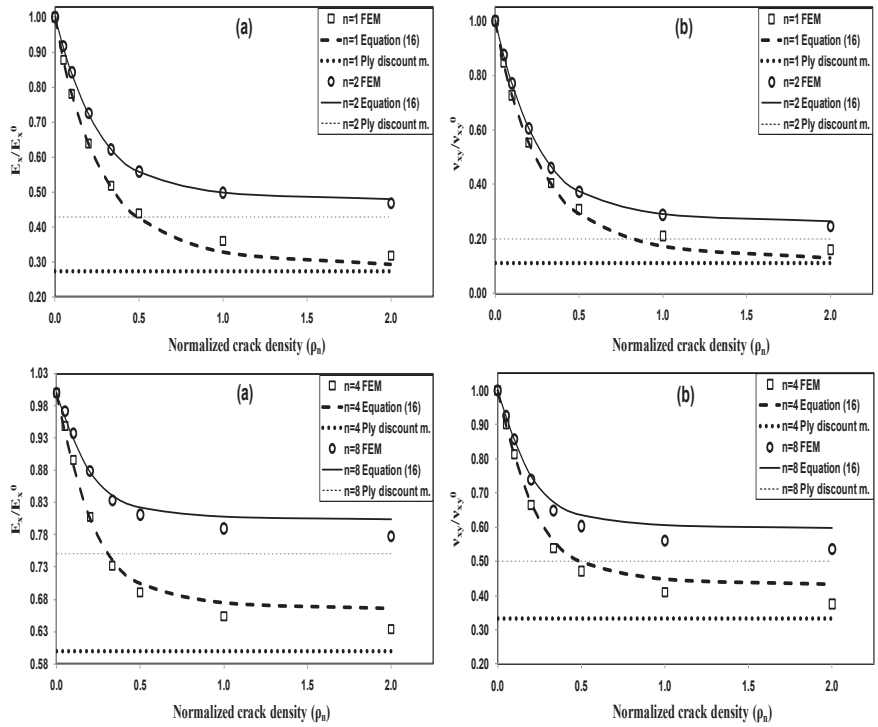

Figure 6 . Elastic modulus (a) Poisson's ratio (b) degradation in $\left[90_8 / 0_n\right]_S$ **GF/EP** laminate due to cracking in 90-layer.

In carbon fiber/epoxy laminates, see Fig. 7, the elastic modulus reduction due to cracks in 90-layer is much smaller, especially for relatively thin 90-layers. The accuracy using the interaction function given in Equation (16) is good also for Poisson's ratio prediction.

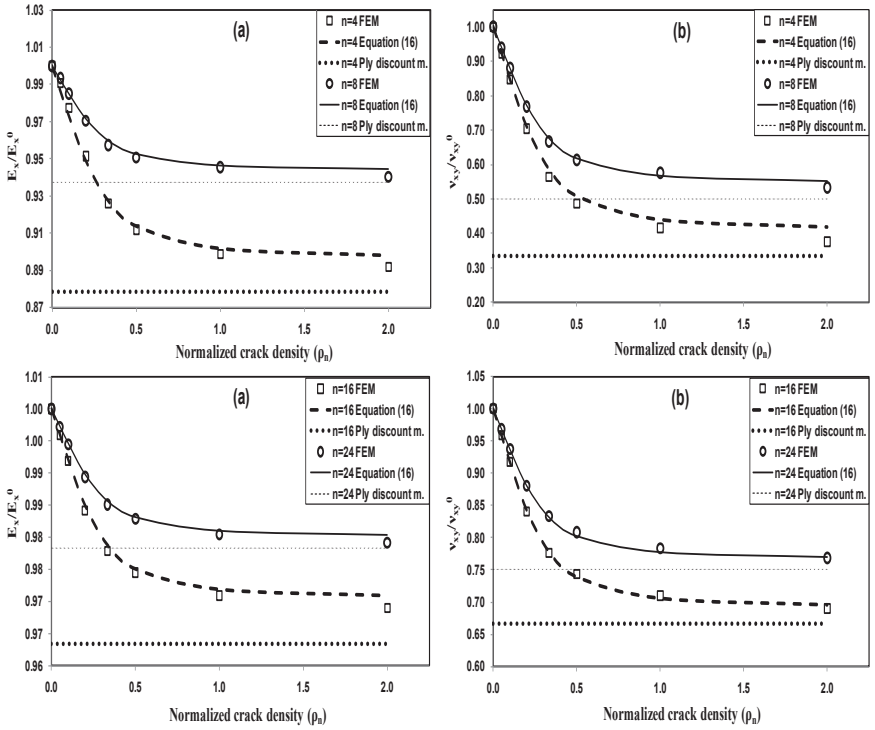

Figure 7. Elastic modulus (a) and Poisson's ratio (b) degradation in $[90_8/0_n]_S$ **CF/EP** laminate due to transverse cracking in 90-layer.

4.2 Stiffness of cross-ply laminates with damage in inside layers

Predicted axial modulus and Poisson's ratio of cross-ply laminates with cracks in inside layers is shown for GF/EP composite in Fig.8 and for CF/EP in Fig. 9. The accuracy of predictions at high crack density is better for CF/EP laminates. The same trends as before with respect to the use of the interaction function (16) have been observed. For large t_s/t_{90} ratio the calculated elastic modulus reduction is slightly underestimated, but the accuracy is good. The same trend is observed for Poisson's ratio reduction.

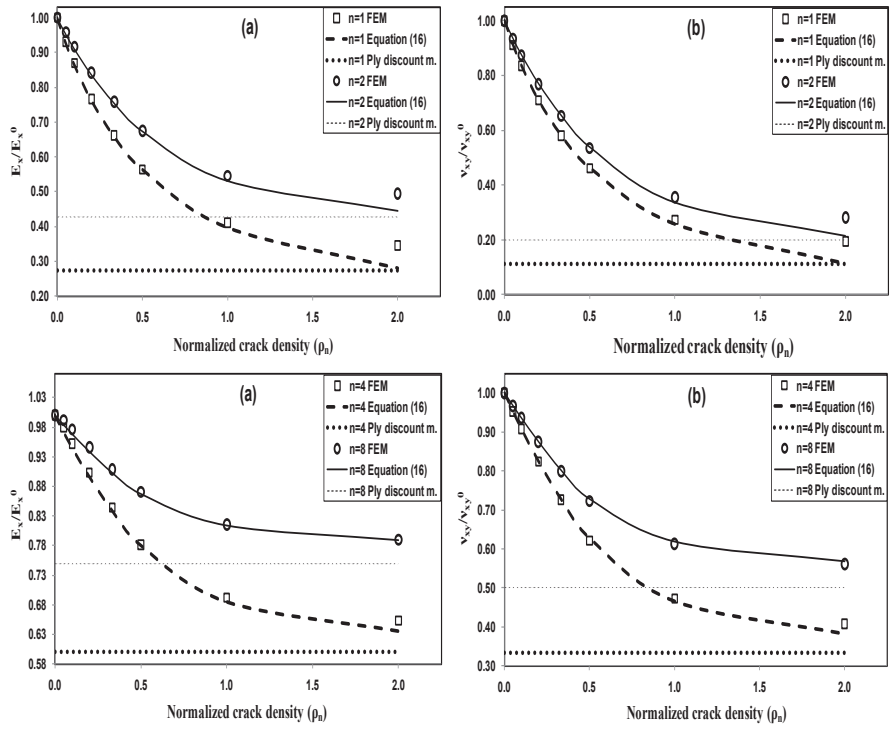

Figure 8. Elastic modulus (a) and Poisson's ratio (b) degradation in $\left[0_n / 90_8\right]_S$ **GF/EP** laminate due to transverse cracking in 90-layer.

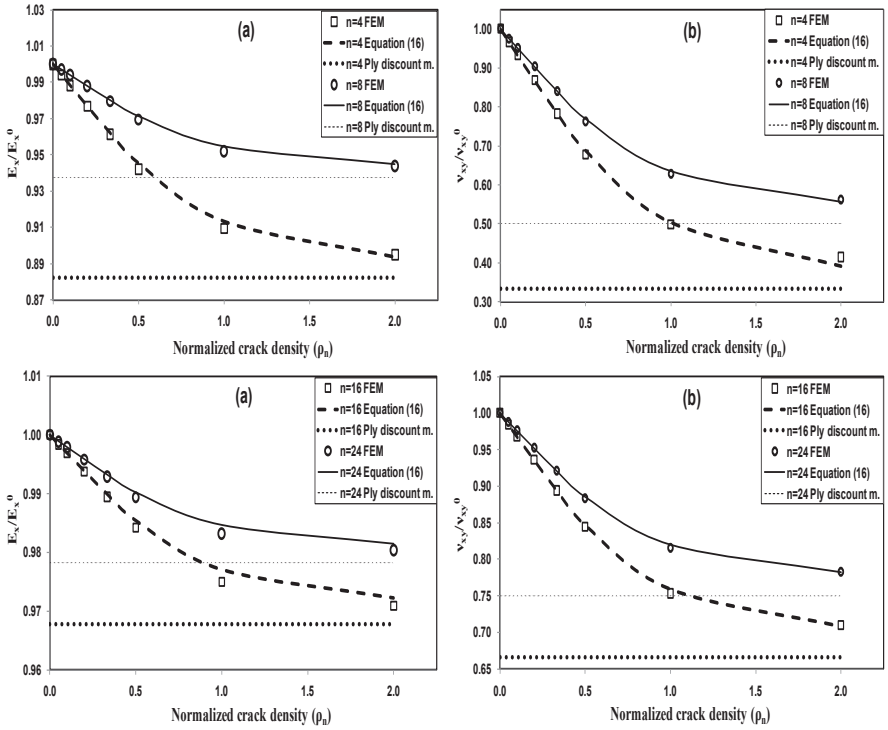

Figure 9. Elastic modulus (a) and Poisson's ratio (b) degradation in $[0_n / 90_8]_S$ **CF/EP** laminate due to transverse cracking in 90-layer.

4.3 Application for quasi-isotropic laminates

4.3.1 Validation of methodology

The objective of the analysis presented in section 3 was to use FEM to analyze crack interaction and to summarize the results in a simple but accurate interaction function. This analytical function together with other expressions can be used to predict stiffness of damaged laminates without any need to involve FEM in this procedure. However, the value of the performed work finding COD interaction function would be rather limited if it can be applied for cross-ply laminates only. In this section we suggest to use the same interaction function $\lambda(\rho_n)$ also for more complex lay-ups, describing the input parameters and comparing the result with numerical values of crack interaction and stiffness for quasi-isotropic laminates obtained directly from FE analysis.

In these calculations the commercial code ANSYS 12.1 was used. The 3-D 8-node structural solid element SOLID185 with three degrees of freedom for each node was used and the number of elements was 86400. Displacement coupling was applied. It means that points on the surface at y=0 has the same displacement in x- and z-directions as the corresponding points on the surface at y=w. In the same way, the points on the surface at x=0 and $x = 2l_{90}$ have the same displacement in y-direction.

The coupling conditions were applied also for normal displacement (Uy=unknown constant) on all nodes at the front edge y=0 and the far-away edge y=w respectively.
CF/EP and GF/EP quasi-isotropic laminates with lay-up [90/0/45/-45]s and [90/45/-45/0]s containing cracks in surface layers as well as [45/-45/0/90]s and [0/45/-45/90]s laminates with cracks in the inside 90-layer were considered.
Applying (16) to "non-cross-ply" laminates further details have to be given with respect to the meaning of E_s and t_s. FEM results show that, when the support layer is much stiffer than the 90-layer (for example 0-layer), the major part of the support is supplied by this layer and it is not really important what the following layers are. In contrary, when the layer closest to the 90-layer is less stiff (for example +45 or -45 layers), this layer alone can not govern crack interaction and the presence of following stiff layer is important (for example, the 0-layer in [0/45/-45/90]s laminate affects interaction of cracks in 90-layer). When this is the case, all neighboring layers have to be included in E_s (for example, considering [0/45/-45]s as sublaminate). Based on these observations the suggestion for E_s and t_s is as follows

$$E_s = \begin{cases} E_1 & \text{if 0 - layer is the closest neighbor} \\ E_x^{subl} & \text{if not} \end{cases} \tag{19}$$

For surface cracks

$$t_s/2 = \begin{cases} t_{0^\circ} & \text{if 0 - layer is the closest} \\ t_{subl}/2 & \text{if not} \end{cases} \tag{20}$$

For inside cracks

$$t_s = \begin{cases} t_{0^\circ} & \text{if 0 - layer is the closest} \\ t_{subl}/2 & \text{if not} \end{cases} \tag{21}$$

4.3.2 Interaction of surface cracks

The fitting function (16) with (17) was adapted for [90/-45/45/0]s laminate as described above. Since the 0° layer is not the closest layer, E_s is calculated using LAP for [0/45/-45]s sublaminate and $t_s/2$ is ½ of its thickness. The obtained values are 62.622 GPa for CF/EP and 25.669 GPa for GF/EP (using data in Table 1). For [90/0/45/-45]s laminate where the 0° layer is the closest layer, $E_s = E_1$ and $t_s/2$ is the thickness of the 0-layer. The values of interaction function are in a good agreement with numerical values calculated directly from FEM, see Fig. 10 for GF/EP laminates.

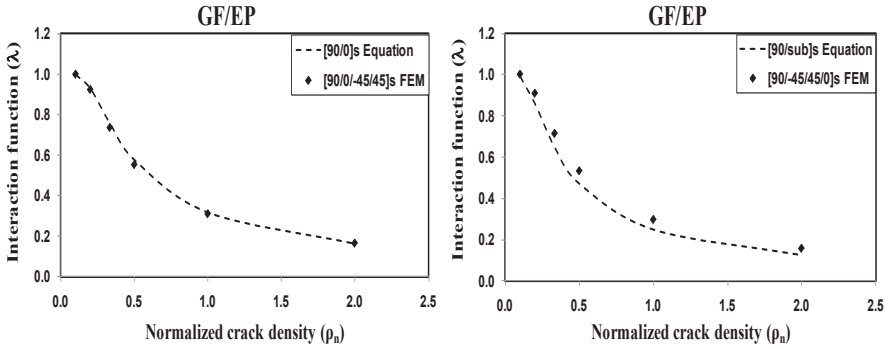

Figure 10. Interaction function according to FEM and equations (16),(17) for GF/EP laminates.

4.3.3 Interaction of inside cracks

The fitting function (16) with (18) was adapted for [0/-45/45/90]s laminate as described above. Since the 0° layer is not the closest layer, E_s is calculated using LAP for [0/45/-45]s sublaminate and t_s is ½ of its thickness. The obtained values are the same as for surface crack case: 62.622 GPa for CF/EP and 25.669 GPa for GF/EP. For [45/-45/0/90]s laminate where the 0° layer is the closest layer, $E_s = E_1$ and t_s is the thickness of the 0-layer. As shown in Fig.11 the interaction function adapted from cross-ply case gives very good approximation of the crack interaction.

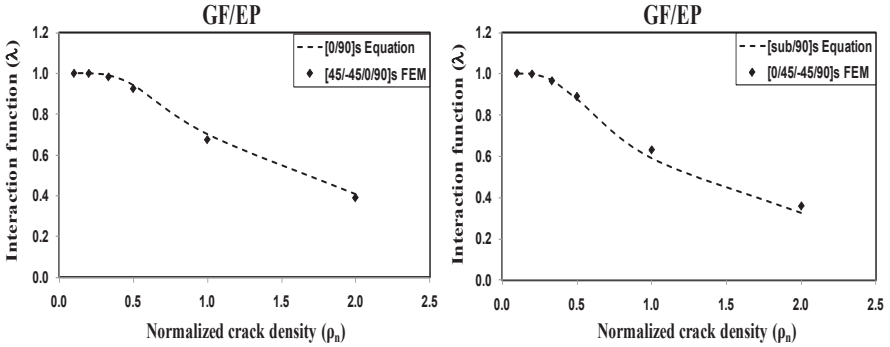

Figure 11. Interaction function according to FEM and equation (16), (18) for GF/EP laminates.

4.3.4 Stiffness of damaged quasi-isotropic laminates

4.3.4.1 Quasi-isotropic laminates with cracks in surface layers

Elastic modulus and Poisson's ratio reduction of quasi-isotropic laminates with cracks in surface layers is shown for GF/EP composite in Fig.12 and for CF/EP in Fig. 13**.** Ply discount model predictions are also shown as dotted lines. The elastic modulus reduction is calculated using Equation (7) to (12) with non-interactive COD's in Table 2 and the interaction function (16) with suggestions (19) and (20). For $[90/0/45/-45]_S$ laminate the accuracy is very good.

For $[90/-45/45/0]_S$ laminate the calculated elastic modulus reduction is slightly underestimated, but the accuracy is good. The same observation holds for Poisson's ratio reduction.

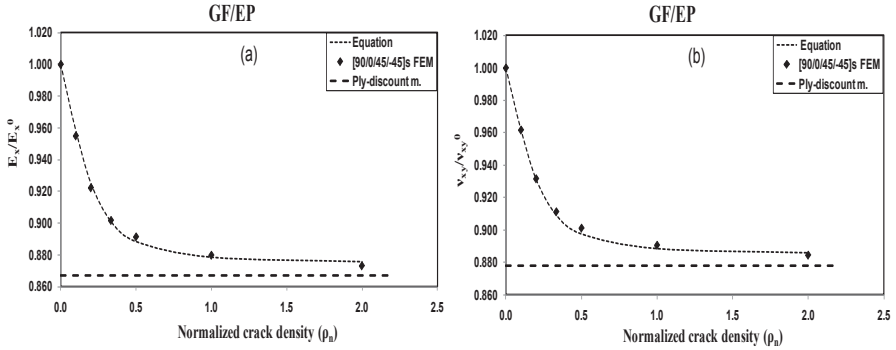

Figure 12. Elastic modulus (a) Poisson's ratio (b) degradation in **GF/EP** quasi-isotropic laminate due to transverse cracking in 90-layer.

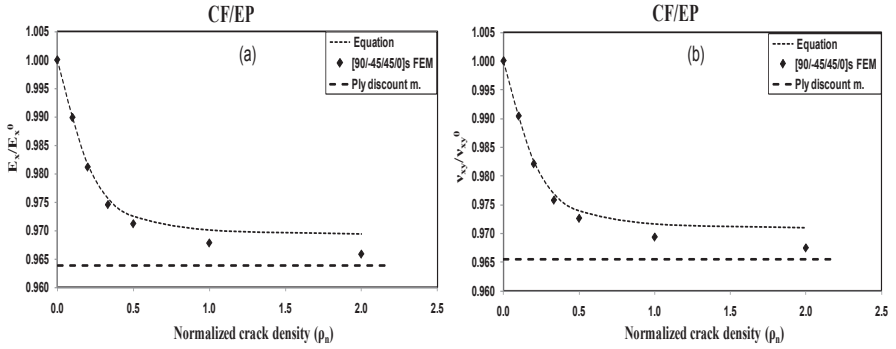

Figure 13. Elastic modulus (a) Poisson's ratio (b) degradation in **CF/EP** quasi-isotropic laminate due to transverse cracking in 90-layer.

4.3.4.2 Quasi-isotropic laminates with cracks in inside layers

Predicted axial modulus and Poisson's ratio of quasi-isotropic laminates with cracks in inside layers is shown for CF/EP composite in Fig.14 and for GF/EP in Fig. 15. The same trends as before with respect to the use of the interaction function (16) with (19) and (21) have been observed.

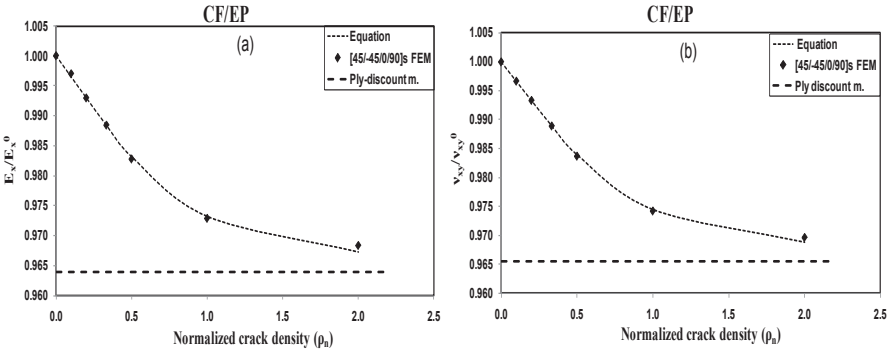

Figure 14. Elastic modulus (a) Poisson's ratio (b) degradation in **CF/EP** quasi-isotropic laminate due to transverse cracking in 90-layer.

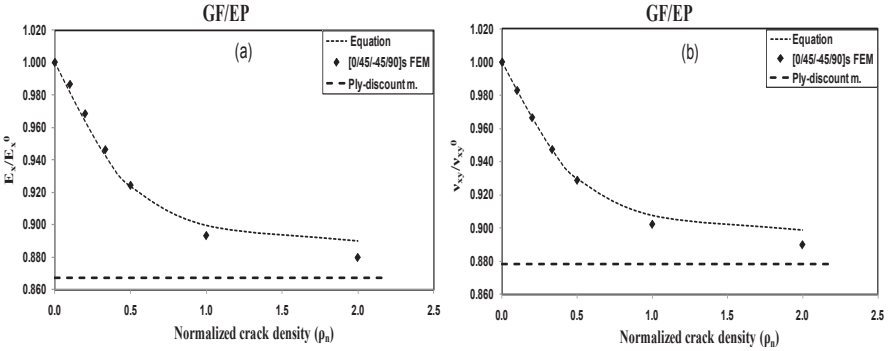

Figure 15. Elastic modulus (a) Poisson's ratio (b) degradation in **GF/EP** quasi-isotropic laminate due to transverse cracking in 90-layer.

5. Conclusions

Expressions for thermo-elastic constants of symmetric and balanced laminates with intralaminar cracks in 90-layers are presented as a special case of the GLOB-LOC model developed in [7,8]. They can be used provided simple and accurate expressions for normalized crack opening (COD) and sliding (CSD) displacements are available. At high crack density where cracks interact they depend on distance between cracks.

The COD of interactive crack are presented as a product of the COD of non-interactive crack and an interaction function which value is equal or smaller than one. The COD of non-interactive cracks is obtained by FEM.

In this paper the tanh() form of the interaction function for COD is introduced and parameters determined using data generated by FEM for large variety of geometrical and material parameters considering cracks in surface as well as inside layers.

Comparison with direct FEM calculations show that the interaction function gives a very good axial modulus and Poisson's ratio prediction for all possible crack densities and cross-ply laminates.

The interaction function derived for cross-ply laminates is adapted for more complex lay-ups and its accuracy is demonstrated for quasi-isotropic laminates.

6. References

1. Smith PA, Wood JR. Poisson's ratio as a damage parameter in the static tensile loading of simple cross-ply laminates. Composites Science and Technology 1990; 38:85-93.
2. Hashin Z. Analysis of cracked laminates: A Variational Approach. Mech. Mater., North-Holland 1985; 4:121-136.
3. Varna J, Berglund LA. Multiple transverse cracking and stiffness reduction in cross-ply laminates. Journal of Composites Technology and Research 1991; 13(2):97-106.
4. Varna J, Berglund LA. Thermo-Elastic properties of composite laminates with transverse cracks. Journal of Composites Technology and Research 1994; 16(1):77-87.
5. Varna J, Krasnikovs A. Transverse cracks in cross-ply laminates. Part 2, Stiffness Degradation, Mechanics of Composite Materials 1998; 34(2):153-170.
6. Krasnikovs A, Varna J. Transverse cracks in cross-ply laminates. Part 1, Stress Analysis, Mechanics of Composite Materials 1997; 33(6):565-582.
7. Lundmark P, Varna J. Constitutive relationships for laminates with ply cracks in in-plane loading. International Journal of Damage Mechanics 2005; 14(3): 235-261.
8. Lundmark P, Varna J. Crack face sliding effect on stiffness of laminates with ply cracks. Composites Science and Technology 2006; 66:1444-1454.
9. Joffe R, Krasnikovs A, Varna J. COD-based simulation of transverse cracking and stiffness reduction in [S/90n]s laminates. Composites Science and Technology 2001; 61:637-656.
10. Farge L, Ayadi Z, Varna J. Optically measured full-field displacements on the edge of a cracked composite laminate. Composites, Part A 2008; 39:1245-1252.
11. Farge L, Varna J, Ayadi Z. Damage characterization of a cross-ply carbon fiber/epoxy laminate by an optical measurement of the displacement field. Composites Science and technology 2010; 70:94-101
12. Varna J, Berglund L.A, Talreja R, Jakovics A. A Study of the crack opening displacement of transverse cracks in cross ply laminates. International Journal of Damage Mechanics 1993; 2:272-289.
13. Varna J, Joffe R, Akshantala NV, Talreja R. Damage in composite laminates with off-axis plies. Composites Science and Technology 1999; 59:2139-2147.
14. Lundmark P, Varna J. Stiffness reduction in laminates at high intralaminar crack density: effect of crack interaction. International Journal of Damage Mechanics 2011; 20:279-297.

Paper II

MS. Loukil, J. Varna and Z. Ayadi

Applicability of solutions for periodic intralaminar crack distributions to non-uniformly damaged laminates

Applicability of solutions for periodic intralaminar crack distributions to non-uniformly damaged laminates

MS. Loukil[1,2], J. Varna[1] and Z. Ayadi[2]

[1]Luleå University of Technology, SE-971 87 Luleå, Sweden
[2]Institut Jean Lamour, EEIGM 6 Rue Bastien Lepage, F-54010 Nancy Cedex, France

Abstract

Stiffness reduction simulation in laminates with intralaminar cracks is usually performed assuming that cracks are equidistant and crack density is the only parameter needed. However, the crack distribution in the damaged layer is very non-uniform, especially in the initial stage of multiple cracking. In this paper the earlier developed model for general symmetric laminates is generalized to account for non-uniform crack distribution. This model, in which the normalized average crack opening (COD) and sliding (CSD) displacements are the main characteristics of the crack, is used to calculate the axial modulus of cross-ply laminates with cracks in internal and surface layers. In parametric analysis the COD and CSD are calculated using FEM, considering the smallest versus the average crack spacing ratio as non-uniformity parameter. It is shown that assuming uniform distribution we obtained lower bond to elastic modulus.
A "double-periodic" approach presented to calculate the COD of a crack in a non-uniform case as the average of two solutions for periodic crack systems is very accurate for cracks in internal layers, whereas for high crack density in surface layers it underestimates the modulus reduction.

Keywords: Laminates, transverse cracking, crack opening displacement, damage mechanics

1. Introduction

Intralaminar cracking in laminates is the most typical mode of damage in laminates. Initiation, evolution and effect of these cracks on laminate stiffness has been discussed in many papers, see for example review papers [1,2]. Intralaminar cracks (called also matrix cracks, transverse cracks, inclined cracks etc) are orthogonal to the laminate midplane, they run parallel to fibers in the layer, usually cover the whole thickness and width of the layer in the specimen.
In the presence of cracks the average stress in the damaged layer is lower than in the same layer in undamaged laminate. The average stress between two cracks depends on the distance between them (normalized spacing). Usually the extent of cracking (number of cracks and distance between them) is characterized in an average sense by average crack spacing and crack density (cracks/mm). Most of the existing stiffness models, for example, [3-6] use this assumption. It is convenient for use and is expected to give sufficient accuracy.
However, the crack distribution in the layer may be highly non-uniform as schematically shown in Fig.1. This is more pronounced in the beginning of the

cracking process when the average crack density is relatively low. At high crack density close to saturation the cracks are more equidistant. The reason is the random distribution of transverse failure properties along the transverse direction of the layer. At low crack density the stress distribution between two existing cracks has a large plateau region and any position there is a site of possible failure. At high crack density there is a distinct maximum in the stress distribution and a new crack most likely will be created in the middle between existing cracks.

The discussion in this paper is focused on the possible inaccuracy introduced in laminate stiffness prediction by using assumption of uniform spacing between cracks in a layer. Numerical results presented here are for two cases: a) when the system of cracks is "non-interactive" in average (low crack density) but some cracks are close to each other and interact; b) the crack density is high and cracks interact "in average".

There are only a few studies where the effect of non-uniformity is addressed, see for example [7-9].

In [7] hypothesis was introduced that for a non-uniformly cracked laminate, the deformation field in the "element" between two neighbouring ply cracks separated by a distance l_k is identical to that in a uniformly cracked laminate where the crack spacing is l_k. Then, for example, the axial strain of the whole Representative Volume Element (RVE) can be calculated by the "rule of mixtures" of average strains of "elements" leading to simple expressions for RVE axial modulus. In [7] this approach was compared with FEM calculations for the whole RVE demonstrating very high accuracy. This assumption is reexamined in our paper analyzing crack opening displacements (COD) of both crack faces and showing that the average stress in the "element" on one side, where the distance to the next crack is smaller, is overestimated by this assumption whereas on the other side it is underestimated. In [8,9] the non-uniform damage evolution is analyzed in a probabilistic way not discussing the effect of non-uniform distribution on stiffness.

The reduced average transverse stress and in-plane shear stress in the damaged layer are responsible for laminate stiffness changes. The average stress change between two cracks is proportional to the average crack face opening (COD) and sliding displacements (CSD) normalized with far field stress [10,11]. The far-field stress at the given load is calculated using laminate theory (CLT). Therefore the damaged laminate stiffness can be expressed also in terms of density of cracks and two parameters: average COD a CSD as done in the GLOB-LOC model [3,12]. These two rather robust parameters depend on the normalized distance to neighboring cracks. Therefore for non-uniform crack distribution they are different for each individual crack. The values of COD and CSD in the commonly assumed uniform crack distribution case correspond to average spacing between cracks and are different than the calculated average over COD's and CSD's of all individual cracks.

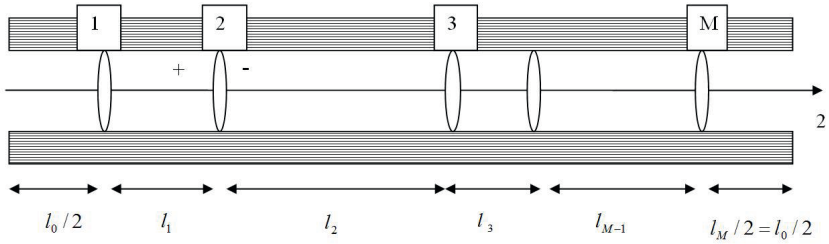

Figure 1. Non-uniform distribution of M cracks in damaged layer shown in its local coordinate system.

In this paper we first will generalize the previously developed expressions for stiffness reduction in symmetric laminates (GLOB-LOC model [3]) for non-uniform spacing case. Then parametric analysis of the effect of geometrical non-uniformity in terms of COD and the laminate axial modulus will be performed for particular cases of $[90m/0n]_s$ and $[0n/90m]_s$ cross-ply laminates with cracks in 90-layers. Cases when sliding displacement CSD affects the stiffness are included in the stiffness expressions in Section 2.2 but they are not numerically analyzed in this paper. Extreme layer thickness ratios and different material anisotropy levels comparing carbon fiber (CF) and glass fiber (GF) composites will be discussed. To simplify stiffness calculations for an arbitrary non-uniform distribution, routine allowing determination of COD's for any crack as a sum of solutions for two periodic systems of cracks, will be formulated and validated (one solution is for periodic system with spacing as on the "+" side of the crack and another one for a periodic system with spacing as on the "-" side of the crack, see Fig.1).

2. Material model of damaged symmetric laminates with intralaminar cracks

2.1 Distances between cracks

We consider representative volume element (RVE) of a layer with M cracks as shown in Fig. 1. The RVE length is L, the average distance between cracks (spacing) is l_{av}, the crack density is ρ

$$L = \sum_{m=0}^{M-1} l_m \qquad l_{av} = \frac{L}{M} \qquad \rho = \frac{1}{l_{av}} \tag{1}$$

Stress state between two cracks in a layer ,see Fig. 1 where the cracked layer is shown in its local coordinates, and also the opening and sliding displacements of crack faces depend on the normalized distance between cracks. Normalization is with respect to the layer thickness t

$$l_{mn} = \frac{l_m}{t} \qquad \text{m=0,1, ... } M\text{,} \qquad l_{avn} = \frac{l_{av}}{t} \tag{2}$$

Index k, used in following sections to identify k-th layer in the laminate, is omitted here for simplicity. Crack with index m has two neighbors located at different distances l_{m-1} and l_m from this crack. Using notation u_{2an}, u_{1an} for the average normalized COD and CSD respectively, we can write for the m-th crack

$$u_{2an}^{m} = u_{2an}^{m}\left(l_{(m-1)n}, l_{mn}\right) \qquad u_{1an}^{m} = u_{1an}^{m}\left(l_{(m-1)n}, l_{mn}\right) \tag{3}$$

If $l_m > l_{m-1}$ the displacements on the "-" side will be larger than on the "+" side.
If the part of the layer shown in Fig. 1 is smaller than the RVE, the methodology of this paper can still be applied but the unknown displacements of the outmost to the left (m=1) and the outmost to the right (m=M) positioned cracks are affecting the calculated homogenized stiffness. The uncertainty is because COD and CSD of these two cracks depend on the distance to the next cracks not shown in Fig. 1 or, in other words, on boundary conditions. The uncertainty is avoided if the shown distribution is considered as "repeating super-element" with M cracks in it. In this case symmetry conditions can be applied on $x = 0$ and $x = 2L$. To model this periodic structure we have to assume $l_0 = l_M$.

2.2 Stiffness Model

The upper part of symmetric *N*- layer laminate with intralaminar cracks is shown in Fig. 2. The *k*-th layer of the laminate has thickness t_k , fiber orientation angle with respect to the global x-axis θ_k and stiffness matrix $[Q]$ in the material symmetry axes, calculated from elastic constants $E_1, E_2, G_{12}, \nu_{12}$. The total thickness of the laminate, $h = \sum_{k=1}^{N} t_k$. The crack density in a layer ρ_k is calculated using (1) where the average distance between cracks l_{av}^{k} is measured transverse to the fiber direction in the k-th layer. Dimensionless crack density ρ_{kn} in the layer is introduced as

$$\rho_{kn} = t_k \rho_k . \tag{4}$$

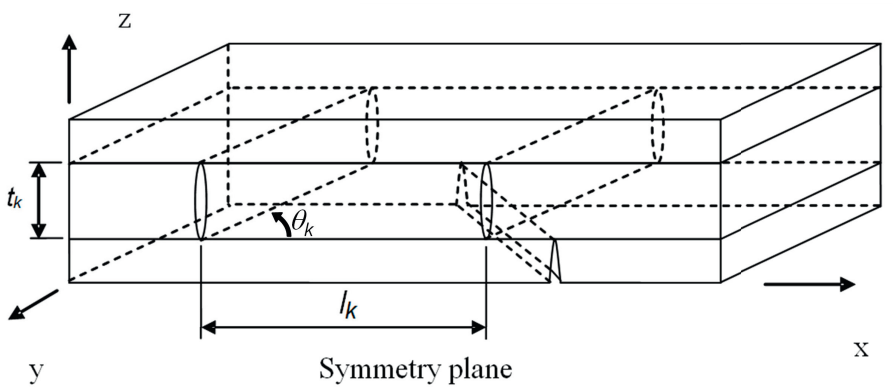

Figure 2. RVE of the damaged laminate with intralaminar cracks in layers.

It is assumed that in the damaged state laminate is still symmetric et est. the crack density in corresponding symmetrically placed layers is the same.
The stiffness matrix of the damaged laminate, $[Q]^{LAM}$ and the stiffness of the undamaged laminate, $[Q]_0^{LAM}$ are defined by the stress-strain relationships

$$\begin{Bmatrix}\sigma_{x0}\\ \sigma_{y0}\\ \sigma_{xy0}\end{Bmatrix}^{LAM} = [Q]^{LAM}\begin{Bmatrix}\varepsilon_x\\ \varepsilon_y\\ \gamma_{xy}\end{Bmatrix}^{LAM}, \qquad \begin{Bmatrix}\sigma_{x0}\\ \sigma_{y0}\\ \sigma_{xy0}\end{Bmatrix}^{LAM} = [Q]_0^{LAM}\begin{Bmatrix}\varepsilon_{x0}\\ \varepsilon_{y0}\\ \gamma_{xy0}\end{Bmatrix}^{LAM} \tag{5}$$

The compliance matrix of the undamaged laminate is $[S]_0^{LAM} = \left([Q]_0^{LAM}\right)^{-1}$.
The expressions below for stiffness matrix of the damaged laminate with non-uniform crack distribution are derived in Appendix 1 and 2 following the procedure described in [3]

$$[Q]^{LAM} = \left([I] + \sum_{k=1}^{N} \rho_{kn} \frac{t_k}{h}[K]_k [S]_0^{LAM}\right)^{-1} [Q]_0^{LAM} \tag{6}$$

$$[S]^{LAM} = [S]_0^{LAM}\left([I] + \sum_{k=1}^{N} \rho_{kn} \frac{t_k}{h}[K]_k [S]_0^{LAM}\right) \tag{7}$$

In (6) and (7) the matrix-function $[K]_k$ for a layer with index k is defined as

$$[K]_k = \frac{1}{E_2}[\overline{Q}]_k [T]_k^T [U]_k [T]_K [\overline{Q}]_k \tag{8}$$

The involved matrices $[T]_k$ and $[\overline{Q}]_k$ are defined according to CLT, upper index T denotes transposed matrix and bar over stiffness matrix indicates that it is written in global coordinates. The influence of cracks in k-th layer is represented by matrix $[U]_k$.

$$[U]_k = 2\begin{bmatrix} 0 & 0 & 0 \\ 0 & u_{2an}^k & 0 \\ 0 & 0 & \dfrac{E_2}{G_{12}} u_{1an}^k \end{bmatrix} \tag{9}$$

Elements of this matrix u_{2an}, u_{1an} are defined in Appendix 2. They are calculated, see (A2.8), using normalized and averaged crack face opening (COD) and sliding displacements (CSD) of all cracks as affected by varying spacing between them.

$$u_{1an} = \frac{1}{M}\sum_{m=1}^{M} u_{1an}^m \left(l_{(m-1)n}, l_{mn}\right) \qquad u_{2an} = \frac{1}{M}\sum_{m=1}^{M} u_{2an}^m \left(l_{(m-1)n}, l_{mn}\right) \tag{10}$$

Index for layer k is omitted in (10). Certainly, since u_{2an}, u_{1an} in k-th layer depend also on neighboring layer properties they are different in different layers. The approach used in appendices is exactly the same as in [3]. The main difference is in Appendix 2 where the two crack faces of any crack may have different displacements due to nonuniformity. Appendix 1 which contains the same information as given in [3] is included to insure consistency of explanation.

2.3 Elastic modulus of balanced laminates with cracks in 90-layer

In case of balanced laminates with damage in 90-layers only, expressions for $[K]_k$ and for $[S]^{LAM}$ have been obtained calculating the matrix products in (7) and (8) analytically. For example, the obtained expression for laminate normalized axial modulus is

$$\frac{E_x}{E_x^0} = \frac{1}{1 + 2\rho_{90n}\frac{t_{90}}{h}u_{2an}^{90}c} \qquad c = \frac{E_2}{E_x^0}\left(\frac{1-\nu_{12}\nu_{xy}^0}{1-\nu_{12}\nu_{21}}\right)^2 \tag{11}$$

Index 90 is used to indicate 90-layer. The quantities with lower index x,y are laminate constants, quantities with additional upper index 0 are undamaged laminate constants and (10) has to be used to calculate u_{2an}^{90}. In the case of uniform crack distribution all COD's in (10) are equal and (11) is just a different form of (31) in [3] leading to numerically identical results.
In the following parametric analysis we consider COD related properties only and validation is based on axial modulus. Therefore damaged laminate shear modulus expression which is related to CSD only is not presented here.

3. Results and discussion

3.1 Formulation of calculation examples

The effect of the non-uniform crack distribution on u_{2an}^{90} was analyzed using FEM for damaged $[0_n/90_8]_S$ and $[90_8/0_n]_S$ laminates (n=1,8) at fixed dimensionless crack density ρ_{90n}, see Fig 3 where the repeating "super-element" with two cracks is shown. To cover large variation in elastic constants both CF/EP and GF/EP composites with constants given in Table 1 were analyzed. All results will be presented in terms of dimensionless crack spacing and crack density. Results depend on layer thickness ratio, not on absolute value of ply thickness.
For laminates with cracks in surface layers staggered crack system where the crack in the bottom layer is located in the middle between cracks in the top layer could be analysed instead of symmetric damage state shown in Fig.3. This case analyzed in [13] by J. Nairn is relevant when the failure analysis is deterministic and the small variation in stress state points on the locus of the next failure (always exactly in the middle between two existing cracks). However, the strength (or the fracture toughness) is not one single value but follows certain statistical distribution. The variation of failure properties along the 90-layer transverse direction is often much larger than the stress perturbation in the bottom layer of the laminate due to crack in the top layer. Therefore the assumption of staggered cracks is as far from reality as the assumed symmetry of the damage with respect to the midplane used in this paper. Starting with symmetric damage state in the stiffness analysis we are trying to create a simple reference case. The interaction effects between systems of cracks in different layers have to be analysed separately. Otherwise the number of parameters changing is too large to draw conclusions.
In all FE calculations the commercial code ABAQUS was used. In order to model the left half of the "super-element" (see Fig. 3), a 3-D model was created. In order to

mesh volumes, 3D continuum elements (C3D8) 8-node linear brick were used. The same fine mesh with total number of elements 86400 was used in each FE model. The (x, z) plane consisted of 21600 elements, with refined mesh near the crack surfaces. In the ply with cracks the number of elements in the thickness direction was 120. The number of elements in y-direction was 4 which as described below is more than sufficient for the used edge conditions. The problem was solved by applying to the right boundary $x = 0$ of the model a given constant displacement in x-direction corresponding to 1% average strain and keeping at the left boundary $u_x = 0$. The top surface was free of tractions. On the front edge (y=0) and the edge (y=w) coupling conditions were applied for normal displacements (u_y= unknown constant). In this way edge effects are avoided and the solution does not depend on y-coordinate. It corresponds to solution for an infinite structure in the width direction. Obviously these conditions lead to generalized plane strain case and corresponding finite elements could be used obtaining the same results. The displacements in direction x for the nodes at the crack surface were used to calculate the average value of the crack face displacement COD.

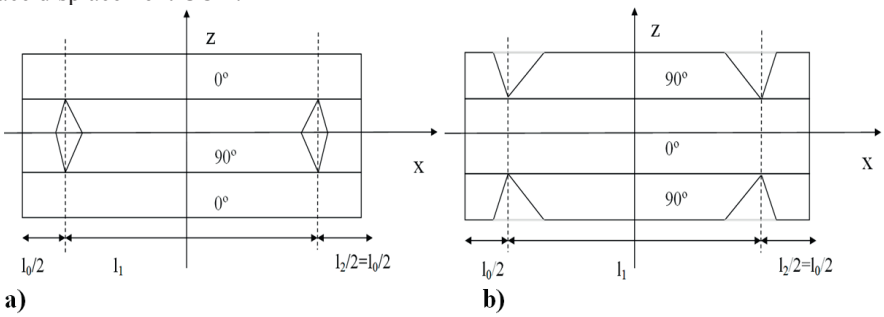

Figure 3. "super-element" models for COD studies with non-uniformly cracked 90-layers: a) cracks in inside layer; b) cracks in surface layer

All plies are considered to be orthotropic considering in calculations a particular case $E_2 = E_3$, $G_{12} = G_{13}$ and $\nu_{12} = \nu_{13}$.

Table 1. Material properties used in simulations.

Material	E_1(GPa)	E_2(GPa)	ν_{12}	ν_{23}	G_{12} (GPa)	G_{23} (GPa)
GF/EP	45	15	0.3	0.4	5	6
CF/EP	150	10	0.3	0.4	5	6

Analyzing the CODs the average crack density was kept constant (two cracks over fixed distance $L = l_0 + l_1$ with average normalized spacing calculated according to (1)

$$l_{avn} = \frac{1}{2}(l_{0n} + l_{1n})$$

In calculations two values of the average normalized spacing were used: a) $l_{avn} = 10$ corresponding to $\rho_{90n} = 0.1$ where the interaction between uniformly spaced cracks

would be negligible; b) $l_{avn} = 2$ corresponding to interactive crack region with crack density $\rho_{90n} = 0.5$.

Studying the effect of non-uniform distribution the normalized spacing l_{0n}, see Fig. 3, was used as a parameter which was lower or equal to the average spacing. In case a) $l_{0n} \in [0.5;10]$ and in case b) $l_{0n} \in [0.5;2]$. It is worth to remind here that at very high crack density (in the so called crack saturation region) the normalized average spacing may be close to 1 (the distance between cracks is equal to the crack size (layer thickness)). Straight intralaminar cracks are almost never observed closer to each other than half of the cracked layer thickness. To characterize the non-uniformity parameter K is introduced as the ratio

$$K = \frac{l_0}{l_{av}} \tag{12}$$

This parameter has value 1 for uniform crack distribution.

3.2 COD parametric analysis at low crack density

In this section results for average normalized spacing $l_{avn} = 10$ ($\rho_{90n} = 0.1$) are presented.

3.2.1 Internal cracks

For internal cracks the profiles of normalized crack face displacements ($u_{2n}^{-}(z_n)$, $u_{2n}^{+}(z_n)$ defined in Appendix 2) along the thickness coordinate $z_n = z\frac{2}{t_{90}} + 1$ are shown in Fig. 4 and Fig. 5. The "+" face of the crack has smaller displacements than the "-" face and the difference is larger when the l_{0n} is smaller than 1 (the neighboring crack to the left is very close). The neighbor to the "-" face is at larger distance than the average spacing and therefore the displacement profile is almost unaffected. For the same geometry the COD's in CF composites are always significantly smaller.

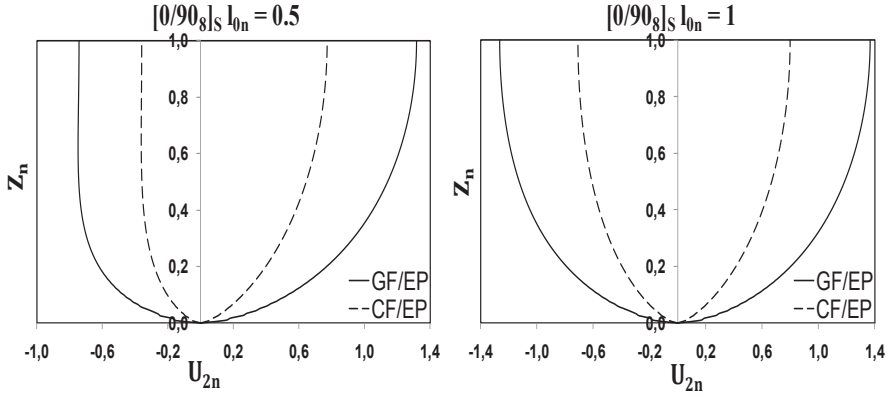

Figure 4. COD profiles of cracks in $[0/90_8]$s laminate with normalized crack density $\rho_{90n} = 0.1$

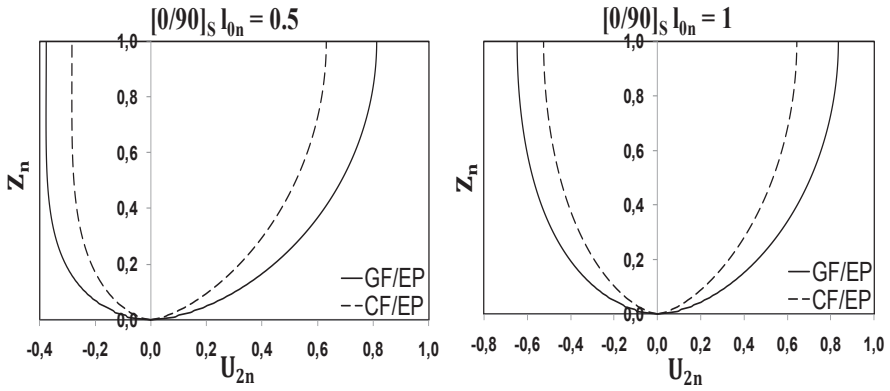

Figure 5. COD profiles of cracks in [0/90]s laminate with normalized crack density $\rho_{90n} = 0.1$

The displacements of both crack faces are significantly smaller when the relative thickness of the neighboring layer is higher, Fig 5. This effect is more pronounced for GF composite where the 0-layer versus 90-layer modulus ratio is not very large.

Using crack face displacements the average normalized COD's u_{2an}^{90} are calculated by numerical integration using expressions in Appendix 2. The obtained dependence on the non-uniformity parameter K is shown in Fig. 6. The average normalized COD is larger if the spacing is uniform. However, the effect is negligible for $K > 0.2$ ($l_0 > 2t_{90}$).

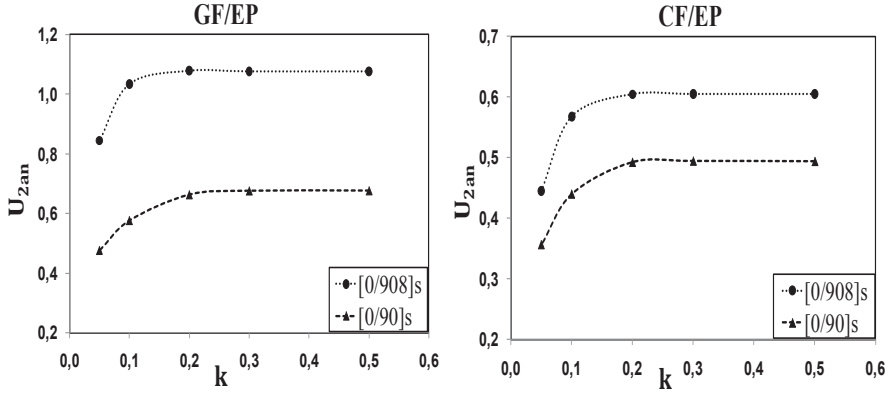

Figure 6. Effect of non-uniform spacing on COD of internal cracks in cross-ply laminates with crack density $\rho_{90n} = 0.1$.

3.2.2 Surface cracks

For surface cracks in [90_8/0]s and [90/0]s laminates the profiles of normalized crack face displacements, $u_{2n}^{-}(z_n)$, $u_{2n}^{+}(z_n)$ along the thickness coordinate $z_n = \dfrac{z - t_0/2}{t_{90}}$ (t_0 is 0-layer thickness) are shown in Fig. 7 and Fig. 8. The trends are the same as for internal cracks but the face displacements are larger and the shape of the profile, especially on the non-interactive side, is different not becoming vertical at outer surface, $z_n = 1$. Since the outer surface is not a symmetry surface this result was expected.

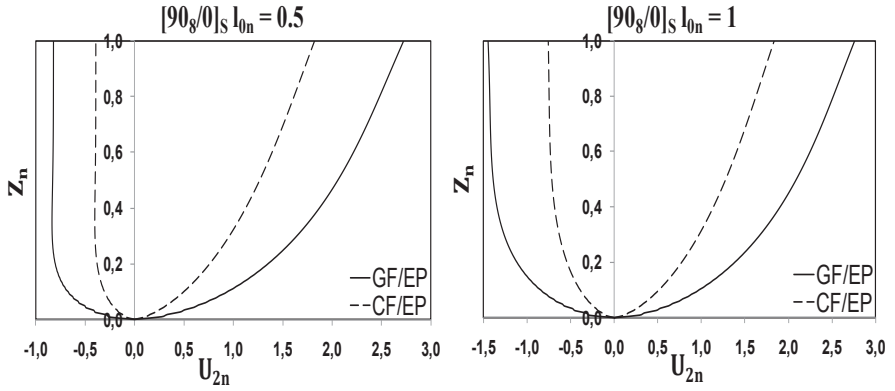

Figure 7. COD profiles of surface cracks in [90_8/0]s laminate with normalized crack density $\rho_{90n} = 0.1$

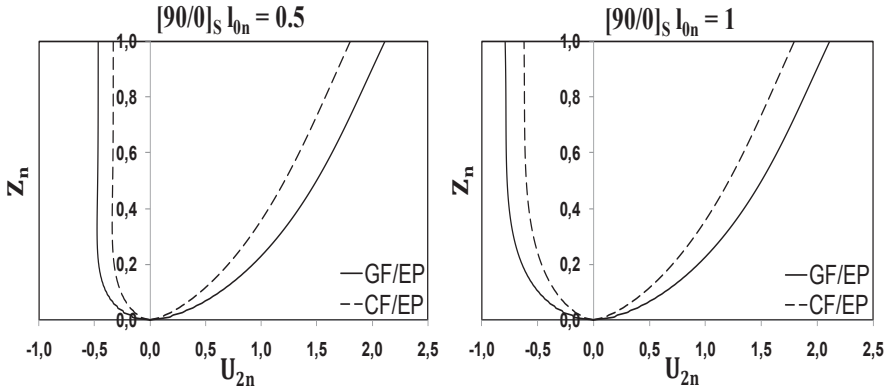

Figure 8. COD profiles of surface cracks in [90/0]s laminate with normalized crack density $\rho_{90n} = 0.1$

The average normalized COD's u_{2an}^{90} are calculated as described in Section 3.2.1. The obtained dependence on the non-uniformity parameter K is shown in Fig. 9. The average normalized COD is smaller if the spacing is non-uniform. According to (11) it will lead to smaller axial modulus reduction. For [90_8/0]s laminate this effect

becomes negligible for $K > 0.3$ ($l_0 > 3t_{90}$) whereas for [90/0]s laminate the transition values are slightly larger ($K > 0.5$, $l_0 > 5t_{90}$).

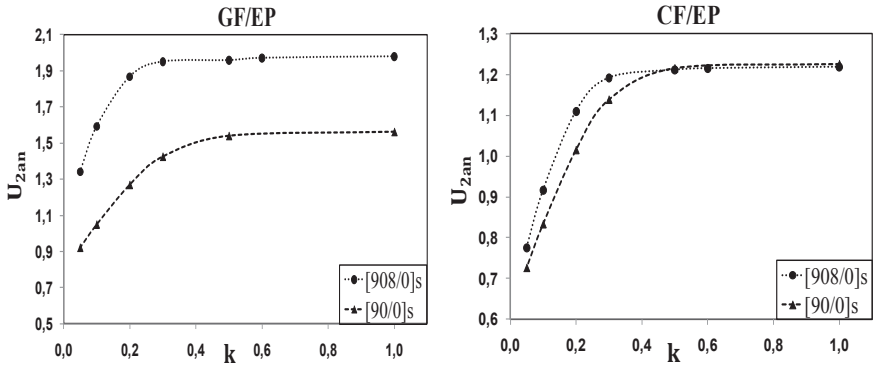

Figure 9. Effect of non-uniform spacing on COD of internal cracks in cross-ply laminates with crack density $\rho_{90n} = 0.1$.

3.3 Approximate COD determination from periodic solutions

The average normalized COD, u_{2an} of a crack in a layer with non-uniform crack distribution can be found considering separately the average normalized COD of the "-" face of the crack and "+" of the crack in Fig. 1.

$$u_{2an} = \frac{1}{2}\left(u^{+}_{2an} + u^{-}_{2an}\right) \tag{13}$$

In this section the following hypothesis will be validated:
" The COD of "-" face depends on the distance to the closest left neighboring crack only and can be calculated considering the region between these two cracks as a periodic element. The COD of the "+" face is obtained in a similar manner, considering the region on the right as periodic element"
This "double-periodic" approach with considering two periodic solutions states that

$$u_{2an} \approx u^{p}_{2an}, \qquad u^{p}_{2an} = \frac{1}{2}\left(u^{p-}_{2an} + u^{p+}_{2an}\right) \tag{14}$$

The two values u^{p+}_{2an}, u^{p-}_{2an} are solutions of the two periodic models.
This hypothesis is equivalent to saying that in Fig. 3 symmetry conditions on the plane $x = \pm l_1/2$ can be applied. This would mean that even in the deformed state the line $x = \pm l_1/2$ in the 0-layer remains straight. Unfortunately there is no symmetry in Fig. 3 and this line will be deformed. The question is how much this additional constraint affects results. Hypothesis that it can be neglected was used by Joffe et al in [11] calculating the work to close the crack for fracture mechanics based damage growth analysis.
If the "double-periodic" approach is accurate enough, the u_{2an} for any crack location with respect to other cracks could be calculated from a master curve for uniform crack distribution. This curve, which is expression of u_{2an} as a function of crack spacing in

layer with uniformly distributed cracks, would be used twice to read the u_{2an}^{p+} , u_{2an}^{p-} values of the right and the left face of the crack.

In order to check the accuracy and validity of the "double-periodic" assumption, the u_{2an} for each value of non-uniformity parameter was calculated in two different ways: a) directly applying FEM to the non-uniform geometry; b) applying FEM two times and using (14), first, for periodic distribution with spacing as on the left from the crack and, second, for periodic distribution with spacing as on the right of the crack.

From Fig. 10 were displacement profiles according to a) and b) are presented we conclude that the trends in the double-periodic approach are described correctly but the values of face displacements are not accurate. On the left face where the interaction is strongest the u_{2n}^{p+} is too small but on the right face, where the next crack is further away, u_{2n}^{p-} is too large. It seems that this result makes the used hypothesis questionable.

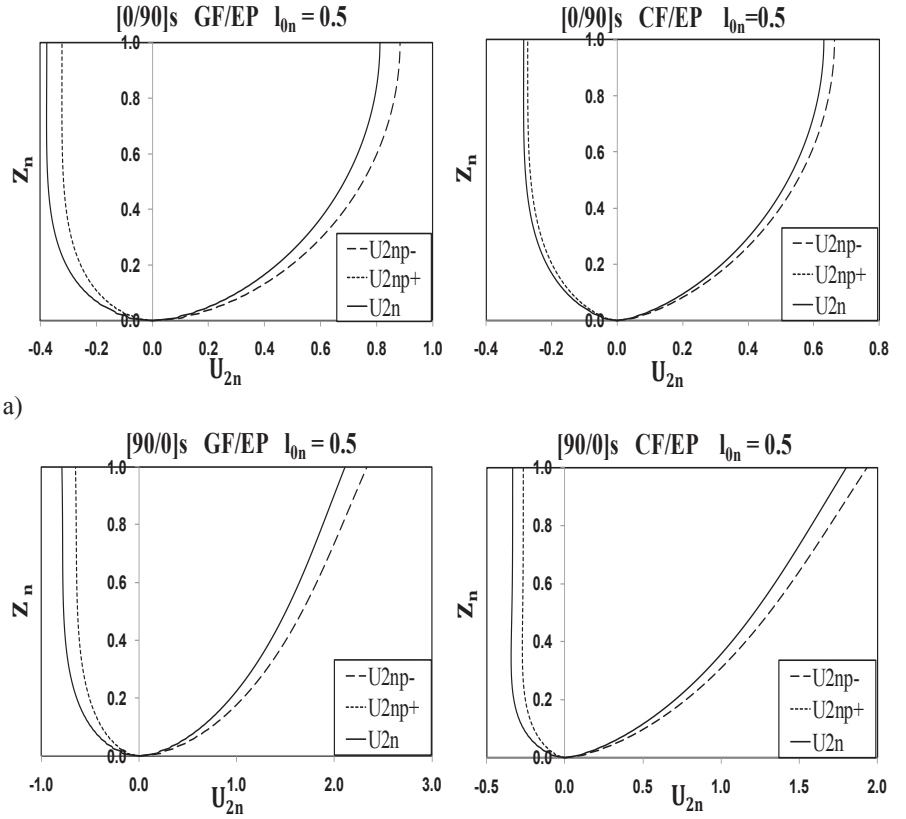

Figure 10. Calculated COD profiles: **a)** of internal cracks in [0/90]s laminate **b)** of surface cracks in [90/0]s laminate

However, for stiffness predictions the average of the COD of both faces, u_{2an}^{p} given by (14) is requested and not value for each face separatelly. The values of u_{2an} and

u_{2an}^{p} can be compared using results presented in Table 2-3 for all lay-ups, materials and non-uniformity parameter values. Amazingly good agreement between values exists for all cases which validates the use of the "double-periodic" hypothesis.

Table 2. Average normalized COD of internal cracks from FEM and from "double-periodic" approach

	[0/90$_8$]s				**[0/90]s**			
	GF/EP		**CF/EP**		**GF/EP**		**CF/EP**	
K	u_{2an}	u_{2an}^{p}	u_{2an}	u_{2an}^{p}	u_{2an}	u_{2an}^{p}	u_{2an}	u_{2an}^{p}
0.50	1.0762	1.0760	0.6045	0.6045	0.6775	0.6760	0.4940	0.4930
0.30	1.0762	1.0760	0.6045	0.6045	0.6770	0.6760	0.4945	0.4935
0.20	1.0784	1.0780	0.6043	0.6090	0.6640	0.6635	0.4925	0.4915
0.10	1.0343	1.0365	0.5676	0.5710	0.5770	0.5810	0.4400	0.4430
0.05	0.8447	0.8670	0.4451	0.4630	0.4760	0.4800	0.3565	0.3625

Table 3. Average normalized COD of surface cracks from FEM and from "double-periodic" approach

	[90$_8$/0]s				**[90/0]s**			
	GF/EP		**CF/EP**		**GF/EP**		**CF/EP**	
K	u_{2an}	u_{2an}^{p}	u_{2an}	u_{2an}^{p}	u_{2an}	u_{2an}^{p}	u_{2an}	u_{2an}^{p}
0.50	1.9575	1.9785	1.2110	1.2180	1.5385	1.5405	1.2160	1.2165
0.30	1.9500	1.9660	1.1915	1.1955	1.4240	1.4290	1.1390	1.1405
0.20	1.8665	1.8810	1.1095	1.1140	1.2685	1.2800	1.0155	1.0220
0.10	1.5920	1.6095	0.9160	0.9220	1.0490	1.0645	0.8335	0.8380
0.05	1.3410	1.3620	0.7755	0.7830	0.9215	0.9325	0.7265	0.7380

The validity of enforcing symmetry in positions like $x = \pm l_1/2$ in Fig.3, is the basic assumption in [7]. In our present paper we have shown, see Fig.10 that it can lead to noticeable inaccuracy in the average COD which is proportional to the average axial stress perturbation between cracks in the cracked layer and is linear with respect to the average stress used in [7]. Since using the symmetry the COD is underestimated on the side where the neighbouring crack is closer and overestimated on the other side, the opposite holds for the average stress: for the given crack it is overestimated in the region with smaller spacing and underestimated on the other side. However, when using (13), (14) as required in stiffness calculation the errors are cancelled out and the sum is very accurate. The high accuracy of the summary effect was found in ref [7] as a result of two numerical procedures.

3.4 Elastic modulus prediction and validation with FEM

The effect of the non-uniform crack distribution on axial modulus of cross-ply laminates is shown in Fig. 11 for GF/EP laminates and in Fig. 12 for CF/EP laminates. All results are for the same normalized crack density $\rho_{90n} = 0.1$. The normalized axial modulus of the laminate is calculated in three different ways:

a) Calculating the average applied stress using FEM and using definition of E_x;

b) Applying (11) and using for u_{2an}^{90} values of u_{2an} obtained from FEM and presented in Tables 2 and 3;

c) Applying (11) and using for u_{2an}^{90} values of u_{2an}^{p} obtained from "double-periodic" approach presented in Tables 2 and 3.

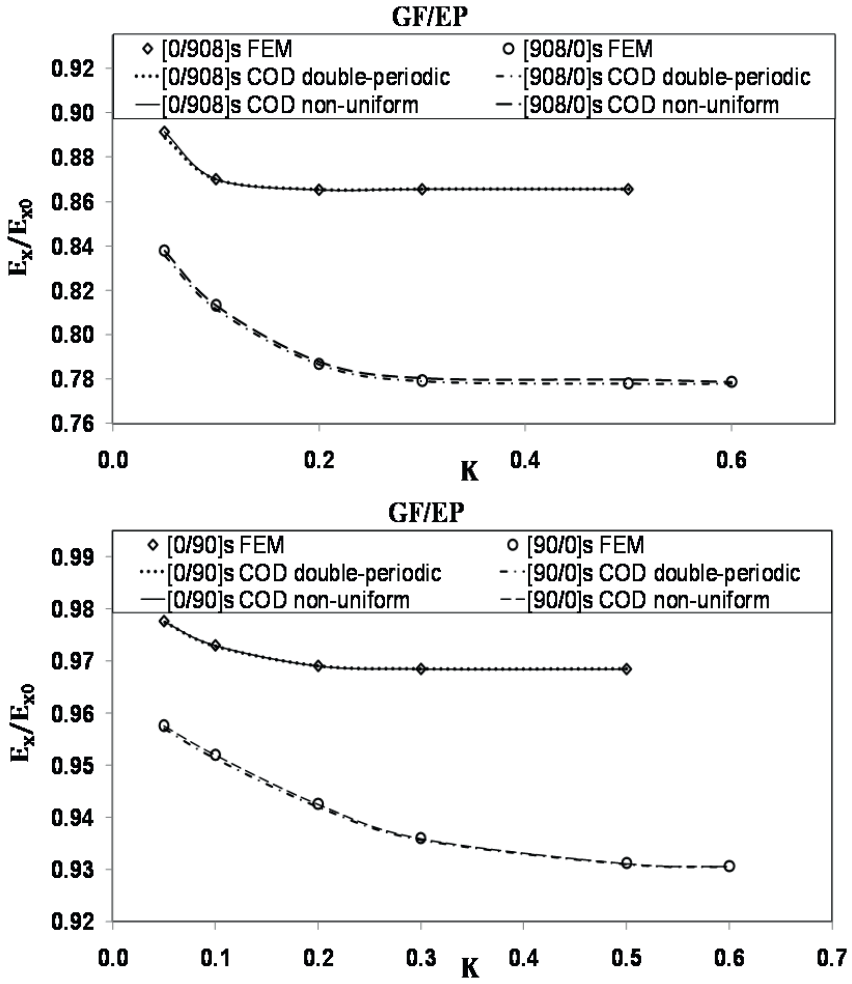

Figure 11. Effect of non-uniform crack distribution on axial modulus of GF/EP cross-ply laminates with normalized crack density $\rho_{90n} = 0.1$

As expected the direct FEM results in Fig.11 coincide with results from (11) using FEM based u_{2an} (equation (11) is exact and its numerical accuracy depends on the accuracy of the input u_{2an}). On other side FEM values practically coincide with the ones where the "double-periodic" approach is used, proving the accuracy and potential of this approach for simulation of systems with multiple non-uniformly spaced cracks.

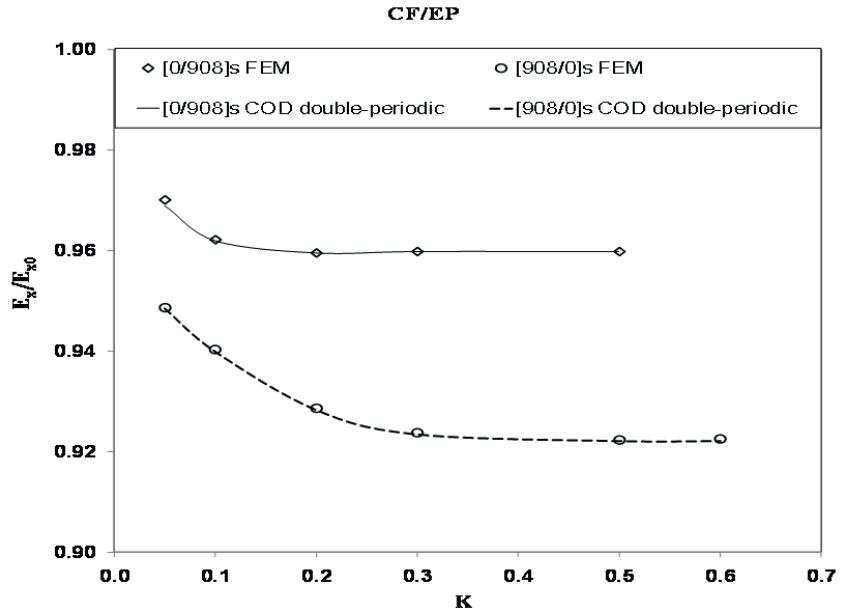

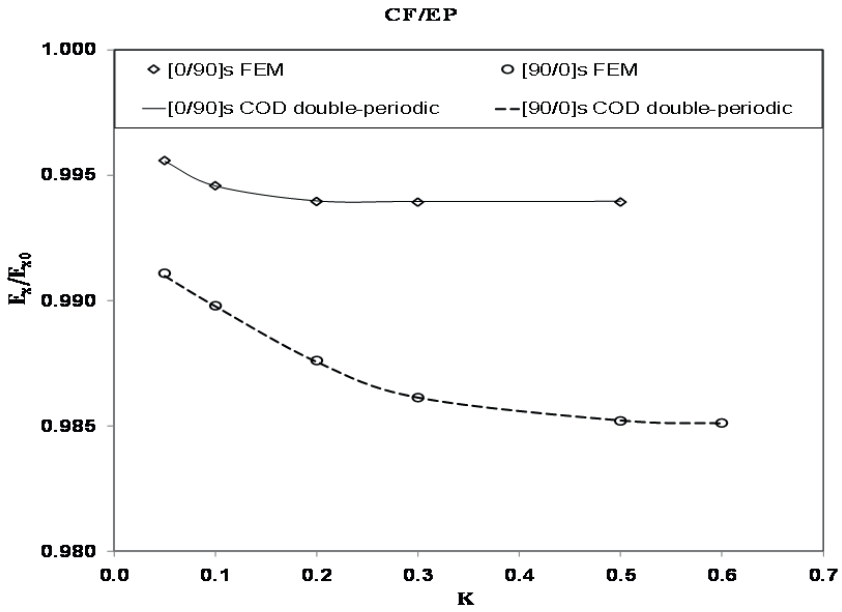

Figure 12. Effect of non-uniform crack distribution on axial modulus of CF/EP cross-ply laminates with normalized crack density $\rho_{90n} = 0.1$.

For the used crack density and all investigated materials and lay-ups the axial modulus reduction is the highest if cracks have uniform distribution. For the reasons described in Introduction the experimental crack distribution at this crack density is

expected to be rather non-uniform and the axial modulus is higher than predicted by models based on periodic crack distribution. The axial modulus value at the highest considered non-uniformity (K =0.05) and at uniform distribution (K =1) are given in Table 4.

The effect of non-uniformity is smallest for CF/EP composite with thin 90-layer. Axial modulus of laminates with relatively thick damaged layers is more sensitive to non-uniform crack distribution: the highest value is 1.077 for GF/EP composite with lay-up $[90_8/0]$s.

The non-uniform distribution of internal cracks does not affect laminate modulus if the non-uniformity parameter $K > 0.2$. For laminates with cracks in surface layers the corresponding value is between 0.3 and 0.5. Note that K values given here are the same as the values when the non-uniformity stops to affect the average normalized COD.

Table 4. Axial modulus of cross ply laminates with non-uniform and uniform (K =1) crack distributions

		$\rho_{90n} = 0.1$			$\rho_{90n} = 0.5$		
Material	Lay-up	**K=0.05** $l_{0n} = 0.5$	**K=1** $l_{0n} = 10$	**Ratio**	**K=0.25** $l_{0n} = 0.5$	**K=1** $l_{0n} = 2$	**Ratio**
GF/EP	$[0/90_8]_s$	0.8915	0.8657	1.0298	0.6213	0.5617	1.1061
GF/EP	$[90_8/0]_s$	0.8380	0.7781	1.0770	0.5068	0.4369	1.1600
GF/EP	$[0/90]_s$	0.9777	0.9685	1.0095	0.8971	0.8638	1.0386
GF/EP	$[90/0]_s$	0.9576	0.9302	1.0295	0.8309	0.8052	1.0319
CF/EP	$[0/90_8]_s$	0.9701	0.9598	1.0107	0.8665	0.8236	1.0521
CF/EP	$[90_8/0]_s$	0.9486	0.9223	1.0285	0.7891	0.7392	1.0675
CF/EP	$[0/90]_s$	0.9956	0.9939	1.0017	0.9782	0.9695	1.0090
CF/EP	$[90/0]_s$	0.9911	0.9850	1.0062	0.9587	0.8505	1.1272

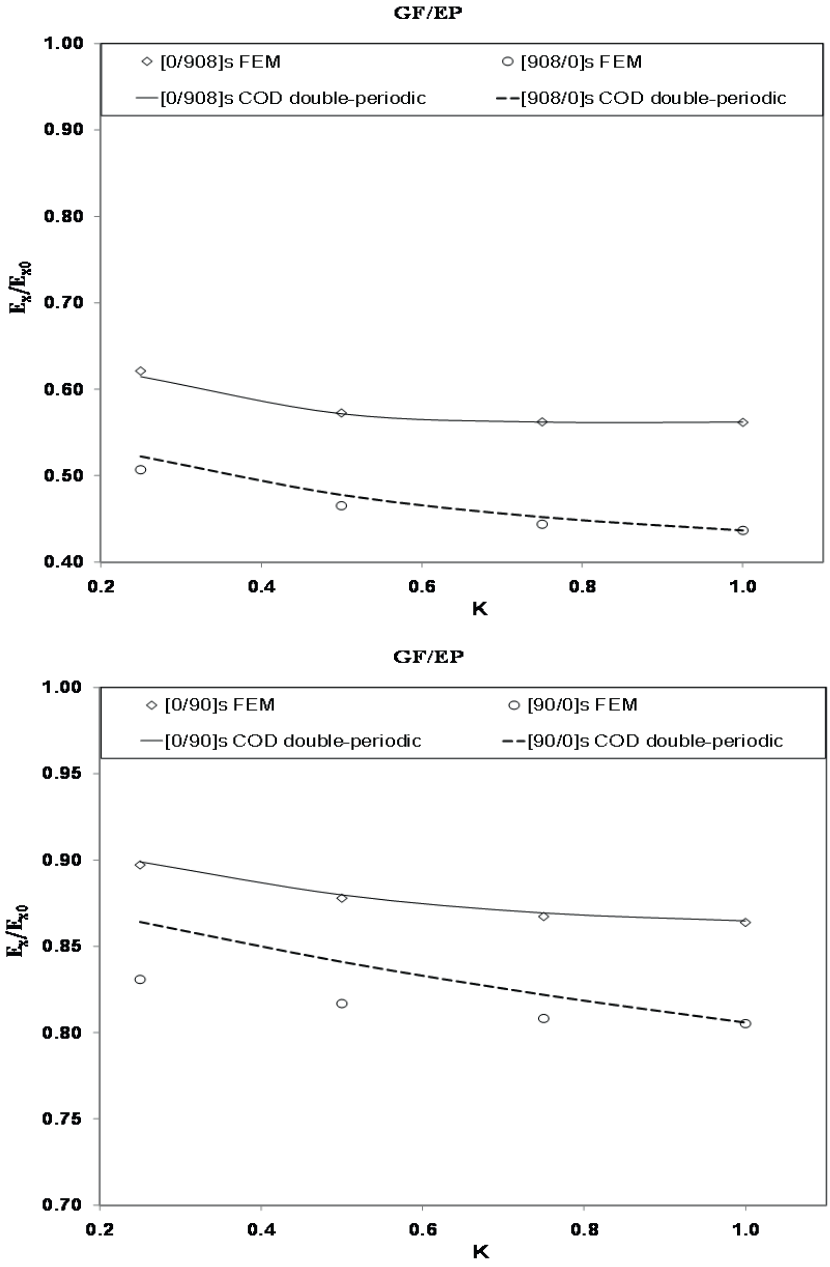

Figure 13. Effect of non-uniform crack distribution on axial modulus of GF/EP cross-ply laminates with normalized crack density $\rho_{90n} = 0.5$

Similar calculations as described above were performed for higher crack density $\rho_{90n} = 0.5$ Results are presented in Table 4 and in Fig 13 and Fig 14. Due to limitations for minimum possible spacing the range of the considered non-uniformity

in calculations is more narrow. Nevertheless the effect of non-uniform distribution is even larger than at low crack density. In contrast to low crack density case, there is no plateau region in Fig. 13 and 14. The "double-periodic" approach at high crack density is still highly accurate for internal cracks. For surface cracks with high non-uniformity this approach underestimates the modulus reduction.

As follows from section 2.2 all thermo-elastic constants of the cross-ply laminate except the shear modulus can be analysed using the calculated u_{2an}. As shown in [7], the reduction of all properties in damaged laminate is linked and the same accuracy and trends as demonstrated for axial modulus apply for other constants. The shear modulus in our formulation in Section 2.2 depends on sliding displacements which may have to be studied separately.

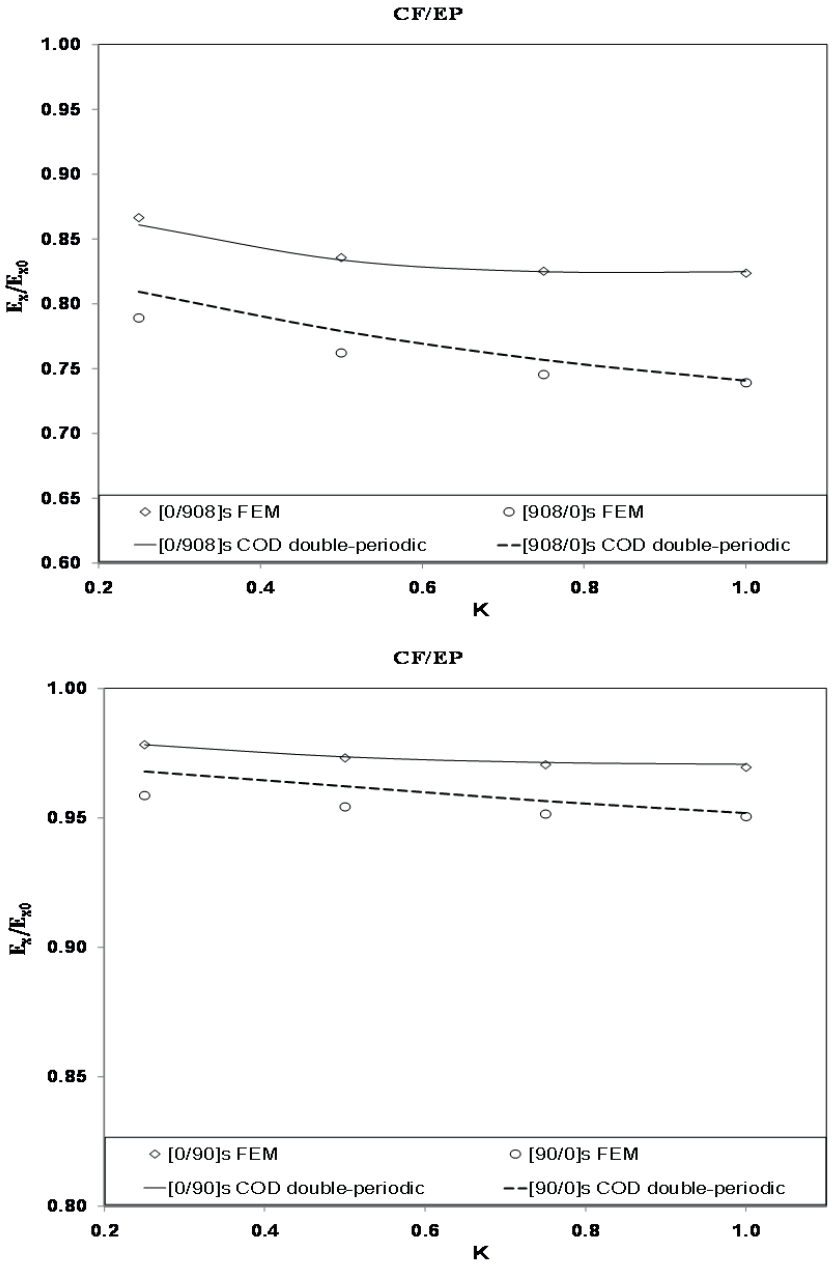

Figure 14. Effect of non-uniform crack distribution on axial modulus of CF/EP cross-ply laminates with normalized crack density $\rho_{90n} = 0.5$

4. Conclusions

Earlier developed model for thermo-elastic properties of damaged symmetric laminates was generalized for case when the intralaminar crack distribution is non-uniform and due to interactions each crack may have different opening (COD) and sliding (CSD) displacements. These displacements and the number of cracks per unit length in the layer are governing the laminate properties reduction.

This model was used to analyze the sensitivity of the damaged cross-ply laminate stiffness with respect to the non-uniformity parameter defined as the ratio of the smallest and the average spacing between cracks in a repeating element containing two cracks. COD values were calculated using FEM in generalized plane strain formulation and stiffness calculations were performed for different GF/EP as well CF/EP laminates with low and also with high crack density.

The trend is the same for all crack densities: if cracks are distributed non-uniformly the damaged laminate modulus is higher. The difference can reach 16 %.

It was shown that in internal layers very accurate COD values for cracks with non-uniform spacing and elastic modulus values can be obtained using “double-periodic” approach stating that the COD is the average of two solutions for periodic systems of cracks. For cracks in surface layers this approach is accurate only for low crack densities.

5. References

1. Nairn, J.A. and Hu, S. (1994). Matrix microcracking, In: Pipes, R.B., Talreja, R. (eds), Damage Mechanics of Composite Materials, Composite Materials series, Vol. 9, pp. 187-243, Elsevier, Amsterdam.
2. Berthelot, J.M. (2003). Transverse Cracking and Delamination in Cross-ply Glass-fiber and Carbon-fiber Reinforced Plastic Laminates: Static and Fatigue Loading, Appl. Mech. Rev., 56(1): 111-147.
3. Lundmark, P. and Varna, J. (2005). Constitutive Relationships for Laminates with Ply Cracks in In-plane Loading, International Journal of Damage Mechanics, 14(3): 235-261.
4. Hashin, Z. (1985). Analysis of Cracked Laminates: A Variational Approach, Mechanics of Materials, 4(2): 121-136.
5. Talreja, R. (1994). Damage characterization by internal variables, In: Pipes, R.B., Talreja, R. (eds), Damage Mechanics of Composite Materials, Composite Materials series, Vol. 9, pp. 53-78, Elsevier, Amsterdam.
6. Kashtalyan, M. and Soutis, C. (2005). Analysis of Composite Laminates with Intra- and Interlaminar Damage, Progress in Aerospace Sciences, 41(2): 152-173.
7. McCartney, L.N. and Schoeppner, G.A. (2000). Predicting the Effect of Non-uniform Ply Cracking on the Thermo-elastic Properties of Cross-ply Laminates, Composites Science and Technology, 62: 1841-1856.
8. Silberschmidt, V.V. (2005). Matrix Cracking in Cross-ply Laminates: Effect of Randomness, Composites: Part A, 36: 129.135.
9. Vinogradov, V. and Hashin, Z. (2005). Probabilistic Energy Based Model for Prediction of Transverse Cracking in Cross-ply Laminates, Int. Journal of Solids and Structures, 42: 365-392.
10. Varna, J., Krasnikovs, A., Kumar, R. and Talreja, R. (2004). A Synergistic Damage Mechanics Approach to Viscoelastic Response of Cracked Cross-ply Laminates, International Journal of Damage Mechanics, 13: 301-334.
11. Joffe, R., Krasnikovs, A. and Varna, J. (2001). COD-based Simulation of Transverse Cracking and Stiffness Reduction in [S/90n]s Laminates, Composites Science and Technology, 61: 637-656.
12. Lundmark, P. and Varna, J. (2006). Crack Face Sliding Effect on Stiffness of Laminates with Ply Cracks, Composites Science and Technology, 66: 1444-1454.
13. Nairn, J.A. and Hu, S. (1992). The Formation and Effect of Outer-ply Microcracks in Cross-ply Laminates: A Variational Approach, Engineering Fracture Mechanics, 41(2): 203-221.
14. Allen, D.H. and Yoon, C. (1998). Homogenization Techniques for Thermo-viscoelastic Solids Containing Cracks, Int. Journal of Solids and Structures, 35:4035-4053.
15. Vakulenko, A.A. and Kachanov, M.L. (1971). Continuum Model of Medium with Cracks, Mekhanika Tverdogo Tela (Mechanics of Solids), 4:159-166.

Appendix 1. Homogenized stiffness of damaged laminate

Using divergence theorem it is easy to show [14] that for stress states that satisfy equilibrium equations the average stress applied to external boundary is equal to volume averaged stress. This statement is correct under assumption that stresses at internal boundaries (cracks) are zero. For laminated composites with applied average stress $\{\sigma_0\}^{LAM}$ this equality can be written as

$$\{\sigma_0\}^{LAM} = \{\overline{\sigma}\}^a = \sum_{k=1}^{N} \{\overline{\sigma}\}_k^a \frac{t_k}{h} \tag{A1.1}$$

In (A1.1) the volume average is calculated expressing the integral over the laminate volume as a sum of volume integrals over N layers. Upper index a is used to indicate volume averages. Using Hook's law and averaging it over a layer we have for averages the same form as for arbitrary point

$$\begin{Bmatrix} \sigma_x^a \\ \sigma_y^a \\ \sigma_{xy}^a \end{Bmatrix}_k = [\overline{Q}]_k \begin{Bmatrix} \varepsilon_x^a \\ \varepsilon_y^a \\ \gamma_{xy}^a \end{Bmatrix}_k \tag{A1.2}$$

Substituting (A1.2) in (A1.1) and using the relationship between volume averaged strain in a layer and the displacements applied to external and internal boundaries [13]

$$\begin{Bmatrix} \varepsilon_x^a \\ \varepsilon_y^a \\ \gamma_{xy}^a \end{Bmatrix}_k = \begin{Bmatrix} \varepsilon_x \\ \varepsilon_y \\ \gamma_{xy} \end{Bmatrix}^{LAM} + \begin{Bmatrix} \beta_x \\ \beta_y \\ 2\beta_{xy} \end{Bmatrix}_k \tag{A1.3}$$

we obtain

$$\begin{Bmatrix} \sigma_{x0} \\ \sigma_{y0} \\ \sigma_{xy0} \end{Bmatrix}^{LAM} = [Q]_0^{LAM} \begin{Bmatrix} \varepsilon_x \\ \varepsilon_y \\ \gamma_{xy} \end{Bmatrix}^{LAM} + \sum_{k=1}^{N} [\overline{Q}]_k \frac{t_k}{h} \begin{Bmatrix} \beta_x \\ \beta_y \\ 2\beta_{xy} \end{Bmatrix}_k \tag{A1.4}$$

In (A1.4) $\{\overline{\beta}\}$ is the Vakulenko-Kachanov tensor written [15] in Voigt notation. In Cartesian coordinates

$$\beta_{ij} = \frac{1}{V} \int_{S_C} \frac{1}{2}\left(u_i n_j + u_j n_i\right) dS \tag{A1.5}$$

Integration in (A1.5) involves the total crack surface S_c in the layer, u_i are displacements of the points on the crack surface, n_i is outer normal to the crack surface, V is the volume of the layer. Obviously (A1.5) represents the effect on stiffness of the crack face displacements (opening and sliding). Since β_{ij} and strain are tensors for both of them we have the same transformation expressions between local and global coordinates et est.

$$\{\overline{\beta}\}_k = [T]_k^T \{\beta\}_k \tag{A1.6}$$

Expression for $\{\beta\}_k$ in local coordinates is given by (A2.9) in Appendix 2

The laminate theory stress $\{\sigma_0\}_k$ in the k-th layer in local coordinates can be expressed in (A2.9) through the applied laminate stress as follows

$$\{\sigma_0\}_k = [T]_k \begin{Bmatrix} \sigma_{x0} \\ \sigma_{y0} \\ \sigma_{xy0} \end{Bmatrix}_k = [T]_k [\overline{Q}]_k \begin{Bmatrix} \varepsilon_{x0} \\ \varepsilon_{y0} \\ \gamma_{xy0} \end{Bmatrix}^{LAM} = [T]_k [\overline{Q}]_k [S]_0^{LAM} \begin{Bmatrix} \sigma_{x0} \\ \sigma_{y0} \\ \sigma_{xy0} \end{Bmatrix}^{LAM} \tag{A1.7}$$

Substituting (A2.9) with (A1.7) in (A1.6) and further in (A1.4) we obtain after arranging the result in form (5) the form of stiffness matrix of damaged laminated given by (6).

Appendix 2. Incorporation of COD and CSD in Valulenko-Kachanov tensor

We consider a representative Volume Element (RVE) of a layer with M cracks. Schematic picture of a non-uniform crack distribution with varying spacing between cracks, $2l_m$, m=1,2…M is shown in Fig. 1. Index denoting k-th layer is omitted to simplify explanation. The cracked layer is considered in its local coordinates with indexes 1, 2 and 3 corresponding to longitudinal, transverse and thickness directions. For transverse cracks the coordinates of the normal vector to the two faces of crack surface are

$$n_1 = n_3 = 0 \qquad n_2 = \pm 1 \tag{A2.1}$$

If the crack density is high the stress perturbation zones of individual cracks overlap and the crack face displacements depend on the distance between cracks. Using the definition (A1.5) for β_{ij} we see that the matrix contains only two non-zero elements: β_{12} and β_{22}

$$\beta_{22} = \frac{1}{2Lt} \sum_{m=1}^{M} \int_{-t/2}^{+t/2} \left[u_2^{m+}(z) - u_2^{m-}(z) \right] dz \qquad \beta_{12} = \frac{1}{2Lt} \sum_{m=1}^{M} \int_{-t/2}^{+t/2} \frac{1}{2} \left[u_1^{m+}(z) - u_1^{m-}(z) \right] dz \tag{A2.2}$$

In (A2.2) t is the cracked layer thickness, $u_1^m(z)$ and $u_2^m(z)$ are sliding and opening displacements of the m-th crack, symbol + or – denotes the particular crack face according to Fig. 1.

As in previous papers for uniform crack distribution [3,12] we introduce also here normalized opening and sliding displacements of crack faces (σ_{20} and σ_{120} are CLT stresses)

$$u_{1n} = u_1 \frac{G_{12}}{t\sigma_{120}} \qquad u_{2n} = u_2 \frac{E_2}{t\sigma_{20}} \tag{A2.3}$$

Introducing average values of displacements of each crack surface over ply thickness

$$u_{1a}^{m+} = -\frac{1}{t} \int_{-t/2}^{+t/2} u_1^{m+}(z) dz \quad u_{1a}^{m-} = \frac{1}{t} \int_{-t/2}^{+t/2} u_1^{m-}(z) dz \quad u_{2a}^{m+} = -\frac{1}{t} \int_{-t/2}^{+t/2} u_2^{m+}(z) dz$$

$$u_{2a}^{m-} = \frac{1}{t} \int_{-t/2}^{+t/2} u_2^{m-}(z) dz \tag{A2.4}$$

The average value of average displacements on both surfaces is

$$u_{1a}^{m} = \frac{1}{2}\left(u_{1a}^{m+} + u_{1a}^{m-}\right) \qquad u_{2a}^{m} = \frac{1}{2}\left(u_{2a}^{m+} + u_{2a}^{m-}\right) \tag{A2.5}$$

Using (A2.4) and (A2.5) the expressions for β_{12} and β_{22} are

$$\beta_{12} = -\frac{1}{2L}\sum_{m=1}^{M} u_{1a}^{m}\left(l_{(m-1)n}, l_{mn}\right) \qquad \beta_{22} = -\frac{2}{2L}\sum_{m=1}^{M} u_{2a}^{m}\left(l_{(m-1)n}, l_{mn}\right) \tag{A2.6}$$

We indicate here that the displacements will be mostly affected by normalized distances to the two closest neighboring cracks. These expressions can be rewritten in terms of average crack density and average (over all cracks) displacements

$$\beta_{12} = -\rho u_{1a} \qquad \beta_{22} = -2\rho u_{2a} \tag{A2.7}$$

$$u_{1a} = \frac{1}{M}\sum_{m=1}^{M} u_{1a}^{m}\left(l_{(m-1)n}, l_{mn}\right) \qquad u_{2a} = \frac{1}{M}\sum_{m=1}^{M} u_{2a}^{m}\left(l_{(m-1)n}, l_{mn}\right) \tag{A2.8}$$

Normalization (A2.3) can be applied also to u_{1a}^{m} and u_{2a}^{m} in (A2.8) using notation u_{1an}^{m}, u_{2an}^{m} for the result. Expressions for β_{ij} in result of normalization are slightly modified. It is easy to check that they can be presented in the following matrix form

$$\{\beta\} = \begin{Bmatrix} 0 \\ \beta_{22} \\ 2\beta_{12} \end{Bmatrix} = -\frac{\rho_n}{E_2}[U]\begin{Bmatrix} \sigma_1 \\ \sigma_2 \\ \sigma_{12} \end{Bmatrix} \qquad [U] = 2\begin{bmatrix} 0 & 0 & 0 \\ 0 & u_{2an} & 0 \\ 0 & 0 & \dfrac{E_2}{G_{12}}u_{1an} \end{bmatrix} \tag{A2.9}$$

In (A2.9) ρ_n is normalized crack density in the layer defined by (4).

Paper III

MS. Loukil, W. Hussain, A. Kirti, A. Pupurs and J. Varna

Thermo-elastic constants of symmetric laminates with cracks in 90-layer: application of simple models

Thermo-elastic constants of symmetric laminates with cracks in 90-layer: application of simple models

MS. Loukil, W. Hussain, A. Kirti, A. Pupurs and J.Varna

Luleå University of Technology, SE-97187 Luleå, Sweden

Abstract

Change of thermo-elastic properties of cross-ply and quasi-isotropic laminates with intralaminar cracks in layers is analyzed. Predictions are performed using previously derived general expressions for stiffness of symmetric damaged laminates as dependent on crack density and crack face opening (COD) and sliding (CSD). It is shown that the average COD can be linked with the average value of axial stress perturbation between two cracks. Using this relationship analytical shear lag and Hashin's models, developed for axial modulus, can be applied for calculating both thermal expansion coefficients, in-plane moduli and Poisson's ratios of damaged laminates. The approach is evaluated using FEM and it is shown that the accuracy is rather similar as in axial modulus calculation.

Keywords: polymer composites, laminates, damage, intralaminar cracks, thermo-elastic properties, modeling, crack opening displacement

1. Introduction

Composite laminates under service loading undergo complex combinations of thermal and mechanical loading leading to microdamage accumulation in layers. The most common damage mode is intralaminar cracking in layers. During service life, the number of these cracks, which are transverse to the midplane, increases reducing laminate thermo-elastic properties.

The stiffness degradation of composite laminates due to cracking can be explained in terms of opening and sliding of crack surface. The crack face relative displacement during loading reduces the average stress in the damaged layer, thus reducing the laminate stiffness.

Numerous analytical models have been developed to study the stiffness degradation due to transverse cracks. They are all based on approximate solution for the stress state between two cracks (repeating element). Reference is given only to papers with direct relevance to the current study [1-16].

The simplest type of models leading to linear second order differential equation with constant coefficients is called shear lag models [1-4]. General for all shear-lag models is that the equilibrium conditions are satisfied in average only and the shear stress free condition on crack surfaces is not satisfied. A "shear lag" parameter which is often a fitting parameter is needed in these models. The stress distribution and the stiffness degradation calculated according to these models in [6,7] are affected by the value of this parameter. The most typical modifications and values of the shear lag parameter compared in [5,6,7] are: a) assuming a resin rich layer of unknown thickness between layers of different orientation where the out-of-plane shear deformation at the crack

tip takes place. In this paper we assume that this layer can not be thicker than fibre diameter; b) assuming that the shear strain acts in the cracked layer only and it is due to linear or parabolic crack opening displacement dependence on the thickness coordinate; c) assuming shear strain also in the constraint layer. The last model was refined by Zhang et al in [8] assuming that the intralaminar shear stress in 0-layer is present only in a part of the constraint layer. Unfortunately, unless experimental full field measurements or FEM are used, the thickness of this zone becomes a fitting parameter.

The first model based on the principle of minimum complementary energy which was free of these assumptions was developed by Hashin [9] to investigate the axial modulus reduction of cross ply laminate with cracks in inside 90 layers. The approximate stress field derived with this approach satisfies all the necessary equilibrium as well as the boundary conditions including zero tractions on the crack surfaces. Since the approximate nature of the selected stress functions lead to increase of the value of the complementary energy, it does not reach the minimum corresponding to the exact solution and the displacement continuity is satisfied only approximately. Hashin's model is relatively simple to use and it renders lower bond for the axial modulus of the damaged laminate. Refined variational models based on minimum principle of the complementary energy with more accurate predictions of axial modulus and Poisson's ratio were developed in [10,11]. However, higher accuracy of analytical solutions is always on the expense of significant increase of complexity. For example, use of the model [11] requires rather complex numerical minimization routine. Therefore [11] as well as models by McCartney [12] and Shoeppner and Pagano [13] could rather be considered as numerical routines.

Two main problems/limitations related to the use of analytical solutions are: a) approximate analytical solutions are available for cross-ply laminates only; b) these models are developed to calculate only one or two of the whole set of laminate thermo-elastic constants (usually axial or shear modulus of the damaged laminate).

In practice a cross-ply laminate lay-up is rarely used. This limitation has been handled by several authors [14,15,16]. Zhang et al [13] introduced the concept of "an equivalent constraint" assuming that the constraint on the damaged layer of the lay-ups above and below the damaged lamina can be replaced by two sublaminates with properties calculated using laminate theory (CLT). Thereby the actual laminate, considered in the coordinate system related to the damaged layer symmetry, could be replaced by a cross-ply with orthotropic constraint layers. Similar approach was used in Lundmark et al [15,16] applying FEM to analyze the effect of surrounding layers. They demonstrated that the modulus and the thickness ratio of the closest neighbor to the damaged layer are the parameters governing the constraint.

In [15] a unique relationship between the damaged laminate thermo-elastic properties and the microdamage parameters was established (GLOB-LOC approach). Exact analytical expressions for thermo-elastic constants of general symmetric laminates with cracks in multiple layers were presented. These matrix expressions are given in Section 2. It was shown that the local parameters in these expressions are the normalized average values of crack opening displacement (COD) and crack sliding displacement (CSD). In addition the laminate lay-up, layer properties and density of cracks in layers has to be given. In this paper we demonstrate how using this framework and the axial stress distributions obtained from shear lag or from Hashin's model one can calculate all thermo-elastic constants of a damaged laminate (except shear modulus). The key point in the procedure is that the average COD can be related to the average stress in a layer between two cracks (see section 3.2).

The accuracy of predictions is evaluated comparing with direct FEM calculations.

2. Material model of damaged symmetric laminates with intralaminar cracks

2.1 Model formulation

The upper part of symmetric *N*- layer laminate is shown in Fig. 1. The *k*-th layer of the laminate is characterized by thickness t_k , fiber orientation angle with respect to the global x-axis θ_k and by stiffness matrix in the local axis $[Q]$ (defined by thermo-elastic constants $E_1, E_2, G_{12}, \nu_{12}, \alpha_1, \alpha_2$). The total thickness of the laminate, $h = \sum_{k=1}^{N} t_k$. The crack density in a layer is $\rho_k = 1/(2l_k \sin\theta_k)$ where average distance between cracks measured on the specimen edge is $2l_k$. Dimensionless crack density ρ_{kn} is introduced as

$$\rho_{kn} = t_k \rho_k \tag{1}$$

It is assumed that the damaged laminate is still symmetric: the crack density in corresponding symmetrically placed layers is the same. The stiffness matrix of the damaged laminate is $[Q]^{LAM}$ and the stiffness of the undamaged laminate is $[Q]_0^{LAM}$. The compliance matrix of the undamaged laminate is $[S]_0^{LAM} = \left([Q]_0^{LAM}\right)^{-1}$, $\{\alpha\}_0^{LAM}$ is the thermal expansion coefficient vector. Constants of the undamaged laminate are calculated using CLT.

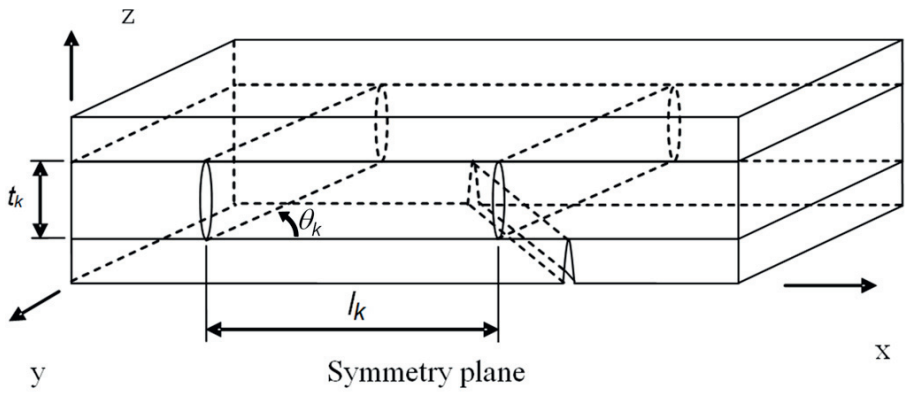

Figure 1. RVE of the damaged laminate with intralaminar cracks in layers

The expressions for compliance matrix and thermal expansion vector of the damaged laminate presented below are exact.

$$[S]^{LAM} = [S]_0^{LAM}\left([I] + \sum_{k=1}^{N} \rho_{kn} \frac{t_k}{h} [K]_k [S]_0^{LAM}\right) \tag{2}$$

$$\{\alpha\}^{LAM} = \left([I] + \sum_{k=1}^{N} \frac{t_k}{h} \rho_{kn} [S]_0^{LAM} [K]_k\right)\{\alpha\}_0^{LAM} - \sum_{k=1}^{N} \frac{t_k}{h} \rho_{kn} [S]_0^{LAM} [K]_k \{\overline{\alpha}\}_k \tag{3}$$

In (2) and (3) $[I]$ is identity matrix. These expressions were derived in [15] expressing the integral effect of cracks in terms of crack density and $[K]_k$, which is a known matrix-function dependent on ply properties and normalized and averaged crack face opening (COD) and sliding displacements (CSD), u_{2an}, u_{1an}, which may be different in different layers. In (3) $\{\overline{\alpha}\}_k$ is the vector of thermal expansion coefficients of the *k*-th layer in global coordinates. The $[K]_k$ matrix for a ply in a laminate is defined as

$$[K]_k = \frac{1}{E_2}[\overline{Q}]_k [T]_k^T [U]_k [T]_K [\overline{Q}]_k \tag{4}$$

The involved matrices $[T]_k$ and $[\overline{Q}]_k$ are defined according to CLT, superscript T denotes transposed matrix and bar over stiffness matrix indicates that it is written in global coordinates. For a layer with fiber orientation angle θ_k, $m = \cos\theta_k$ and $n = \sin\theta_k$

$$[T]_k = \begin{bmatrix} m^2 & n^2 & +2mn \\ n^2 & m^2 & -2mn \\ -mn & +mn & m^2 - n^2 \end{bmatrix}, \qquad [\overline{Q}]_k = [T]_k^{-1}[Q]\left([T]_k^{-1}\right)^T \tag{5}$$

The influence of each crack is represented in (4) by matrix $[U]_k$, which contains the normalized average COD and normalized average CSD of the crack surfaces in k-th layer

$$[U]_k = 2\begin{bmatrix} 0 & 0 & 0 \\ 0 & u_{2an}^k & 0 \\ 0 & 0 & \dfrac{E_2}{G_{12}} u_{1an}^k \end{bmatrix} \tag{6}$$

Correlation of u_{2an}, u_{1an} with the stress state between cracks is the key point in this paper.

2.2 Thermo-elastic constants of balanced laminates with cracks in 90-layers

For balanced laminates with cracked 90-layer, $[K]_k$ can be calculated analytically. Using the result in (2) and (3) the following expressions for laminate thermo-elastic constants were obtained for the case with only one cracked 90-layer (if laminate has several cracked 90-layers summation is required in the denominator).

$$\frac{E_x^{LAM}}{E_{x0}^{LAM}} = \frac{1}{1 + 2\rho_{90n}\dfrac{t_{90}}{h} u_{2an}^{90} c_2} \qquad \frac{E_y^{LAM}}{E_{y0}^{LAM}} \frac{1}{1 + 2\rho_{90n}\dfrac{t_{90}}{h} u_{2an}^{90} c_4} \tag{7}$$

$$\frac{\nu_{xy}^{LAM}}{\nu_{xy0}^{LAM}}=\frac{1+2\rho_{90n}\dfrac{t_{90}}{h}u_{2an}^{90}c_1\left(1-\dfrac{\nu_{12}}{\nu_{yx0}^{LAM}}\right)}{1+2\rho_{90n}\dfrac{t_{90}}{h}u_{2an}^{90}c_2} \qquad \frac{G_{xy}^{LAM}}{G_{xy0}^{LAM}}=\frac{1}{1+2\rho_{90n}\dfrac{t_{90}}{h}u_{1an}^{90}\dfrac{G_{12}}{G_{xy0}^{LAM}}} \tag{8}$$

$$\frac{\alpha_x^{LAM}}{\alpha_{x0}^{LAM}}=1-2\rho_{90n}\frac{t_{90}}{h}u_{2an}^{90}\frac{c_1}{\alpha_{x0}^{LAM}}\left(\alpha_2-\alpha_{x0}^{LAM}-\nu_{12}\left(\alpha_{y0}^{LAM}-\alpha_1\right)\right) \tag{9}$$

$$\frac{\alpha_y^{LAM}}{\alpha_{y0}^{LAM}}=1-2\rho_{90n}\frac{t_{90}}{h}u_{2an}^{90}\frac{c_3}{\alpha_{y0}^{LAM}}\left(\alpha_2-\alpha_{x0}^{LAM}-\nu_{12}\left(\alpha_{y0}^{LAM}-\alpha_1\right)\right) \tag{10}$$

$$c_1=\frac{E_2}{E_{x0}^{LAM}}\frac{1-\nu_{12}\nu_{xy0}^{LAM}}{\left(1-\nu_{12}\nu_{21}\right)^2} \qquad c_2=c_1\left(1-\nu_{12}\nu_{xy0}^{LAM}\right) \tag{11}$$

$$c_3=\frac{E_2}{E_{y0}^{LAM}}\frac{\nu_{12}-\nu_{yx0}^{LAM}}{\left(1-\nu_{12}\nu_{21}\right)^2} \qquad c_4=c_3\left(\nu_{12}-\nu_{yx0}^{LAM}\right) \tag{12}$$

Index 90 is used for thickness, crack density and COD in 90-layer. The quantities with subscripts x,y and superscript LAM are laminate constants, quantities with additional subscript 0 are undamaged laminate constants. It is noteworthy that

a) If Poisson's effects are neglected $c_3=c_4=0$. In this approximation E_y^{LAM} and α_y^{LAM} do not change because of damage in 90-ply.

b) Shear modulus is not related to COD and depends on sliding displacement only. It is not analyzed in the present paper.

The class of laminates covered by these expressions is broader than just cross ply laminates or laminates with 90-layers. For example, any quasi-isotropic laminate with an arbitrary cracked layer can be rotated to have the damaged layer as a 90-layer. The only limitation of (7)-(12) is that the laminate after rotation is balanced with zero coupling terms in $[S]_0^{LAM}$.

Application of (7)-(12) requires values of u_{2an}, u_{1an}. Three different expressions of u_{2an} are presented in section 3 according to FEM, shear-lag and Hashin's models.

3. Determination of COD

3.1 Crack face displacements

It is assumed that all cracks in the same layer are equal and equidistant. The average CSD and COD are defined as

$$u_{1a}^{90}=\frac{1}{2t_{90}}\int_{-\frac{t_{90}}{2}}^{\frac{t_{90}}{2}}\Delta u_1^{90}(x_3)\,dx_3 \qquad u_{2a}^{90}=\frac{1}{2t_{90}}\int_{-\frac{t_{90}}{2}}^{\frac{t_{90}}{2}}\Delta u_2^{90}(x_3)\,dx_3 \tag{13}$$

Here Δu_i is the displacement gap between corresponding points at both crack faces. Subscript 1 denotes the displacement in fiber direction (sliding) and subscript 2 in the transverse direction (opening).

In linear model the average displacements u_{2a}^{90} and u_{1a}^{90} are linear functions of the applied stress and the ply thickness. Therefore, they are normalized with respect to the far field (CLT) shear stress σ_{xy0}^{90} and transverse stress σ_{x0}^{90} in the layer (resulting from the macro-load $\{\sigma\}_0^{LAM}$ and temperature difference ΔT) and with respect to the thickness of the cracked layer t_{90}

$$u_{1an}^{90} = u_{1a}^{90} \frac{G_{12}}{t_{90}\sigma_{xy0}^{90}} \qquad u_{2an}^{90} = u_{2a}^{90} \frac{E_2}{t_{90}\sigma_{x0}^{90}} \tag{14}$$

Elastic constants E_2 and G_{12} of the UD composite are introduced in (14) to have dimensionless descriptors. The influence of each crack on thermo-elastic laminate constants is represented by u_{2a}^{90} and u_{1a}^{90}.

3.2 Average COD relation to stress perturbation

Part of the deformed laminate with an open crack is shown in Fig.2. Thickness of the supporting sublaminate is t_s and its effective modulus in the axial direction is E_x^s. Denoting the displacement of the undamaged sublaminate at $x = l_{90}$ (l_{90} is the half distance between cracks) by $u_s(l_0)$ and the displacement of the crack face by $u_{90}(l_0, z)$ we can write that the average COD is

$$u_{2a}^{90} = \frac{2}{t_{90}} \int_0^{\frac{t_{90}}{2}} \left[u_s(l_{90}) - u_{90}(l_{90}, z)\right] dz = u_s(l_{90}) - \frac{2}{t_{90}} \int_0^{\frac{t_{90}}{2}} u_{90}(l_{90}, z) dz \tag{15}$$

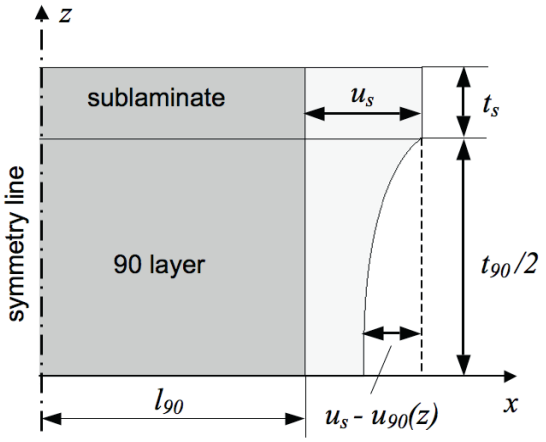

Figure 2. Schematic showing of the deformation of the laminate in the vicinity of transverse crack

The crack opening leads to reduction of axial stress in the 90-layer. The stress between two cracks in the 90-layer can be written in the following general form

$$\sigma_x^{90} = \sigma_{x0}^{90}\left[1 - f(x, z, l_{90})\right] \tag{16}$$

Function f in (16) represents the stress perturbation and σ_{x0}^{90} is the axial stress in the undamaged 90-layer (CLT). The average value of the stress between two cracks is defined as

$$\sigma_{xa}^{90} = \sigma_{x0}^{90}\left[1 - f_a\left(\rho_{90n}\right)\right] \tag{17}$$

$$f_a\left(\rho_{90}\right) = \frac{2}{l_{90}t_{90}} \int_0^{l_{90}} \int_0^{\frac{t_{90}}{2}} f\left(x,z,l_{90}\right) dxdz \tag{18}$$

The average stress in the sublaminate can be obtained from force balance

$$\sigma_{xa}^{s} = \sigma_{x0}^{s}\left(1 + \frac{t_{90}}{2t_s}\frac{E_2}{E_x^s} f_a\left(\rho_{90n}\right)\right) \tag{19}$$

In this section we will establish relationship between u_{2a}^{90} and f_a.
Neglecting Poisson's effects the $u_{90}\left(l_0, z\right)$ can be written as

$$u_{90}\left(l_{90}, z\right) = \int_0^{l_{90}} \varepsilon_x^{90}\left(x,z\right) dx = \frac{1}{E_2} \int_0^{l_{90}} \sigma_x^{90}\left(x,z\right) dx \tag{20}$$

Similarly for $u_s\left(l_{90}\right)$ we can write

$$u_s\left(l_{90}\right) = \int_0^{l_{90}} \varepsilon_x^{s}\left(x,z\right) dx = \frac{2}{t_{90}} \int_0^{\frac{t_{90}}{2}} \int_0^{l_{90}} \varepsilon_x^{s}\left(x,z\right) dxdz = \frac{2}{E_x^s t_{90}} \int_0^{\frac{t_{90}}{2}} \int_0^{l_{90}} \sigma_x^{90}\left(x,z\right) dxdz = \frac{l_{90}}{E_x^s}\sigma_{xa}^{s} \tag{21}$$

Substituting (20) and (21) in (15) we obtain

$$u_{2a}^{90} = l_{90}\left(\frac{\sigma_{xa}^{s}}{E_x^s} - \frac{\sigma_{xa}^{90}}{E_2}\right) \tag{22}$$

Substituting (17), (19) in (22) and using approximate expressions

$$\frac{\sigma_{x0}^{90}}{E_2} = \frac{\sigma_{x0}^{s}}{E_x^s} \qquad\qquad E_{x0}^{LAM} = \frac{E_2\frac{t_{90}}{2} + E_x^S t_s}{\frac{t_{90}}{2} + t_s} \tag{23}$$

we obtain

$$u_{2a}^{90} = f_a \cdot l_{90}\sigma_{x0}^{90}E_{x0}^{LAM}\frac{\frac{t_{90}}{2} + t_s}{t_s E_2 E_x^s} \tag{24}$$

Using (14) the relationship between normalized average COD and stress perturbation f_a is written as

$$u_{2an}^{90} = f_a\left(\rho_{90n}\right)\cdot\frac{1}{\rho_{90n}}\frac{E_{x0}^{LAM}}{E_x^s}\frac{\frac{t_{90}}{2} + t_s}{2t_s} \tag{25}$$

3.3 Shear-lag model

The stress perturbation function for shear lag models is given in [5]. Using expression (40) from [5] in (25) we obtain (note that $f_a = \frac{\rho_{90n}}{2} R$ used in [5])

$$u_{2an}^{90} = \frac{E_{x0}^{LAM}\left(t_s + \frac{t_{90}}{2}\right)}{2E_x^s t_s} \frac{1}{\xi} \tanh\left(\frac{\xi}{\rho_{90n}}\right) \tag{26}$$

The shear lag parameter ξ depends on the chosen modification of the shear lag model. Assuming existence of a resin rich layer with shear modulus G_m and thickness d_0 at the 0/90 interface we have the following expression

$$\xi^2 = \frac{G_m}{d_0} \frac{\frac{t_{90}}{2}\left(E_2 \frac{t_{90}}{2} + E_x^s t_s\right)}{t_s E_2 E_x^s} \tag{27}$$

Usually the thickness of the resin layer is taken equal to one fiber diameter. It seems physically unrealistic to have it larger than that (if any). In other modifications of the shear lag model [3,4] the expressions for the shear lag parameter are different. In one of the most common modifications G_m / d_0 in (27) is replaced by $2G_{23} / t_{90}$, whereas in modification assuming parabolic displacement distribution it is equal to $6G_{23} / t_{90}$.

3.4 Hashin´s model

Expressions for Hashin's model for the case when 90-layer is supported by orthotropic sublaminate are given in [5]. Expression for stress perturbation function is also given there. After substituting these expressions in (25) and using our notation we obtain

$$u_{2an}^{90} = \frac{E_{x0}^{LAM}\left(t_s + \frac{t_{90}}{2}\right)}{2E_x^s t_s} \frac{2\alpha\beta}{\alpha^2 + \beta^2} \frac{\cosh\left(\frac{2\alpha}{\rho_{90n}}\right) - \cos\left(\frac{2\beta}{\rho_{90n}}\right)}{\beta \sinh\left(\frac{2\alpha}{\rho_{90n}}\right) + \alpha \sin\left(\frac{2\beta}{\rho_{90n}}\right)} \tag{28}$$

$$\text{Here } \alpha = q^{1/4} \cos\frac{\theta}{2},\ \beta = q^{1/4} \sin\frac{\theta}{2},\ \tan\theta = \sqrt{\frac{4q}{p^2} - 1} \tag{29}$$

$$p = \frac{C_{02} - C_{11}}{C_{22}},\ q = \frac{C_{00}}{C_{22}} \tag{30}$$

$$C_{00} = \frac{1}{E_2} + \frac{t_{90}}{2E_x^s t_s} \qquad C_{02} = \frac{\nu_{23}}{E_2}\left(\frac{2t_s}{t_{90}} + \frac{2}{3}\right) - \frac{\nu_{xz}^s}{3E_x^s} \frac{2t_s}{t_{90}} \tag{31}$$

$$C_{11} = \frac{1}{3G_{23}} + \frac{1}{3G_{xz}^s} \frac{2t_s}{t_{90}} \qquad C_{22} = \frac{1}{E_2}\left(\left(\frac{t_s}{t_{90}}\right)^2 + \frac{2t_s}{3t_{90}} + \frac{8}{60}\right) + \frac{2}{5E_z^s}\left(\frac{t_s}{t_{90}}\right)^3 \tag{32}$$

For cross-ply laminates $E_x^s = E_1$, $E_z^s = E_2$, $G_{xz}^s = G_{12}$, $\nu_{xz}^s = \nu_{12}$ and t_s is equal to the thickness of 0 layer.
For "non cross-ply laminate", GF/EP2 [±15/90$_4$]s laminate (in section 4.3) and GF/EP [0/±45/90]s laminate (in section 4.4) E_x^s is calculated using CLT, t_s is the thickness of the sublaminate. E_z^s, G_{xz}^s and ν_{xz}^s in this case are calculated using FEM.

3.5 Ply discount model

In the ply discount model it is assumed that as soon as damage appears in a layer its load bearing capacity reduces to zero. This assumption corresponds to infinite number of cracks in the layer. Zero load bearing by the layer can be obtained by changing elastic properties of the layer to zero. In the most conservative form of this model all elastic constants are assumed zero. More representative for the case of transverse cracking is assumption used in this paper stating that the transverse and the shear modulus of the damaged layer is close to zero whereas the longitudinal modulus and Poisson's ratio have not changed. The stiffness of the damaged laminate is calculated using CLT.
The transverse elastic modulus E_2 and shear modulus G_{12} were reduced to 0.01 of their initial values. In section 4.5, where the ply discount model is used for case with neglected Poisson's effects the CLT analysis is reduced to the rule of mixtures.

4. Results and discussion

4.1. Material properties

The elastic properties of the unidirectional composites relevant to this study are given in Table 1. Elastic properties of GF/EP and CF/EP used in simulations were arbitrary assumed to represent materials like glass fiber/epoxy and carbon fiber/epoxy respectively.
Elastic properties of GF/EP2 were taken from [5] where the properties (except the out-of-plane Poisson's ratio ν_{23}, which was assumed) were obtained experimentally.
It has to be noted that the GF/EP and CF/EP in Table 1 do not have isotropy in the transverse plane and the out-of-plane shear modulus is slightly different than it would be for transverse isotropic material. Reason for the increased anisotropy could be through the thickness stitching observable in many composites. However, shear lag model does not contain G_{23} and Hashin's model, which has it in C_{11} is insensitive to it.

Table 1. Ply properties of the studied materials

	E_1	E_2	ν_{12}	ν_{23}	G_{12}	G_{23}	α_1	α_2	t_0	d_0
Material	[GPa]	[GPa]	[-]	[-]	[GPa]	[GPa]	[°C^{-1}]	[°C^{-1}]	[mm]	[mm]
GF/EP	45	15	0.3	0.4	5	6	1.0e-5	2.0e-5	0.13	0.007
CF/EP	150	10	0.3	0.4	5	6	4.3e-7	2.6e-5	0.13	0.0035
GF/EP2	44.73	12.76	0.297	0.42	5.8	4.49	-	-	0.144	0.007

d_0 is the thickness of the shear layer ($d_0 = 0.5 \cdot d_f$, where d_f is the diameter of one fiber)

4.2. Parametric analysis on cross-ply laminates

In all figures below the notation "Shear-lag" is used to indicate results calculated using COD obtained from shear lag stress analysis (26) in expressions (7)-(12). The thickness of the shear layer is given in Table 1 or indicated in figures if selected differently. The notation "Hashin" is used for predictions where the stress perturbation function from Hashin's model (generalized for orthotropic support layers/sublaminates) (28) is used. The notation used for considered cross-ply lay-ups is shown in Table 2.

Table 2. Cross-ply laminate lay-ups and used notation

Notation	Lay-up
{1}	[0/90/0]
{2}	[0/90]s
{3}	[0/90_2]s

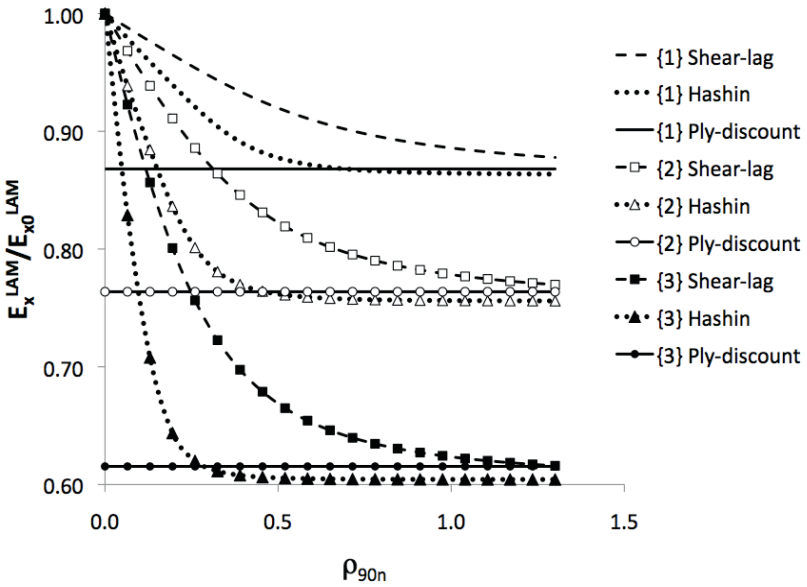

Figure 3. Simulation results showing changes in the axial modulus of the laminate E_x^{LAM} for GF/EP.

In Fig. 3 and 4 the axial modulus reduction normalized with respect to its initial value is shown for all three lay-ups and for GF/EP and CF/EP composites. Predictions of the ply-discount model are shown as horizontal lines. The modulus reduction behavior is well known and described in literature: a) more modulus reduction in laminates with relatively thick cracked plies; b) much more modulus reduction in GF/EP composites because the damaged layer has relatively high modulus as compared with the longitudinal modulus; c) more modulus reduction according to Hashin's model which as a consequence of the used minimum principle always gives conservative results.

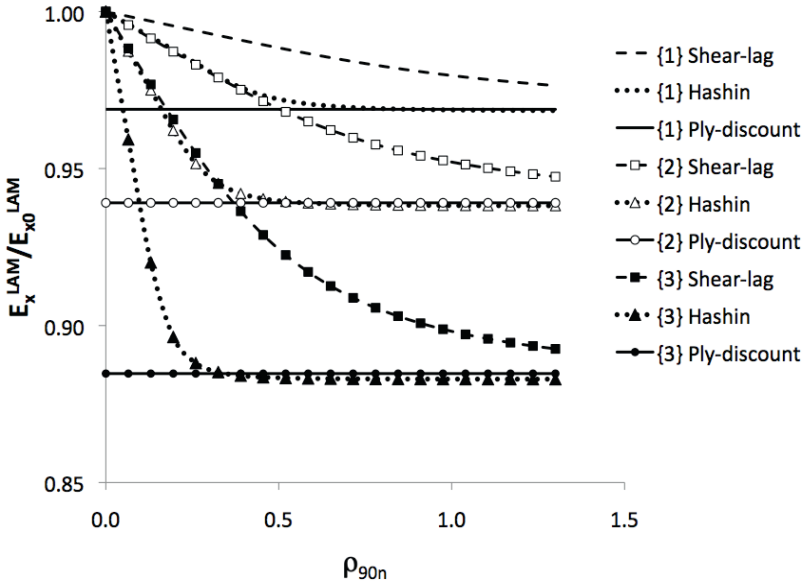

Figure 4. Simulation results showing changes in the axial modulus of the laminate E_x^{LAM} for CF/EP.

The rate of the modulus reduction according to the shear lag model depends on the shear lag parameter (related to the thickness of the resin layer d_0). The values given in Table 1 lead to much slower decrease rate than in Hashin's model. All simulated curves approach to the ply discount value. Surprisingly, the asymptotic values of both models go slightly below the ply-discount value. Since ply-discount model corresponds to an infinite number of cracks this trend needs an explanation which is given in section 4.5.

The normalized transverse modulus E_y^{LAM} / E_{y0}^{LAM} of the damaged laminate reduction is marginal, see Fig 5 and 6, which validates the usual assumption that due to cracks in 90-layer it is not changing at all. Also for this elastic property the Hashin's model predicts faster reduction with increasing crack density than the shear lag model. The change is very similar for GF/EP and CF/EP and the asymptotic values are very insensitive to the damaged ply thickness.

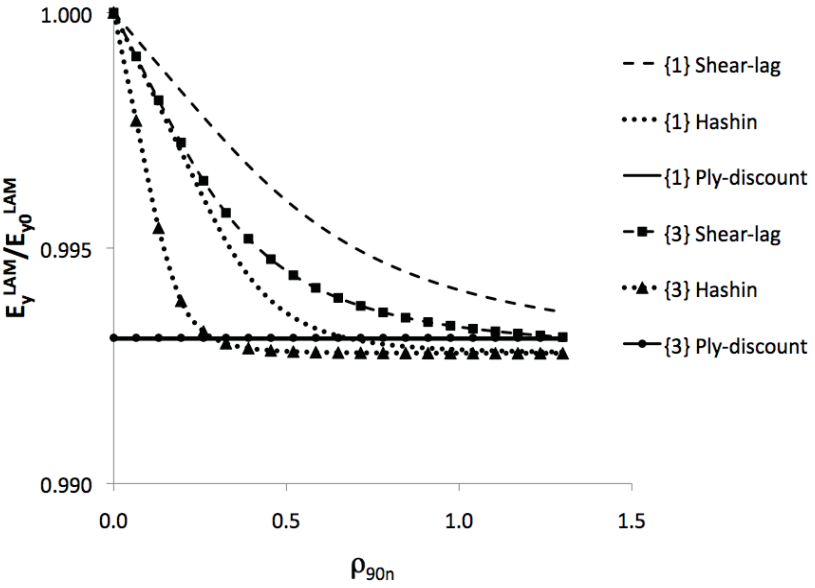

Figure 5. Simulation results showing changes in the transverse modulus of the laminate E_y^{LAM} for GF/EP

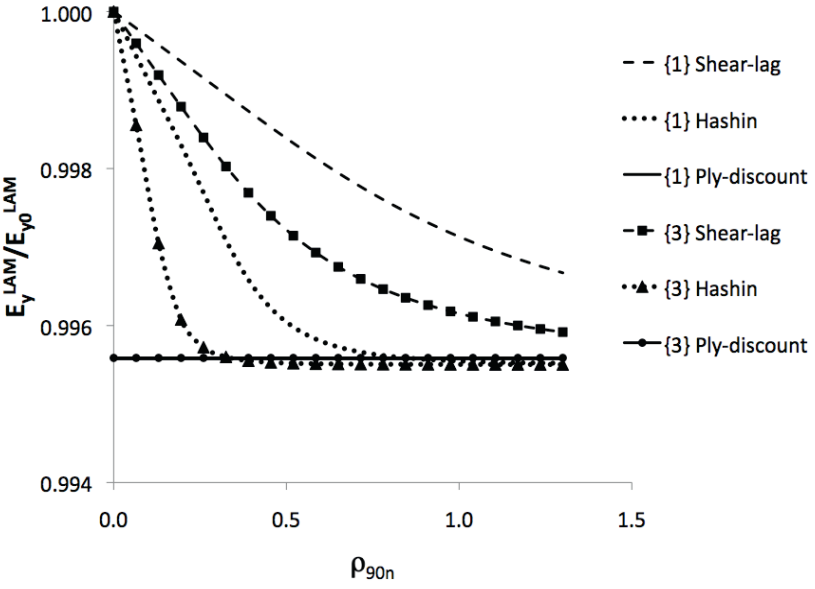

Figure 6. Simulation results showing changes in the transverse modulus of the laminate E_y^{LAM} for CF/EP

Similar results for the normalized Poisson's ratio are given in Fig.7 and 8. For this property the asymptotic values does not depend on the used material but the rate of

approaching to these values is material dependent, especially according to the shear lag model. The asymptotic value for damaged cross-ply laminate depends only on ply-thickness ratio.

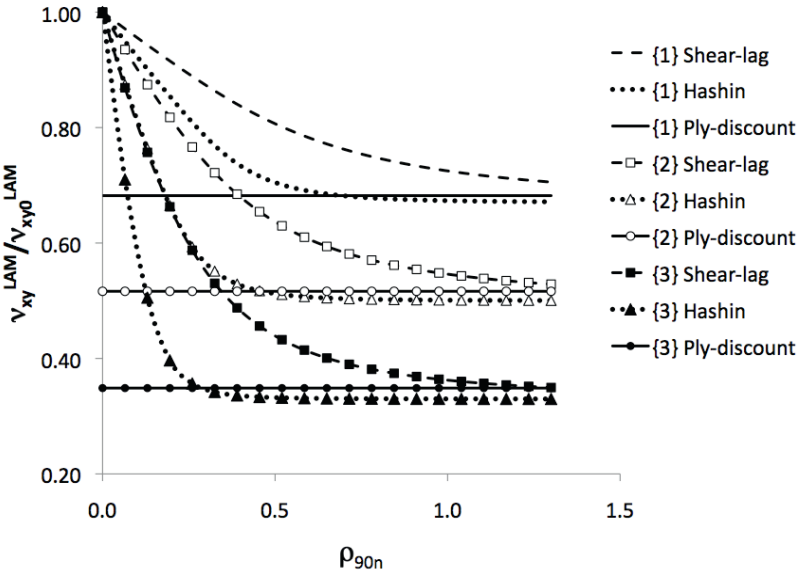

Figure 7. Simulation results showing changes in the major Poisson's ratio of the laminate ν_{xy}^{LAM} for GF/EP

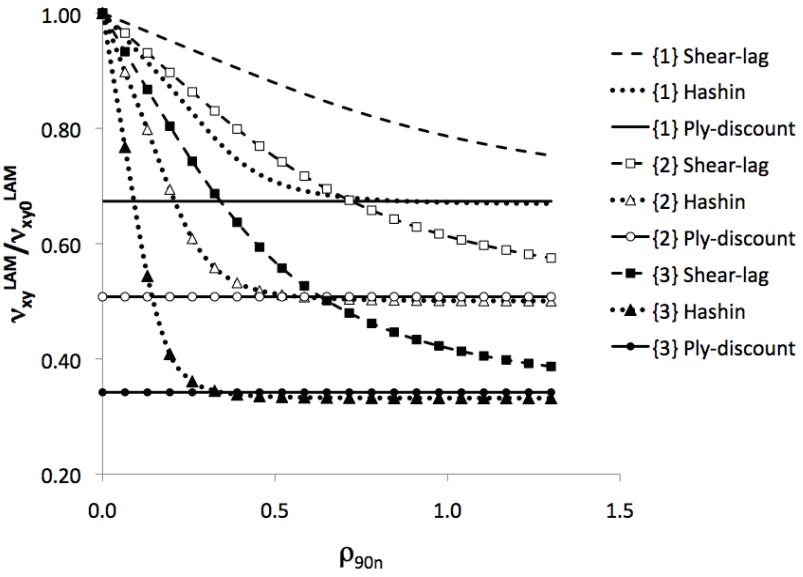

Figure 8. Simulation results showing changes in the major Poisson's ratio of the laminate ν_{xy}^{LAM} for CF/EP

Change of thermal expansion coefficients, which is seldom discussed in analytical models is shown in Fig. 9 and 10 for $\alpha_x^{LAM}/\alpha_{x0}^{LAM}$ and in Fig. 11 and 12 for $\alpha_y^{LAM}/\alpha_{y0}^{LAM}$. The relative change is much larger for CF/EP laminates but the absolute values are, certainly, much smaller. The trend is the same: Hashin's model predicts much faster properties reduction. It is noteworthy that for CF/EP laminate the transverse thermal expansion coefficient change is more than 20% (for lay-up with thickest 90-layer).

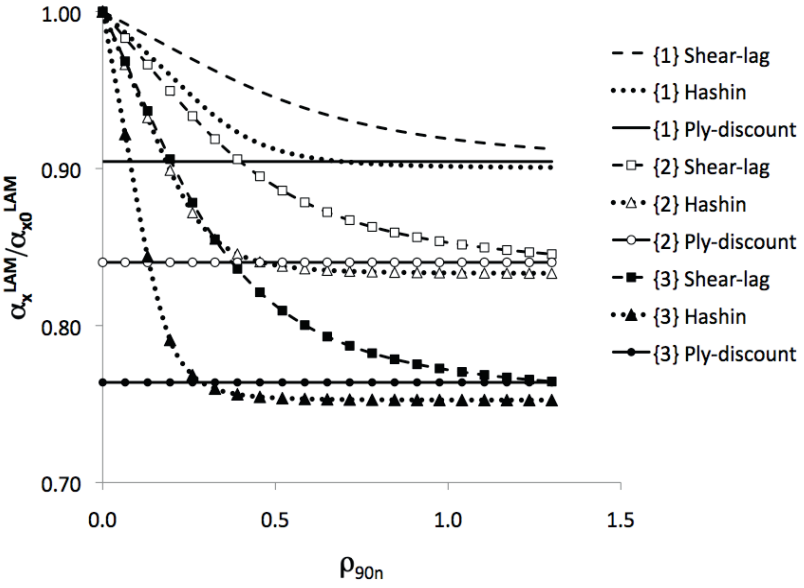

Figure 9. Simulation results showing changes in the axial coefficient of thermal expansion of the laminate α_x^{LAM} for GF/EP

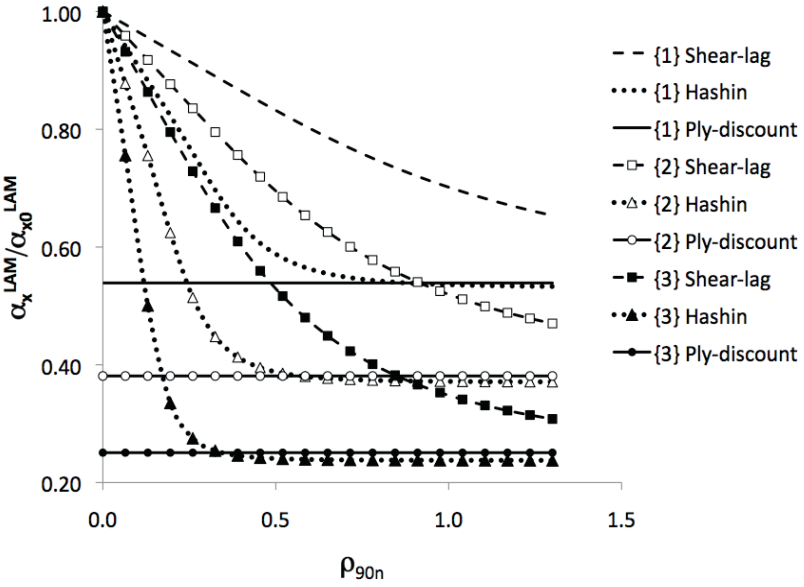

Figure 10. Simulation results showing changes in the axial coefficient of thermal expansion of the laminate α_x^{LAM} for CF/EP

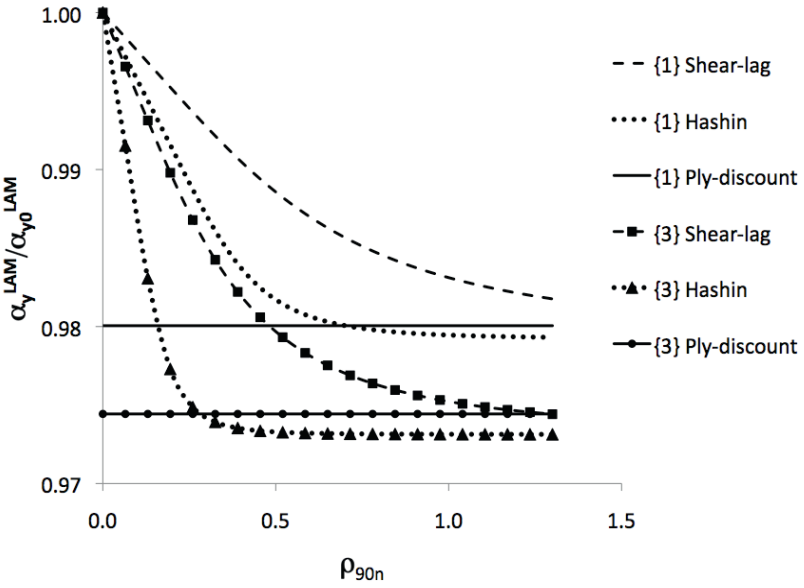

Figure 11. Simulation results showing changes in the transverse coefficient of thermal expansion of the laminate α_y^{LAM} for GF/EP

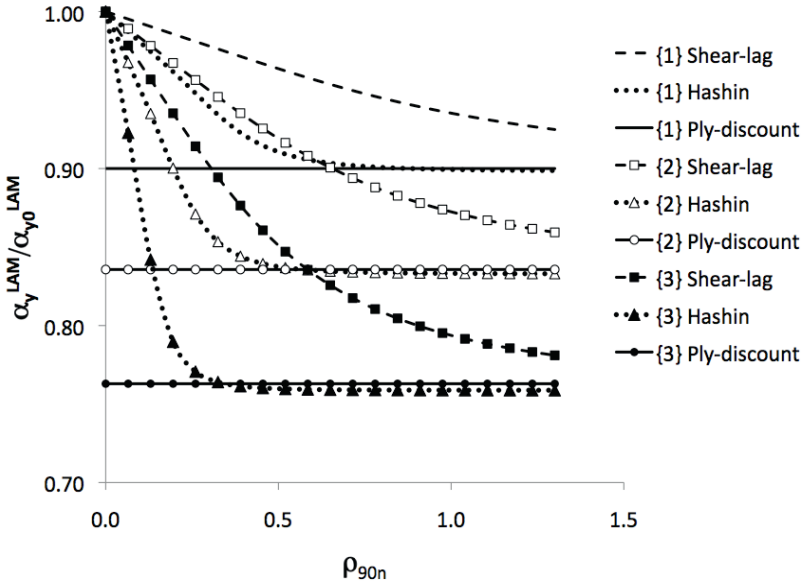

Figure 12. Simulation results showing changes in the transverse coefficient of thermal expansion of the laminate α_y^{LAM} for CF/EP

4.3. Comparison between simulations and experimental data.

The shear lag model and the Hashin's model predictions are compared with experimental data in Fig 13 to 16. It is obvious that for both GF/EP2 laminate lay-ups ($[0_2/90_4]$s and $[\pm 15/90_4]$s) Hashin's model describes the axial modulus and Poisson's ratio reduction more accurate than the shear lag model. Still, the Hashin's model gives conservative values, especially for the $[\pm 15/90_4]$s lay-up. The shear lag model by far under-predicts the reduction of these constants.

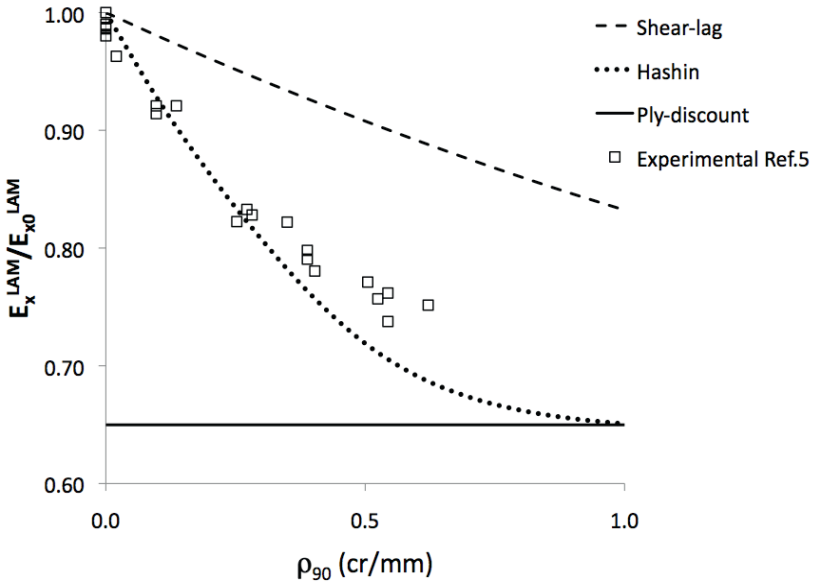

Figure 13. Simulations and experimental data showing the change in axial modulus E_x^{LAM} of GF/EP2 $[0_2/90_4]$s laminate

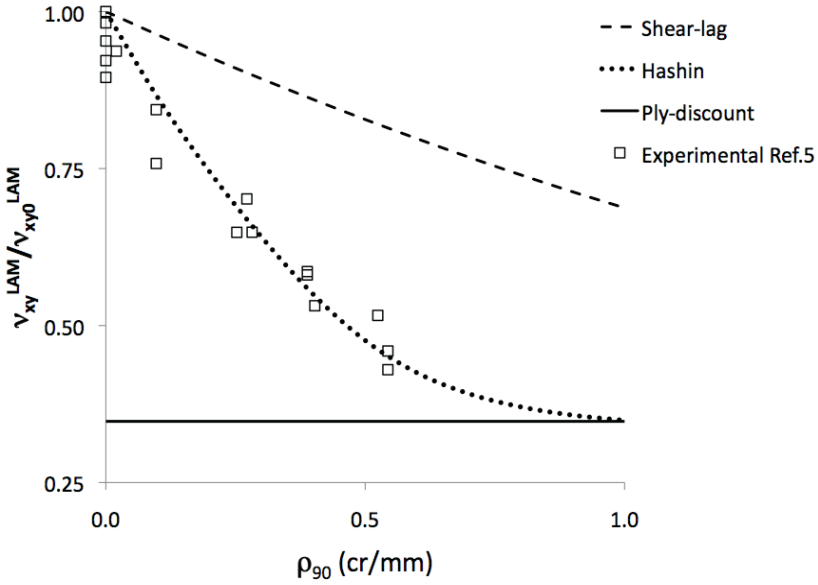

Figure14. Simulations and experimental data showing the change in Poisson's ratio ν_{xy}^{LAM} of GF/EP2 $[0_2/90_4]$s laminate.

The excellent agreement between the test results and the predictions of the Hashin's model, which suppose to give a lower bond to stiffness, requires an explanation. 90-layer thickness was rather large (1.15mm) and much thicker than the constraint layer.

Laminates with such geometry are prone to local delaminations starting from transverse crack tip. These local delaminations would increase the crack opening and lead to more modulus reduction than in the case without delaminations and improve the agreement with Hashin's model. FEM results for this laminate presented in [5] are higher than experimental data indicating that in this case indeed the crack model without delaminations may not correspond to reality.

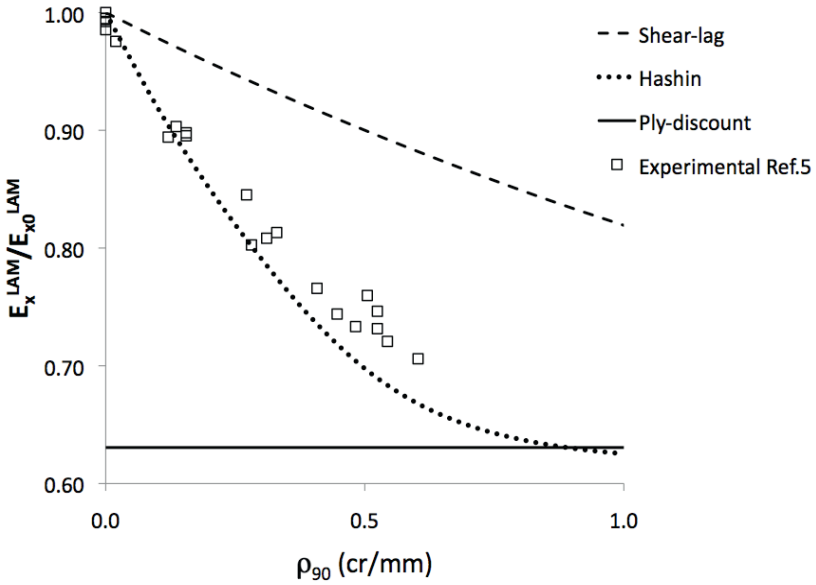

Figure 15. Simulations and experimental data showing the change in axial modulus E_x^{LAM} of GF/EP2 [±15/90_4]s laminate

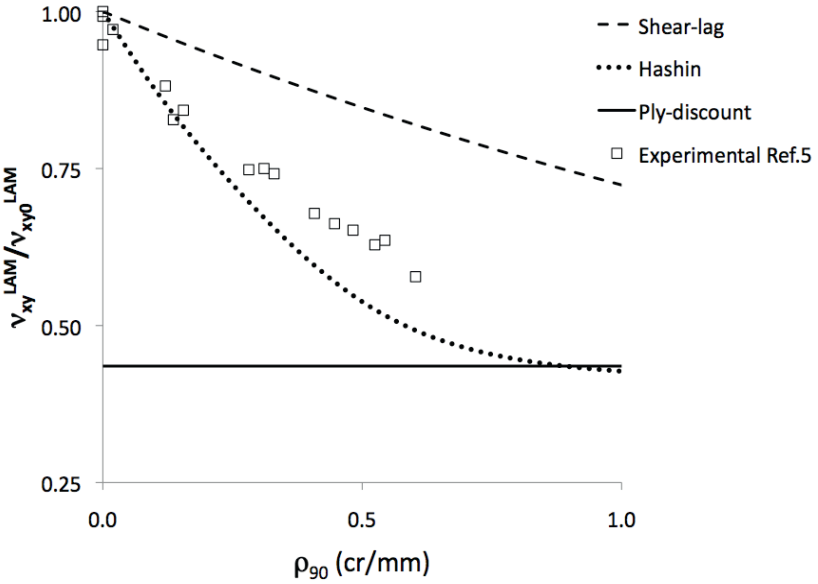

Figure16. Simulations and experimental data showing the changes in Poisson's ratio ν_{xy}^{LAM} of GF/EP2 [±15/90$_4$]s laminate

4.4. Comparison between analytical simulations and FEM data.

To validate the results and trends presented in section 4.2 FEM analysis was performed and the thermo-elastic properties of damaged laminates were analyzed directly from the FEM model or indirectly (for example, thermal expansion coefficients) determining COD with FEM and using (7)-(12). Results are presented in Fig. 17 to 24.

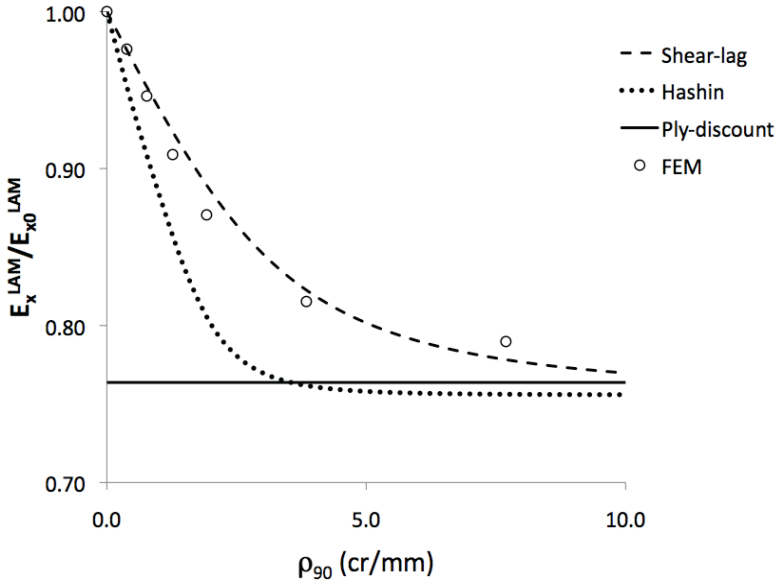

Figure17. Simulations and FEM data showing the changes in axial modulus E_x^{LAM} of GF/EP [0/90]s laminate

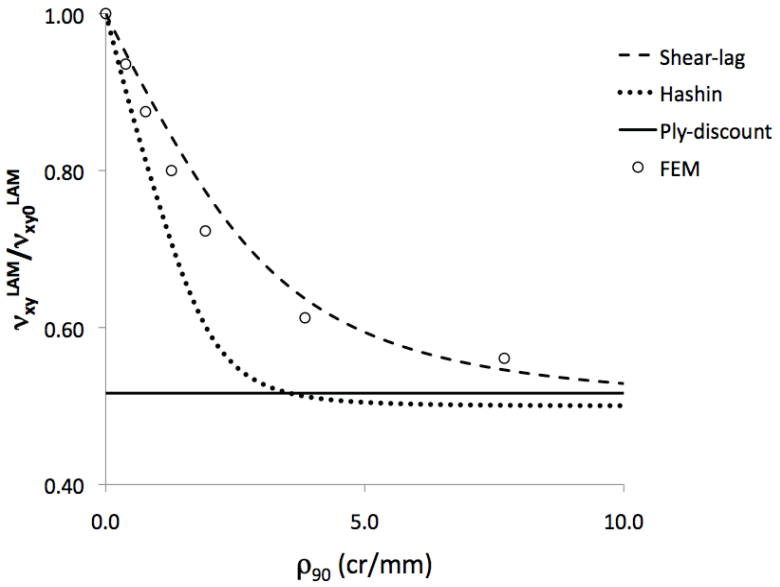

Figure 18. Simulations and FEM data showing the changes in Poisson's ratio ν_{xy}^{LAM} of GF/EP [0/90]s laminate

Comparison for GF/EP [0/90]s laminates can be based on data presented in Fig.17 to 19. The shear lag model with the selected resin layer thickness of 0.007 mm gives excellent accuracy for axial modulus and for thermal expansion coefficient and

slightly larger differences for Poisson's ratio. Noteworthy, the differences have the same trends with crack density change for all three properties. Hashin's model largely overestimates changes of all three properties.

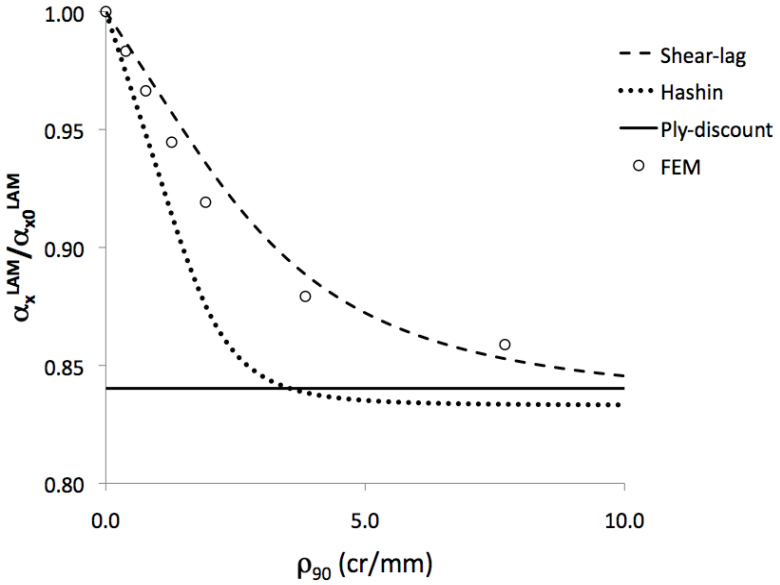

Figure 19. Simulations and FEM data showing the changes in axial coefficient of thermal expansion α_x^{LAM} of GF/EP [0/90]s laminate

In CF/EP [0/90]s laminate, see Fig 20 to 22, the situation is different: the shear lag model with $d_0 = 0.0035$ mm (half of the carbon fiber diameter) gives very poor prediction. Voluntarily taking it two times larger (equal to the value for glass fiber radius) improves the agreement but it still underestimates the properties reduction.

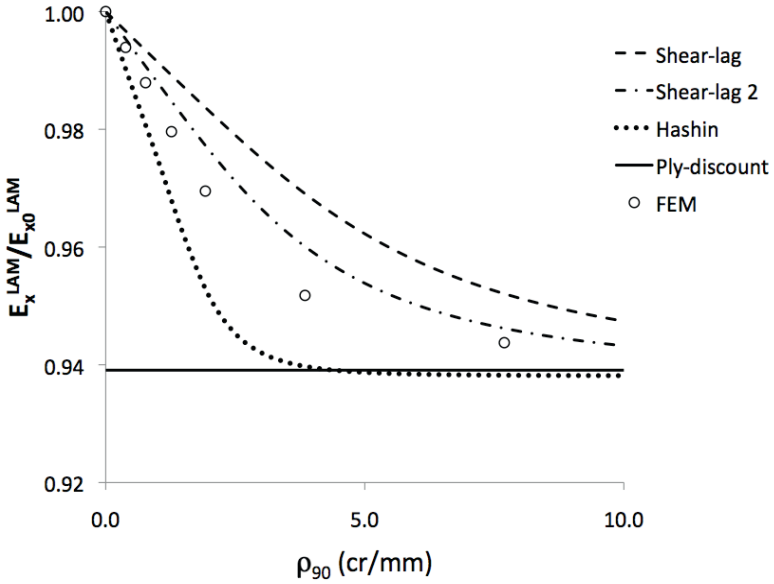

Figure 20. Simulations and FEM data showing the changes in axial modulus E_x^{LAM} of CF/EP [0/90]s laminate. "Shear-lag" corresponds to $d_0 = 0.0035$ mm, "Shear-lag 2" to $d_0 = 0.007$ mm

The lower bond from Hashin's model is much lower than the FEM data. Fig. 20 to 22 reveal the features of the shear lag model: using the resin layer thickness as a fitting parameter we could find a value which gives a very good fitting for all three considered properties. This is useful result suggesting approximate procedure: find this fitting parameter from FEM data for axial modulus and use it for all thermo-elastic properties.

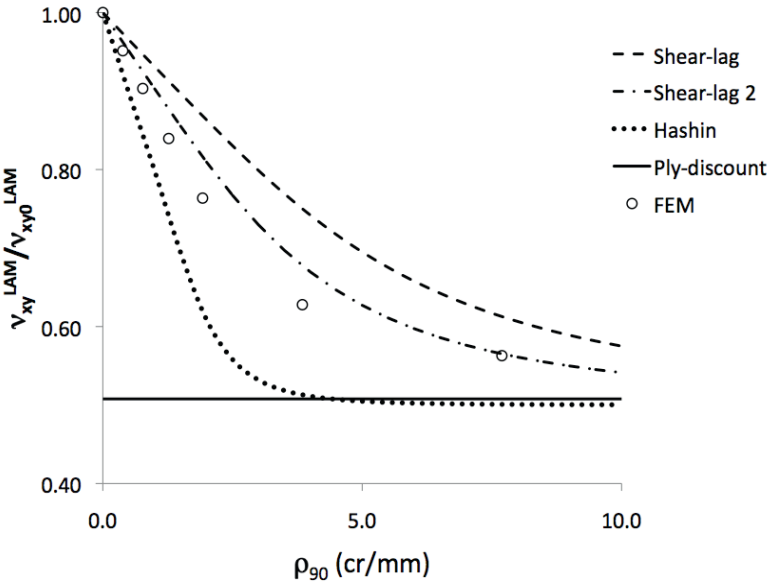

Figure 21. Simulations and FEM data showing the changes in Poisson's ratio ν_{xy}^{LAM} for CF/EP [0/90]s laminate. "Shear-lag" corresponds to $d_0 = 0.0035$ mm, "Shear-lag 2" to $d_0 = 0.007$ mm

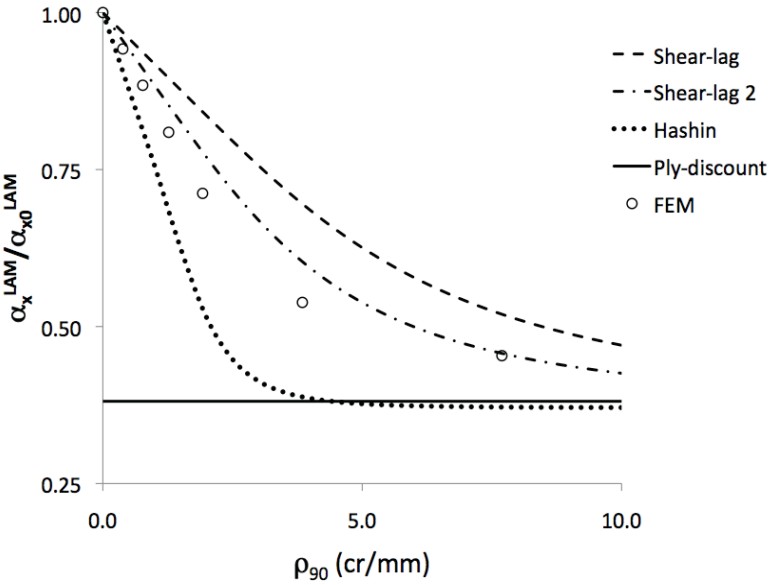

Figure 22. Simulations and FEM data showing the changes in longitudinal coefficient of thermal expansion α_x^{LAM} of CF/EP [0/90]s laminate. "Shear-lag" corresponds to $d_0 = 0.0035$ mm, "shear-lag 2" to $d_0 = 0.007$ mm

Unfortunately, the value, which gives the best fit, will be different for different materials and lay-ups. In addition, this value of resin layer thickness in our case has no physical meaning because it is too large (more than one fiber diameter).
Application of the suggested calculation approach to quasi-isotropic laminates is demonstrated in Fig. 23 and 24. The material is GF/EP and the 90-layer thickness is the same as for cross-ply laminates analyzed in Fig. 17 to 19. The agreement of the shear lag model with FEM results is as good as in case of cross-ply laminates (using the same resin layer thickness). The Hashin's model even in this case strongly overestimates the rate of the reduction.

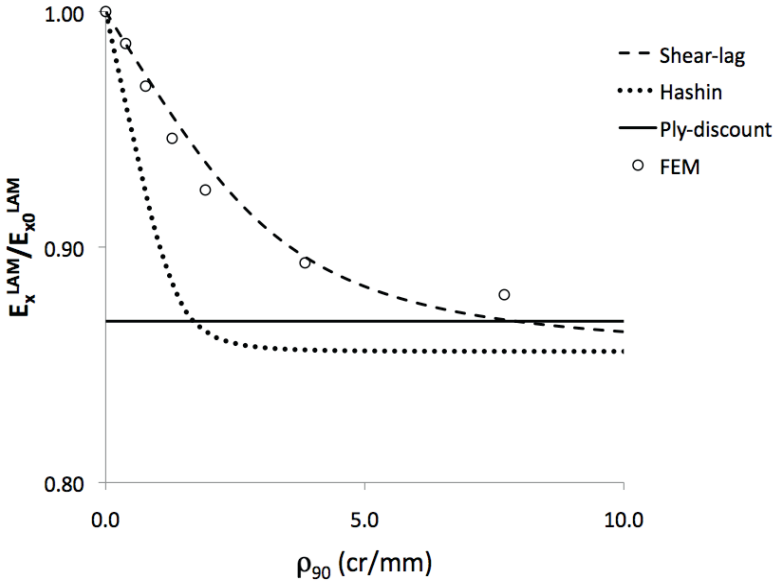

Figure 23. Simulations and FEM data showing the changes in longitudinal modulus E_x^{LAM} of GF/EP [0/±45/90]s laminate

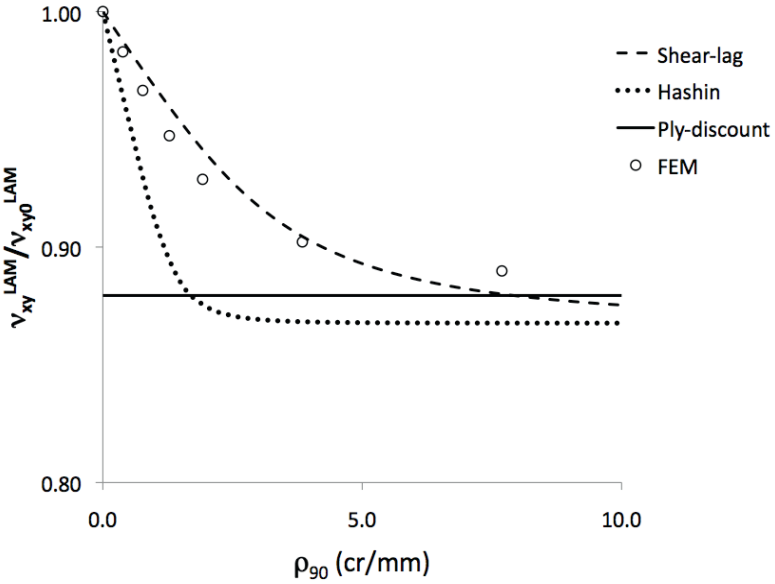

Figure 24. Simulations and FEM data showing the changes in Poisson's ratio ν_{xy}^{LAM} of GF/EP [0/±45/90]s laminate.

4.5 Ply-discount model and the asymptotic behavior of stiffness reduction

In this section we will address the observation from all presented figures that both models predict asymptotic values of thermo-elastic properties that are slightly lower than the ply-discount value calculated using CLT. It seems to be theoretically impossible. Nevertheless it is possible because in both analytical models the stress analysis is 2-dimensional, neglecting Poisson's interactions in layers and stress components in the specimen width direction. The used ply discount model was based on use of CLT which accounts for these interactions. In other words the comparison of asymptotic values in the way we did is inconsistent. The ply discount model used to compare asymptotic values should be based on the same assumptions as the stress analysis. In this particular case instead of CLT we should use rule of mixtures (ROM), for example, to calculate degraded laminate axial modulus with ply-discount.

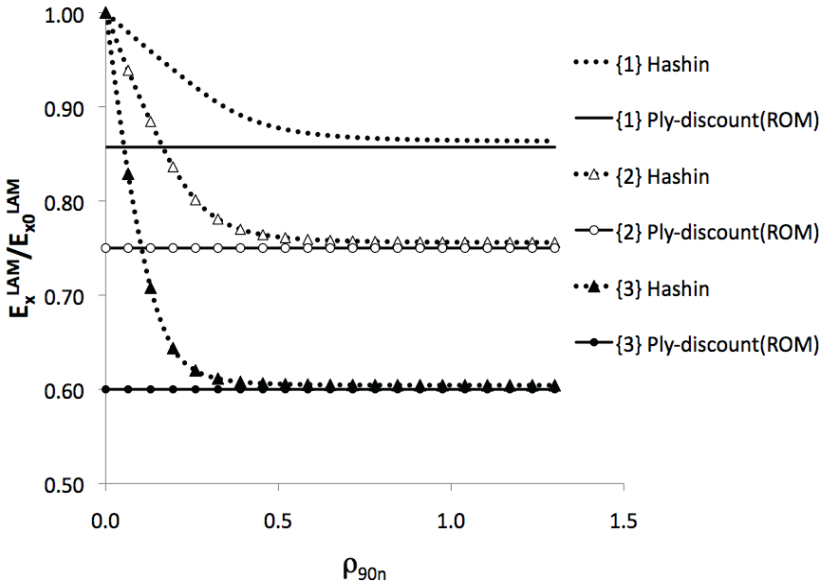

Figure 25. Simulation results showing changes in the axial modulus of the laminate E_x^{LAM} for GF/EP

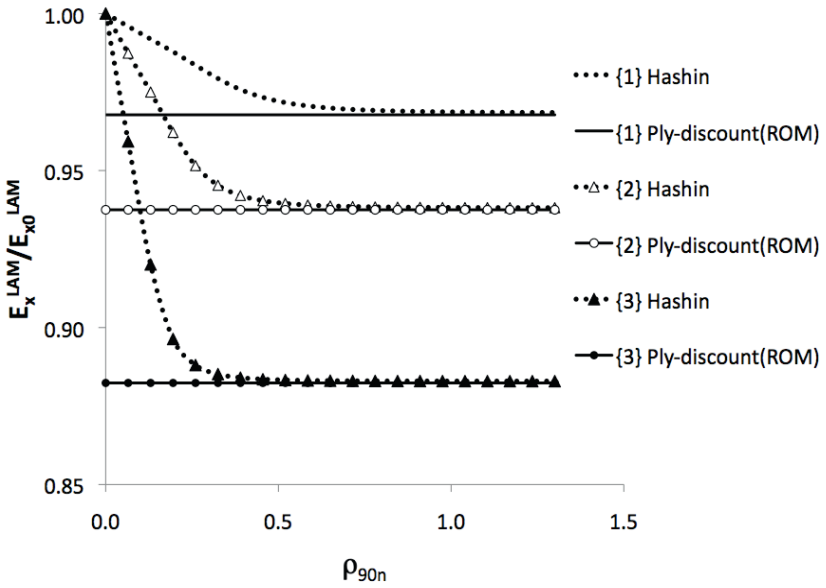

Figure 26. Simulation results showing changes in the axial modulus of the laminate E_x^{LAM} for CF/EP

The results presented in Fig. 25 and 26 show that the asymptotic values coincide with the ply-discount values based on rule of mixture analysis (instead of CLT).

This result explains the observed discrepancies but it does not mean that the rule of mixtures based ply-discount value is more accurate than the CLT based.

5. Conclusions

Methodology has been developed for approximate evaluation of all thermo-elastic constants of general symmetric laminates with cracked 90-layers. It is based on use of stress solutions from shear lag and Hashin's models in a general framework where laminate macroscopic properties are expressed through average stress perturbation between two cracks. This methodology has been validated with FEM and experimental data.

As expected all predicted curves approach to the ply-discount model predictions which assume almost zero transverse and shear properties of the damaged layer.

The predictions of the Hashin's model are always conservative but may be close to experimental data if the layer is relatively thick and local delaminations occur.

Comparing the shear lag model with FEM the accuracy of axial modulus determination is the same as the accuracy of thermal expansion coefficients. The shape function of the elastic property reduction from shear lag model can give a good agreement to FEM results if the shear lag parameter (thickness of the resin layer in our case) is used as a fitting parameter. For given material and lay-up all properties can be fitted with the same value of the parameter. It applies even for quasi-isotropic laminates if the ply thickness is the same.

References

1. A.L. Highsmith and K.L. Reifsnider: Damage in composite materials, ASTM STP 775, Philadelphia (PA), USA, 1982.
2. Y.M. Han, and H.T. Hahn: Compos. Sci. Tech., 1989, 35, 377-397.
3. P.A. Smith and J.R. Wood: Compos. Sci. Tech., 1990, 38, 85-93.
4. S.G. Lim and C.S. Hong: J. Compos. Mater., 1989, 23, 695-713.
5. R. Joffe and J. Varna: Compos. Sci. Tech., 1999, 59, 1641-1652.
6. A. Krasnikovs and J. Varna: Mech. Compos. Mater., 1997, 33, 565-582.
7. J. Varna and A. Krasnikovs: Mech. Compos. Mater., 1998, 34, 153-170.
8. J. Zhang, J. Fan and C. Soutis: Composites, 1992, 23, 291-304.
9. Z. Hashin: Mech. Mater., 1985, 4, 121-136.
10. J. Varna and L.A. Berglund: J. Compos. Tech. Res., 1994, 16, 77-87.
11. J. Varna and L.A. Berglund: Eur. J. Mech. Solid., 1993, 12, 699-723.
12. L.N. McCartney: 'A recursive method of calculating stress transfer in multiple ply cross-ply laminates subject to biaxial loading', NPL report DMMA(A)150, 1995.
13. G.A. Schoeppner and N. Pagano: Int. J. Solid. Struct., 1998, 35, 1025-1055.
14. J. Fan and J. Zhang: Compos. Sci. Tech., 1993, 47, 107-118.
15. P. Lundmark and J.Varna., International Journal of Damage Mechanics, 2005, 14, 235-261.
16. P. Lundmark and J. Varna: Compos. Sci. Tech., 2006, 66, 1444–1454.